CHAPTER V

EXPERIMENTAL RESULTS FOR A SINGLE HEAT PIPE AND DISCUSSIONS

In this chapter, the heat transfer characteristics of the heat pipes which contain Freon-113 or Freon-22 as working fluid are presented and discussed. For each type of working fluid, the effects of fill ratio, hot and cold fluid flowrates, inclination angle of the pipe and temperature difference across the pipe will be investigated experimentally. Then the experimental results will be presented as well as compared with those published by other investigators.

5.1 Experimental Conditions

In order to study the performance characteristics of a single heat pipe, tests were conducted on heat pipes with various fill quantities, under various flow rates of the external fluids, inclination angles and temperature differences. The ranges of these parameters are summarized in Table 5.1.

Table 5.1 The experimental conditions investigated

Parameters	Range
Working Fluid	Freon-113, Freon-22
Fill Ratio, % (respect to total volume)	4.9, 9.3, 18.5, 30 for Freon-113, and 16.4, 30 for Freon-22
Reynolds Number of Hot Water	800-5,000
Reynolds Number of Cold Water	1,000-5,000
Tilt Angle, degree	10-90
Temperature Difference, ^{o}C (between hot and cold waters)	5, 10, 20

5.2 Effect of Fill Ratio on a Wickless Heat Pipe

In the present study, two types of working fluids have been used, that is, Freon-113 and Freon-22. The following discussion will touch on each type.

From the heat transfer mechanism of heat pipe, the circulation of the working fluid has an important role in its operation. A maximum possible circulation is required to obtain the maximum heat transport capacity. The optional quantity of each type of working fluid depends on the physical properties of the working fluid and the tube geometry and the operating conditions such as tilt angle. When a large quantity of the working fluid is used, the two-phase mixture which forms by pool boiling will overflow into the condensing section, leading to a reduction in the condensation heat transfer area. On the other hand, if the liquid fill charge is too small, some of the heated

evaporation surface may be dry. This adversely affects the evaporation heat transfer coefficient. The optimum amount of the working fluid is thus the amount that suffices to wet all the evaporation surface and form a small liquid supply pool at the end of the evaporation section.

The term "fill ratio" in this study is defined as the percentage of the working fluid volume compared to the total heat pipe inside volume. In order to study the effect of the fill ratio, 6 heat pipes have been constructed. Four of them use Freon-113 as working fluid, and the rest Freon-22.

In the case of Freon-113, to determine an optimum amount of Freon-113 the heat pipes were manufactured at fill ratio of 4.9%, 9.3%, 18.5% and 30% (11%, 20.9%, 41.6%, 67.5% with respect to the evaporator volume). The experiments were conducted at a tilt angle of 50 degrees with the hot and cold water temperatures being 35 and 30, respectively. The results are shown in Figures 5.1-5.3. Figure 5.1 shows the average heat transfer rate versus the average temperature difference observed between the outer surfaces of the evaporator and condenser at each fill ratio. At the fill ratio of 9.3, 18.5 and 30%, the heat rate is very high, but for 30% fill ratio, the observed temperature difference is also high. So the optimum fill charge should be around 9.3-18.5%.

To comfirm the above analysis, the ratio of the effective thermal conductivity of the heat pipe to that of an equal-size copper rod (386 $W/m^{o}C$) is plotted against the Reynolds number of the hot and cold water in Figures 5.2 and 5.3, respectively. It can be seen in Figure 5.2 that the heat pipe with 9.3% fill ratio has the highest effective thermal conductivity ratio (about 600-860 times of copper).

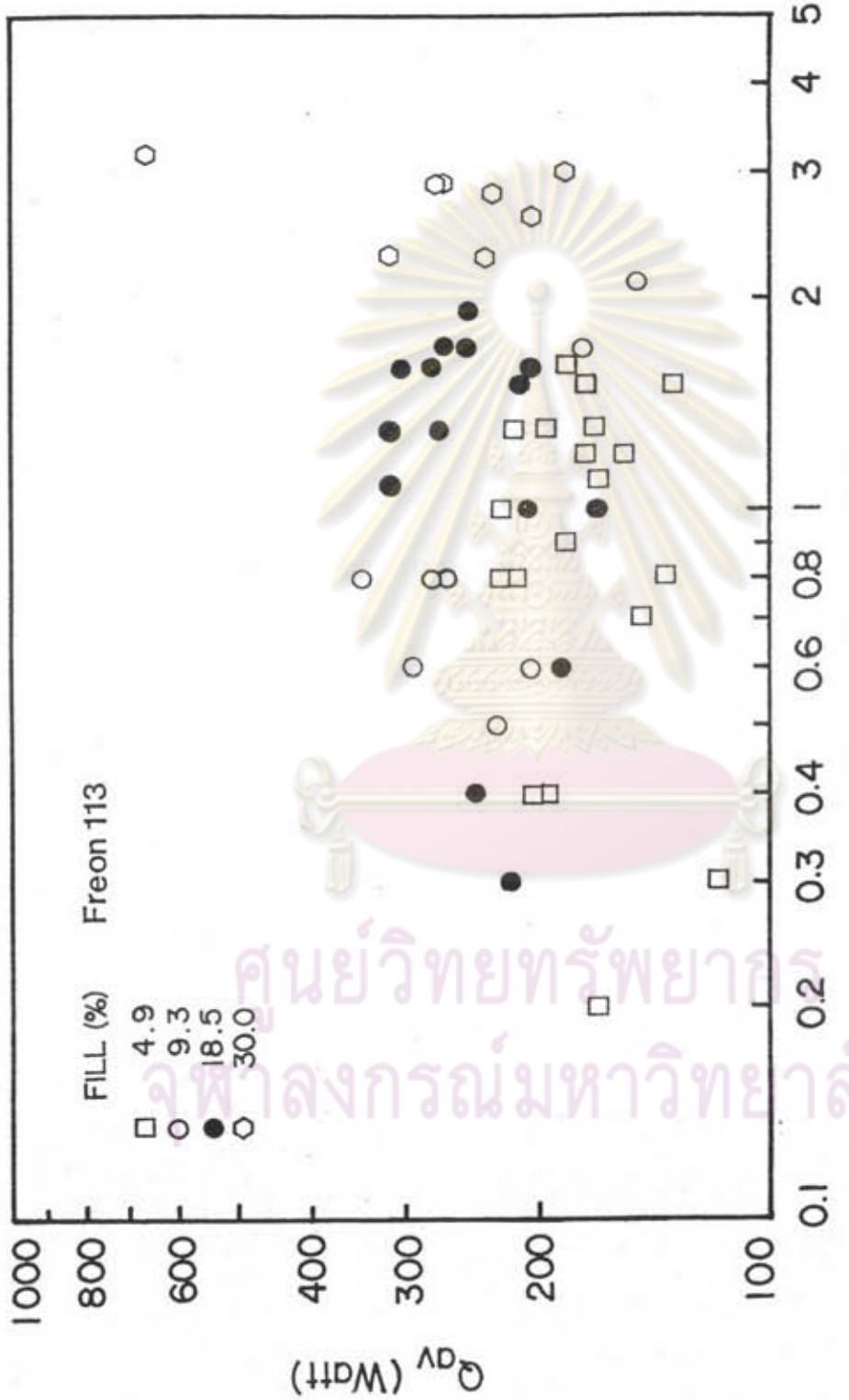

Figure 5.1 The effect of the heat rate versus temperature difference between the evaporator and condenser surface at various fill ratios (tilt angle 50 degrees, $T_h - T_c$ = 35-30 °C).

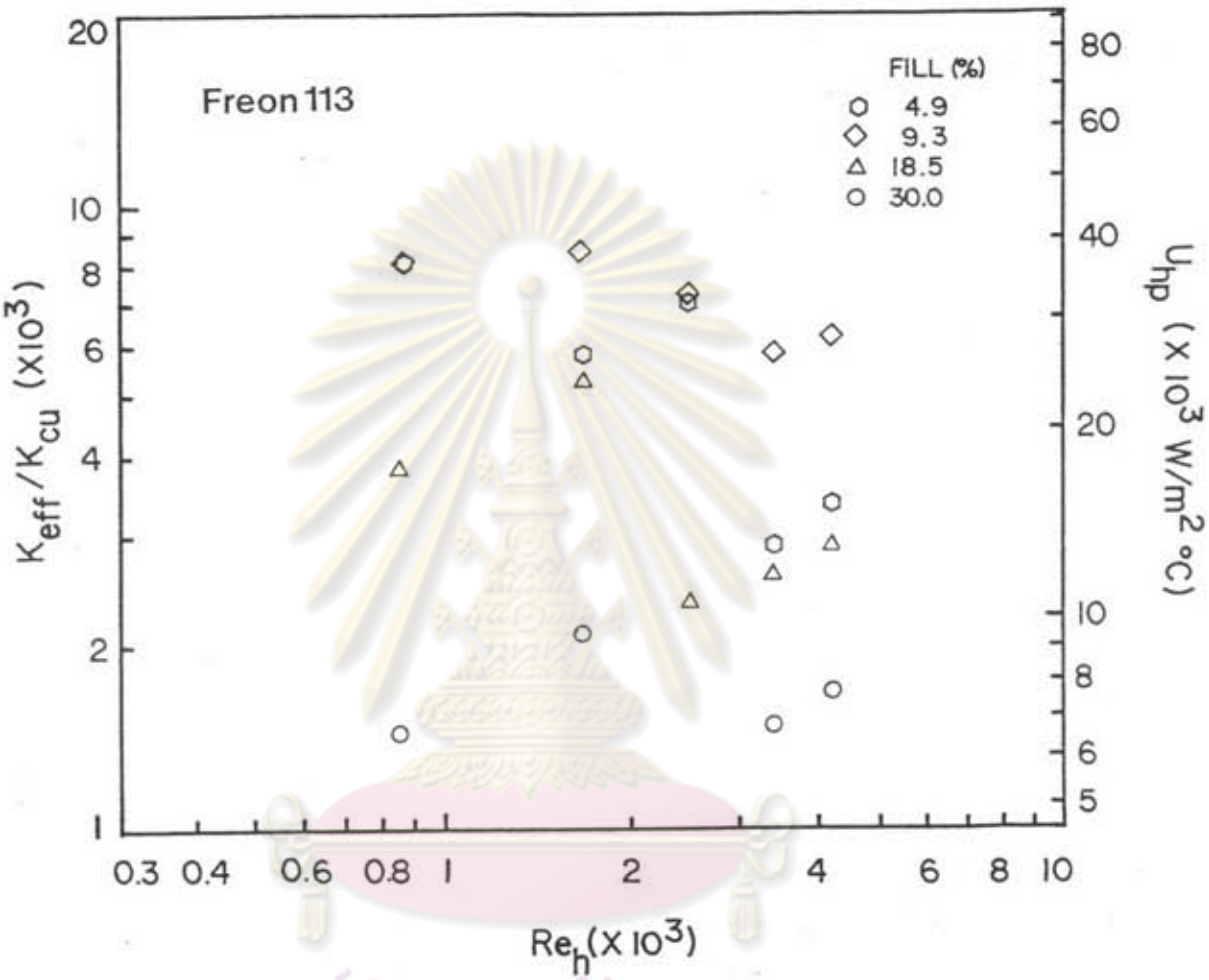

Figure 5.2 Ratio of effective thermal conductivity versus Reynolds number of hot water at various fill ratios (tilt angle 50 degrees, $T_h - T_c$ = 35-30 °C).

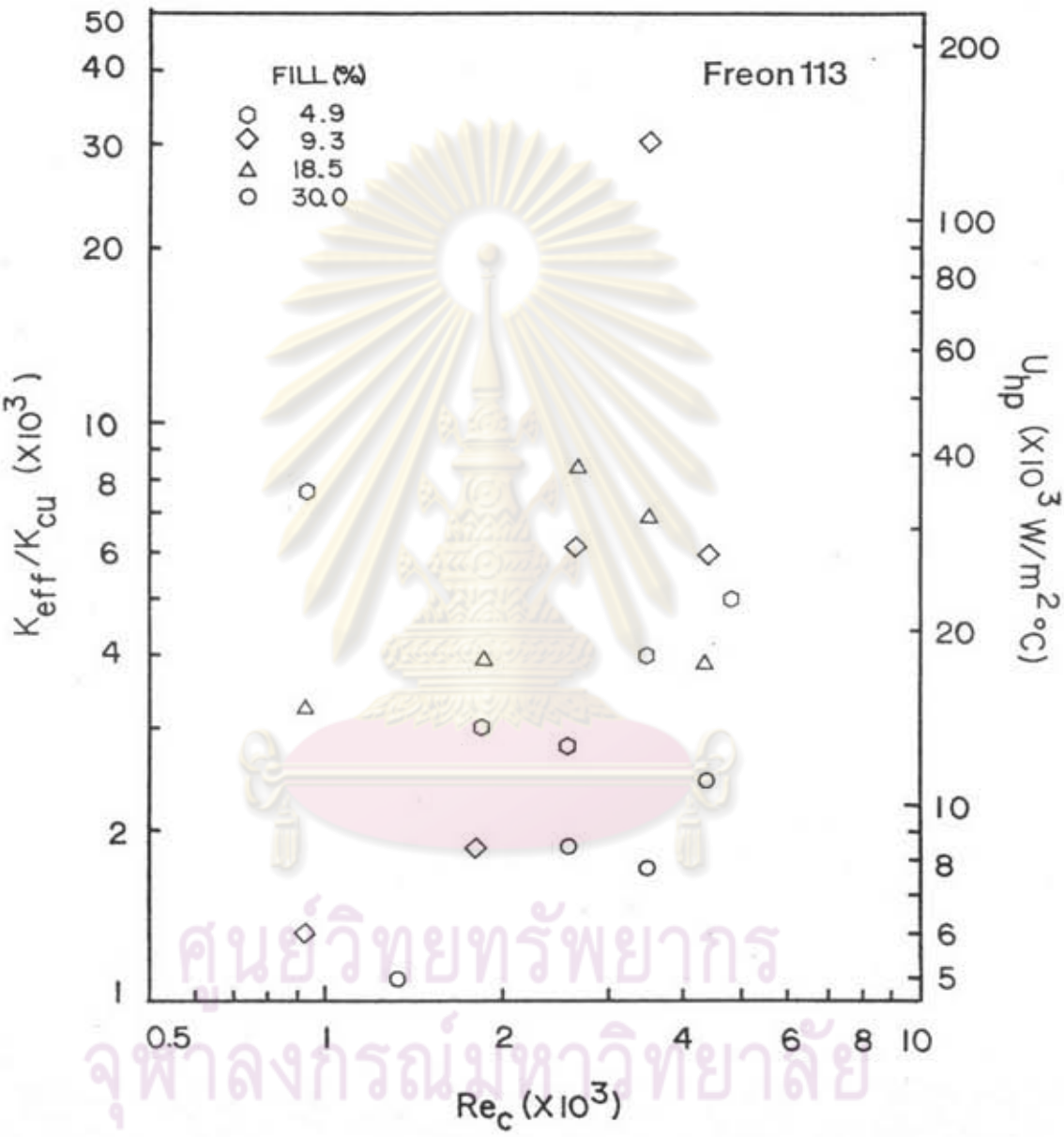

Figure 5.3 Ratio of effective thermal conductivity versus Reynolds number of cold water at various fill ratios (tilt angle 50 degrees, $T_h - T_c$ = 35-30 °C).

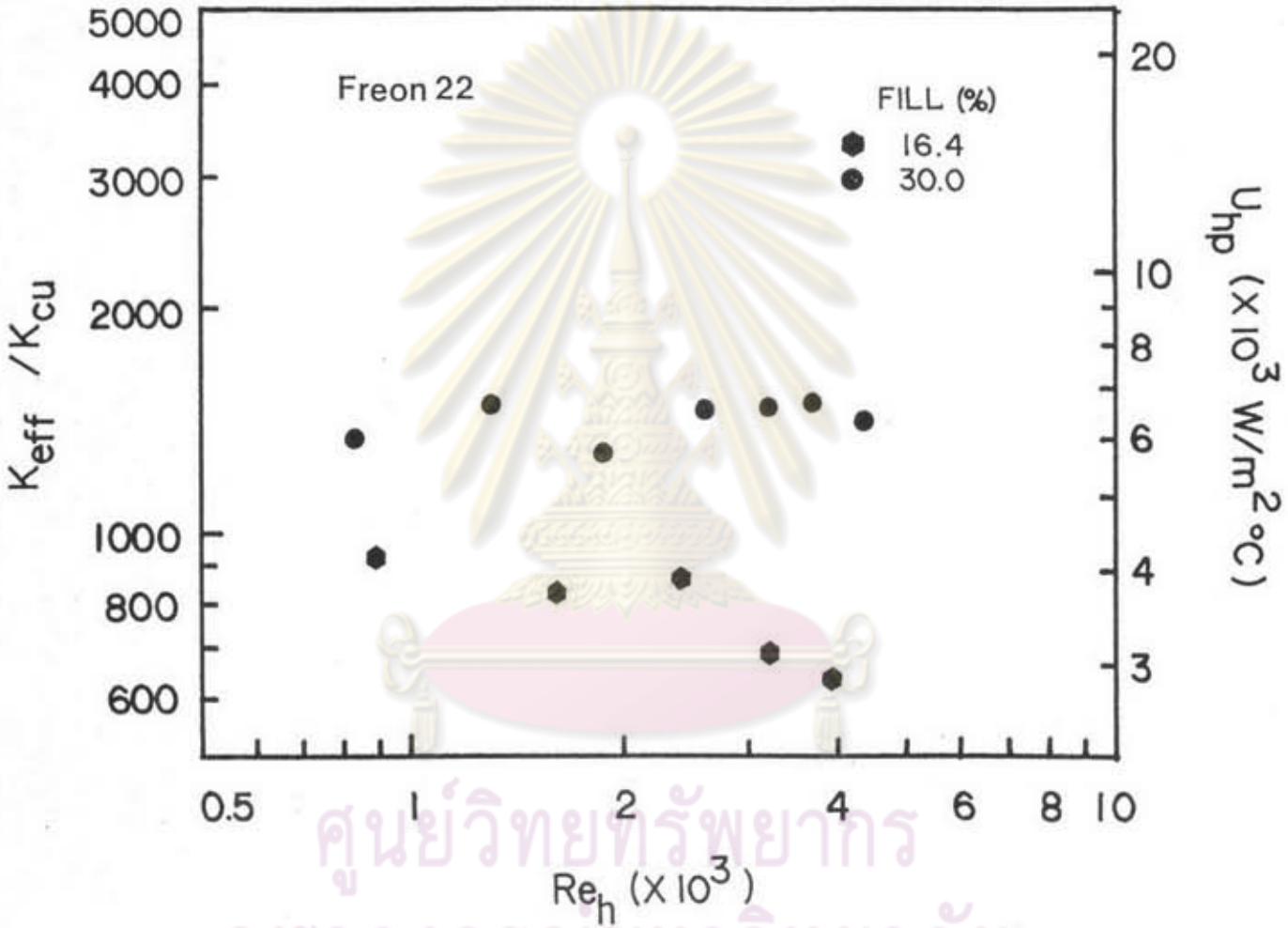

Figure 5.4 Ratio of effective thermal conductivity versus Reynolds number of hot water at various fill ratios (tilt angle 50 degrees, $T_h - T_c = 40\text{-}20\ ^{o}C$).

Although the effective thermal conductivity at the fill ratio of 4.9% is also high in Figure 5.3 but the results are not so good in the other cases. Thus it can be concluded that the optimum fill for Freon-113 is in the range of 9.3-18.5%. The conclusion indicates that at a large fill ratio, most of the evaporator is covered by the liquid pool and the mechanism of heat transfer in the evaporator is dominated by surface evaporation from a thick liquid film. The depth of the pool also tends to suppress nucleate boiling. On the otherhand, when the fill ratio is suitable, the evaporator surface is mostly covered by a thin film. So the dominant mechanism in the evaporator may change from thick film evaporation to thin film evaporation and nucleate boiling in the supply liquid pool. However, if the liquid fill is too small, part of the evaporation surface will dry out leading to reduced heat transfer.

In the case of Freon-22, only two fill ratios, 16.4 and 30% have been investigated. The results are shown in Figure 5.4. Figure 5.4 reveals that the fill ratio of 30% is more suitable than 16.4%, which is different from the case of Freon-113. Althuogh the latent heat (per unit mass) of Freon-22 is higher than that of Freon-113, its density is much less (see Table B-1 - B-2 in Appendix B). So suitable fill ratio of Freon-22 is larger than that of Freon-113.

5.3 Effect of the Inclination Angle of the Heat Pipe

The results of the experiments for the case of the Freon-113 heat pipe are shown in Figures 5.5-5.7. The experiments were conducted on the heat pipe with fill ratio of 30% and at 30 ^{o}C and 25 ^{o}C of hot and cold water temperatures. In Figure 5.5 the heat transfer rate is plotted against the temperature difference between

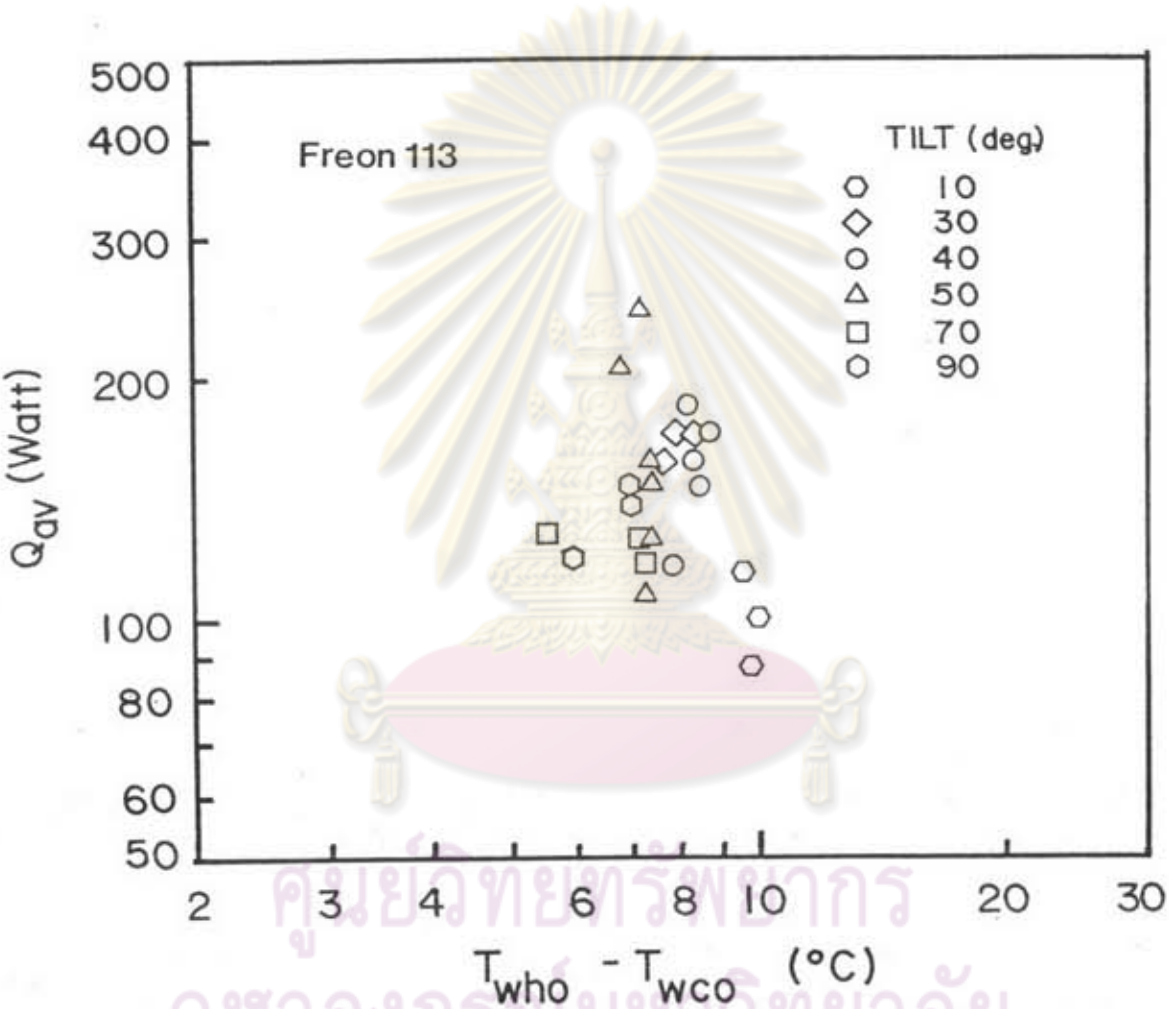

Figure 5.5 Heat rate versus temperature difference between the evaporator and condenser surface at various tilt angle (fill ratio 30%, $T_h - T_c \simeq 35\text{-}25$ °C).

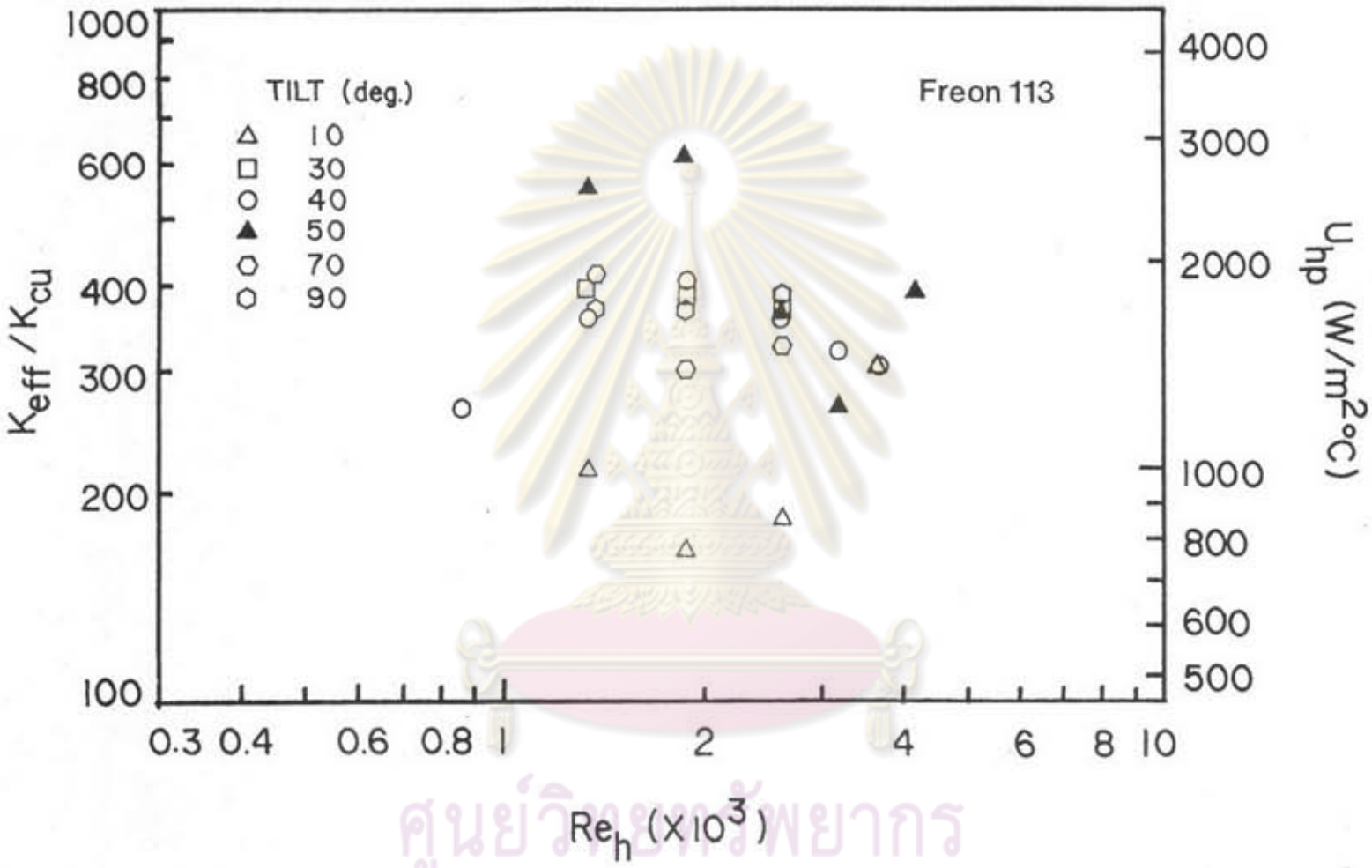

Figure 5.6 Ratio of effective thermal conductivity versus Reynolds number of hot water at various tilt angles (fill ratio 30%, $T_h - T_c$ = 35-25 °C).

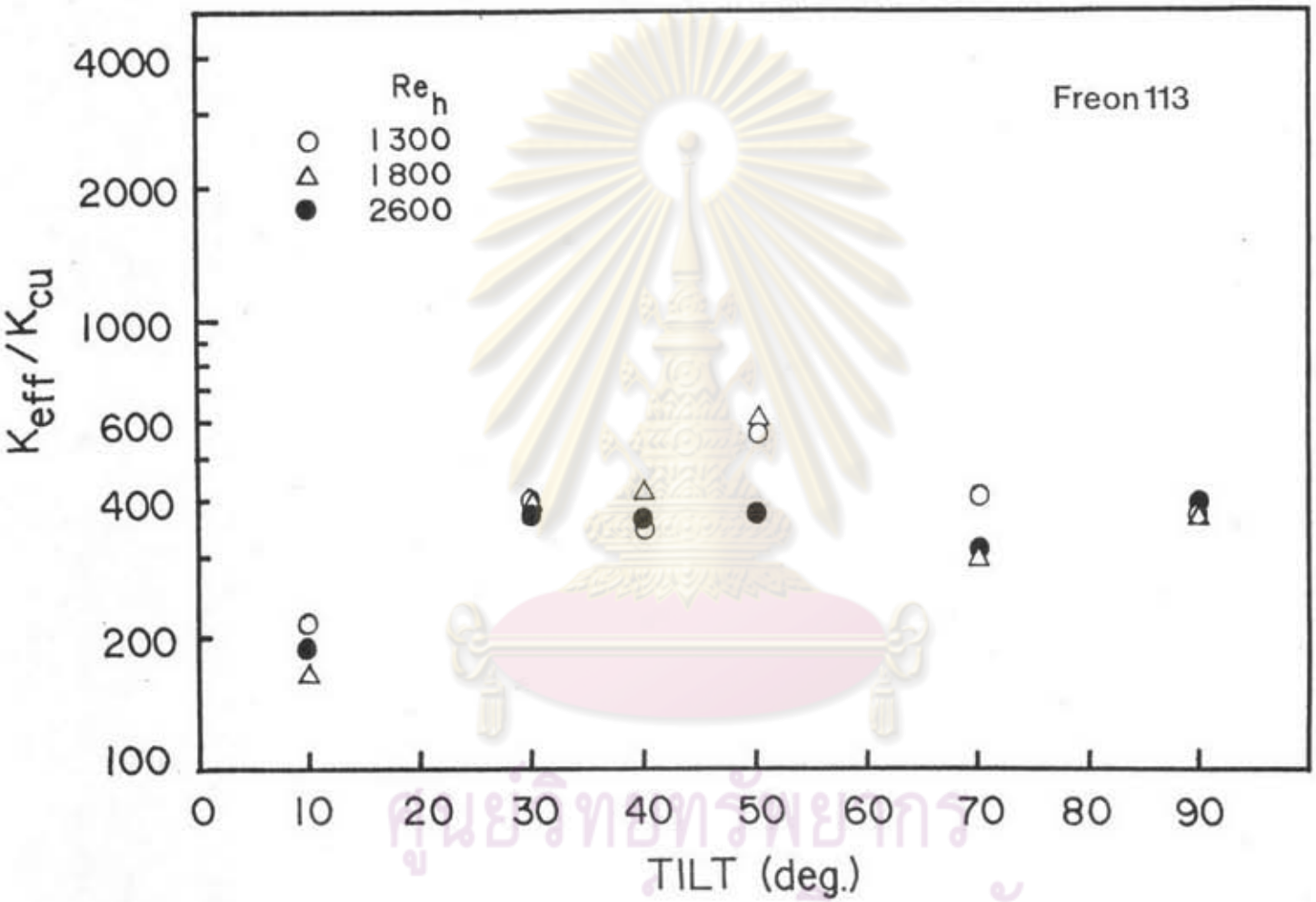

Figure 5.7 Ratio of effective thermal conductivity versus tilt angle at various hot Reynolds numbers (fill ratio 30%, $T_h - T_c$ = 35-25 °C).

the hot and cold surfaces at each tilt angle. The results show that the heat pipe which inclines at 50 degree from the horizontal can transfer more heat than at the other angles. Figure 5.6, a plot of the effective thermal conductivity ratio versus the hot Reynolds number, shows the same result. That is a tilt angle of 50 degrees gives the highest effective thermal conductivity.

The effective thermal conductivity ratio is next shown as a function of the tilt angle in Figure 5.7. The effective conductivity of the heat pipe increases as the tilt angle increases up to 50 degrees. Further increase in the tilt angle instead reduce the effective thermal conductivity. At a small tilt angle, some of the working fluid may overflow into the condenser section resulting in a reduction of heat pipe performance. The condensate of the thermosyphon or wickless heat pipe generally returns to the evaporator by the gravity force. When the pipe is inclined the vertical force acting on the condensate will be $g\sin\theta$, where θ is the tilt angle with respect to the horizontal. This means that the condensate return force will increase as the tilt angle increases. Thus the heat transfer rate is controlled more by the phenomena in the evaporator than in the condenser.

However, when the heat pipe is tilted at more than 50 degrees, the wetting of the evaporator surface covers less area and a deep pool is formed at the end of the evaporator. All these hamper heat transfer rate in the evaporator, even if the condensed liquid is promptly returned.

Besides the gravity force, the shear force resulting from the counter flow of the vapor and liquid inside the thermosyphon also has an effect on the condensate flow. In a properly inclined tube, the

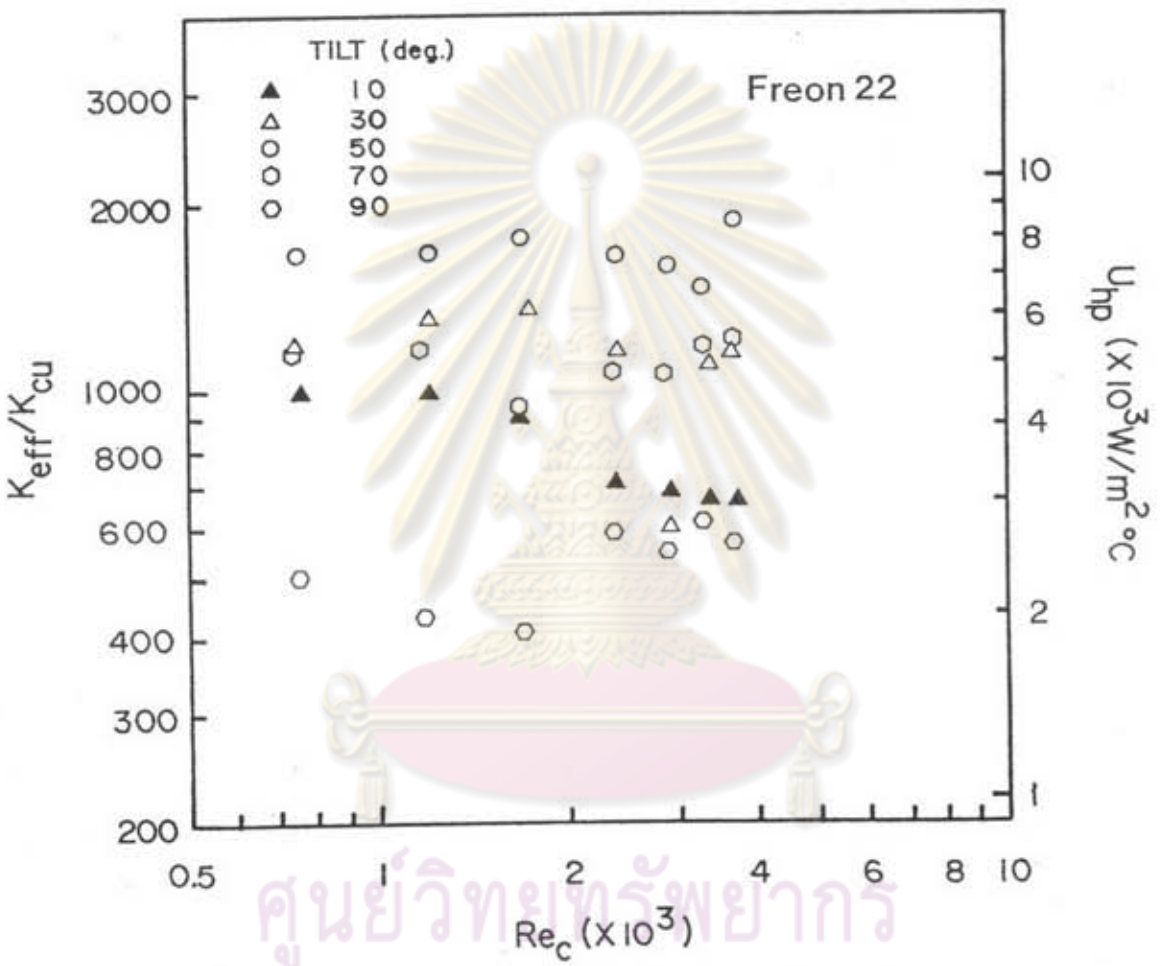

Figure 5.8 Ratio of effective thermal conductivity versus Reynolds number of cold water at various tilt angles (fill ratio 30%, $T_h - T_c$ = 40-20 °C, Re_h = 4,200).

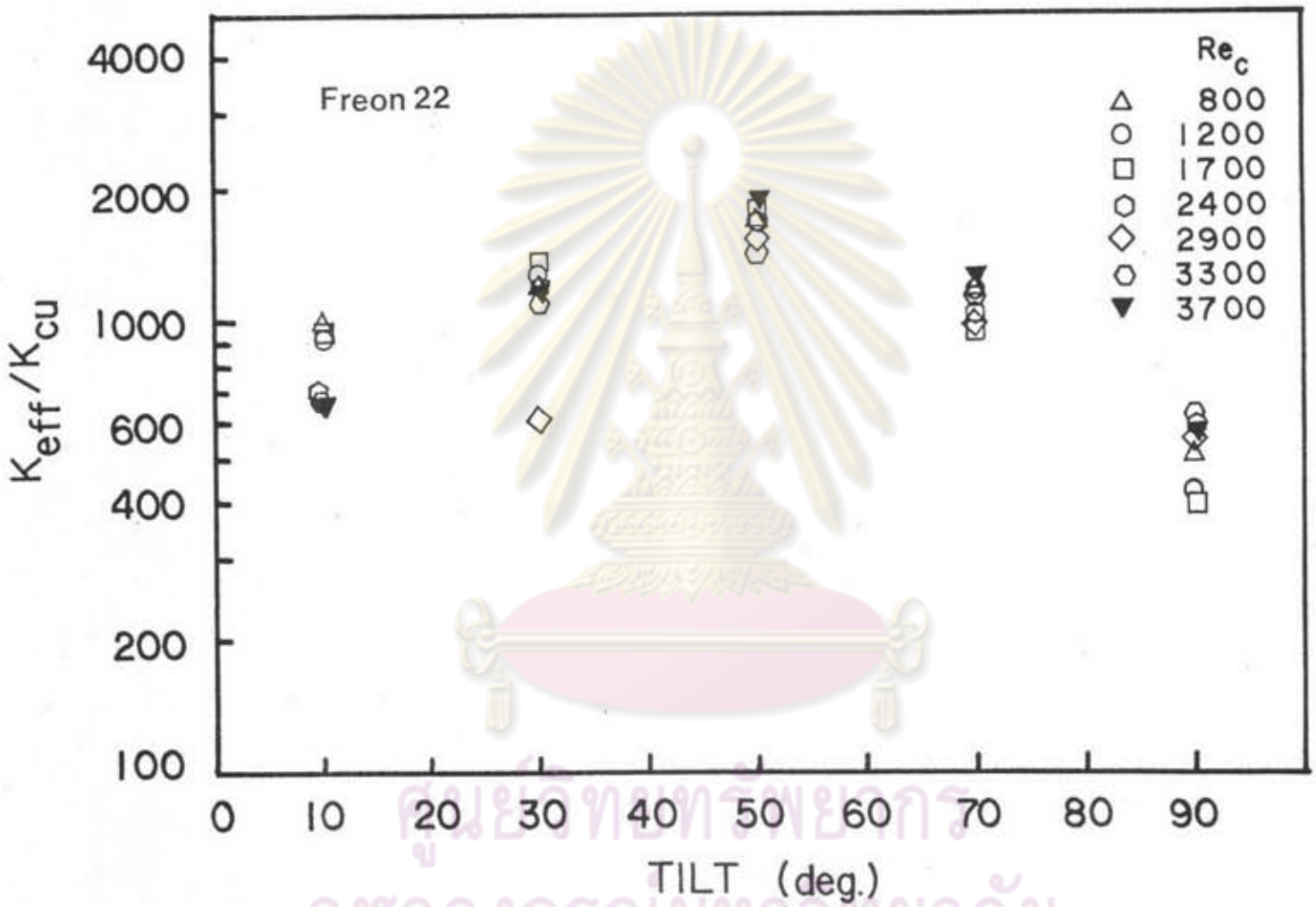

Figure 5.9 Ratio of effective thermal conductivity versus tilt angle at various cold Reynolds numbers (fill ratio 30%, $T_h - T_c$ = 35-30 °C, Re_h = 4,200).

vapor tends to flow along the upper side of the tube while the liquid is collected at the lower side, thus reducing the interface acted upon by the shear forces, and liquid return is not hampered.

For the case of Freon-22, the results are shown in Figures 5.8-5.9. The trends are similar to those of Freon-113. It can be concluded that the optimum tilt angle for both types of heat pipes is about 50 degrees from the horizontal.

5.4 Effect of Flow Rates of External Fluids

For the case of Freon -113, to understand the effect of the water flow rates on the performance of the heat pipes, the effective thermal conductivity ratio is plotted against the hot Reynolds number and cold Reynolds number respectively in Figures 5.10 and 5.11. In Figure 5.10, as the hot Reynolds number increases, the effective thermal conductivity decreases stepwise around Re_h = 2,300. Above and below Re_h = 2,300 the effective conductivity is almost constant. This implies that the transition of the flow regime may be the cause. In the case of increasing cold Reynolds number (Figure 5.11), the effective conductivity is found to be more or less constant, except for a few data points at Re_h above 3,500. Again the change in flow regime is the suspected cause.

Figures 5.12-5.13 show that an increase in either the hot and cold Reynolds number does not affect the percentage of the external or outer film resistances compared to the total resistance. It can be seen that the share of the heat pipe internal resistances is much larger than that of the outer film resistances. This means the internal mechanism of the heat pipe plays an important role here. Figures 5.14-5.18 show the effect of the Reynolds numbers on both the

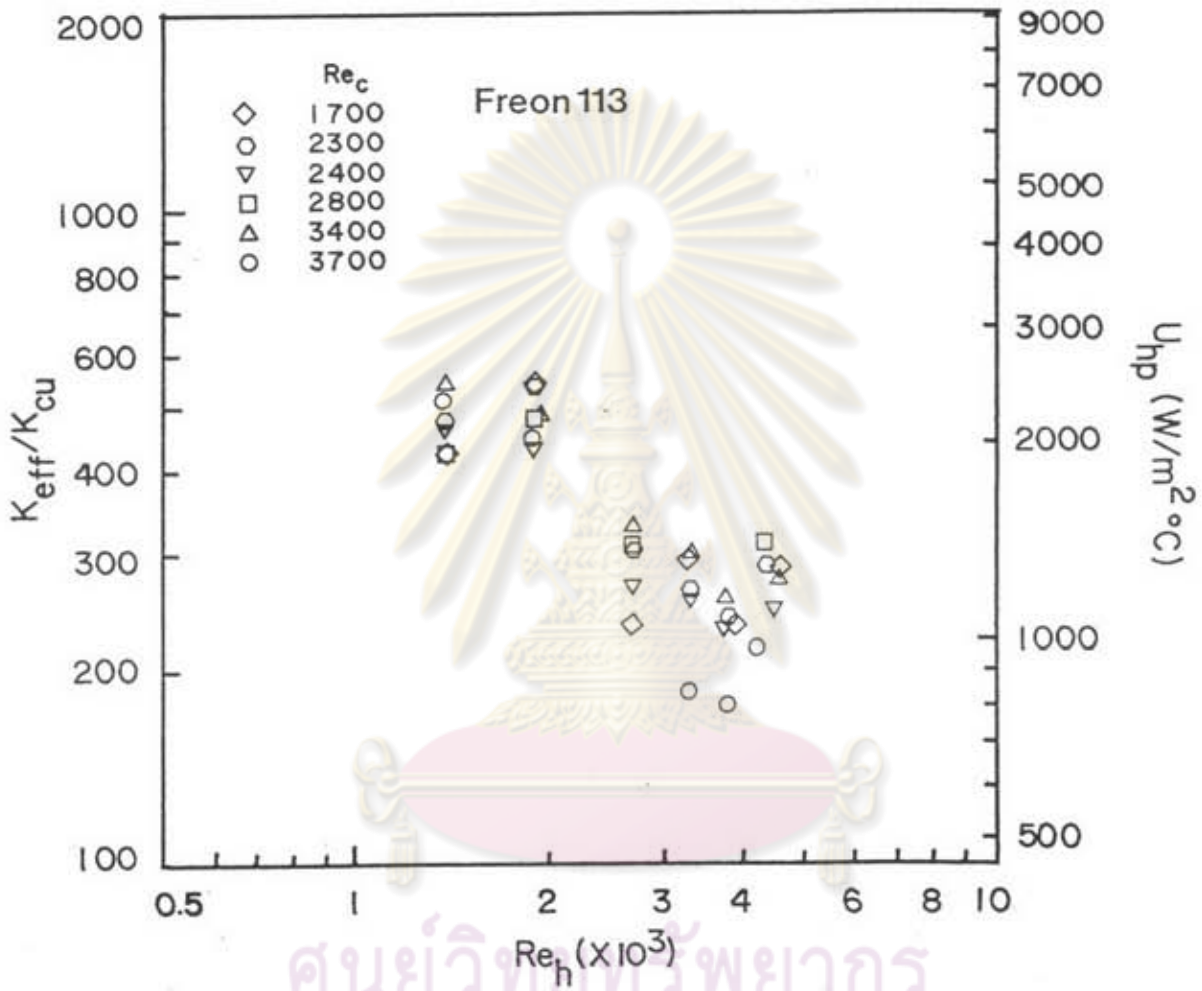

Figure 5.10 Ratio of effective thermal conductivity versus Reynolds number of hot water at various cold Reynolds numbers (tilt angle 50 degrees, $T_h - T_c$ = 40-20 °C, fill ratio 30%).

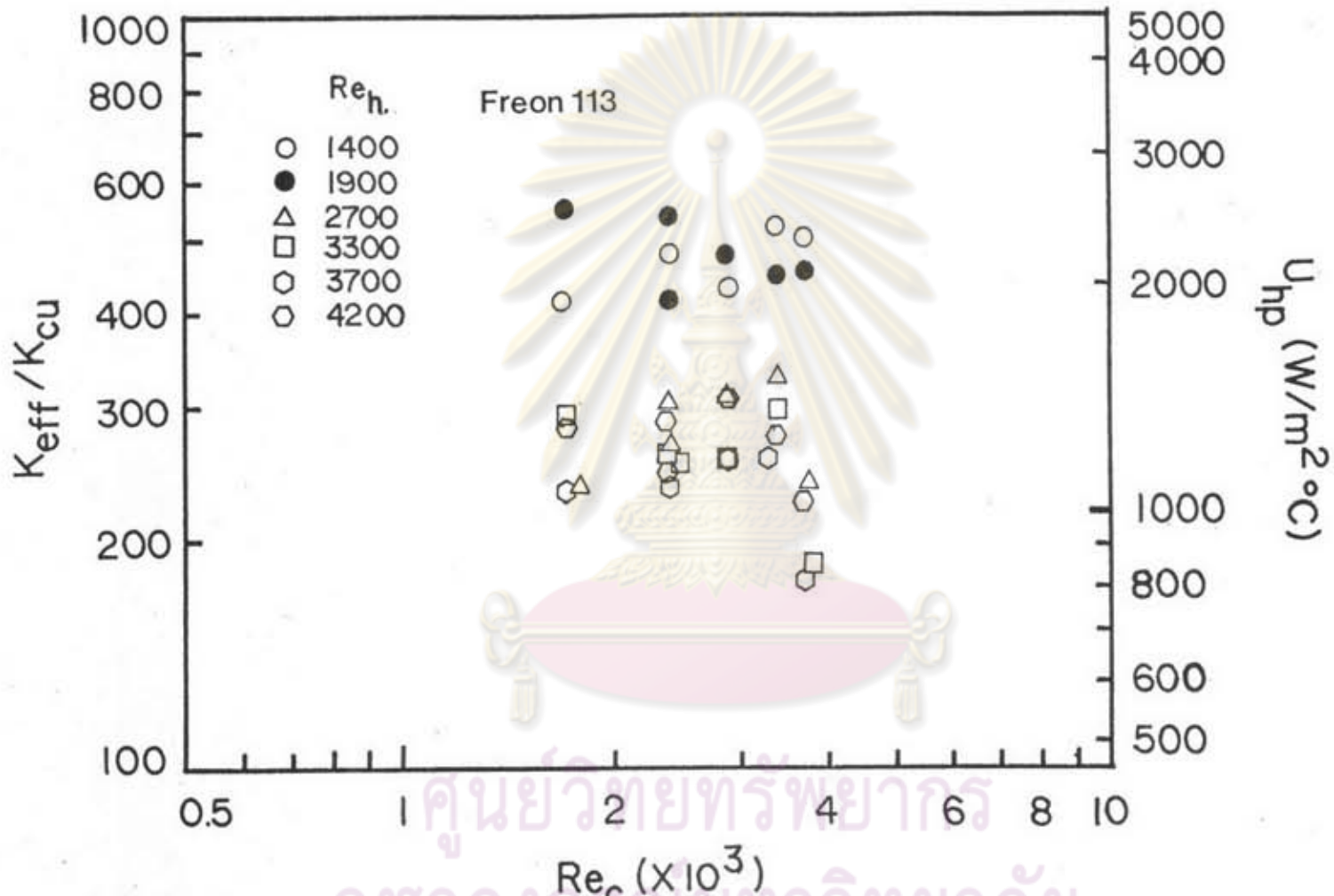

Figure 5.11 Ratio of effective thermal conductivity versus Reynolds number of cold water at various hot Reynolds numbers (tilt angle 50 degrees, $T_h - T_c$ = 40-20 °C, fill ratio 30%).

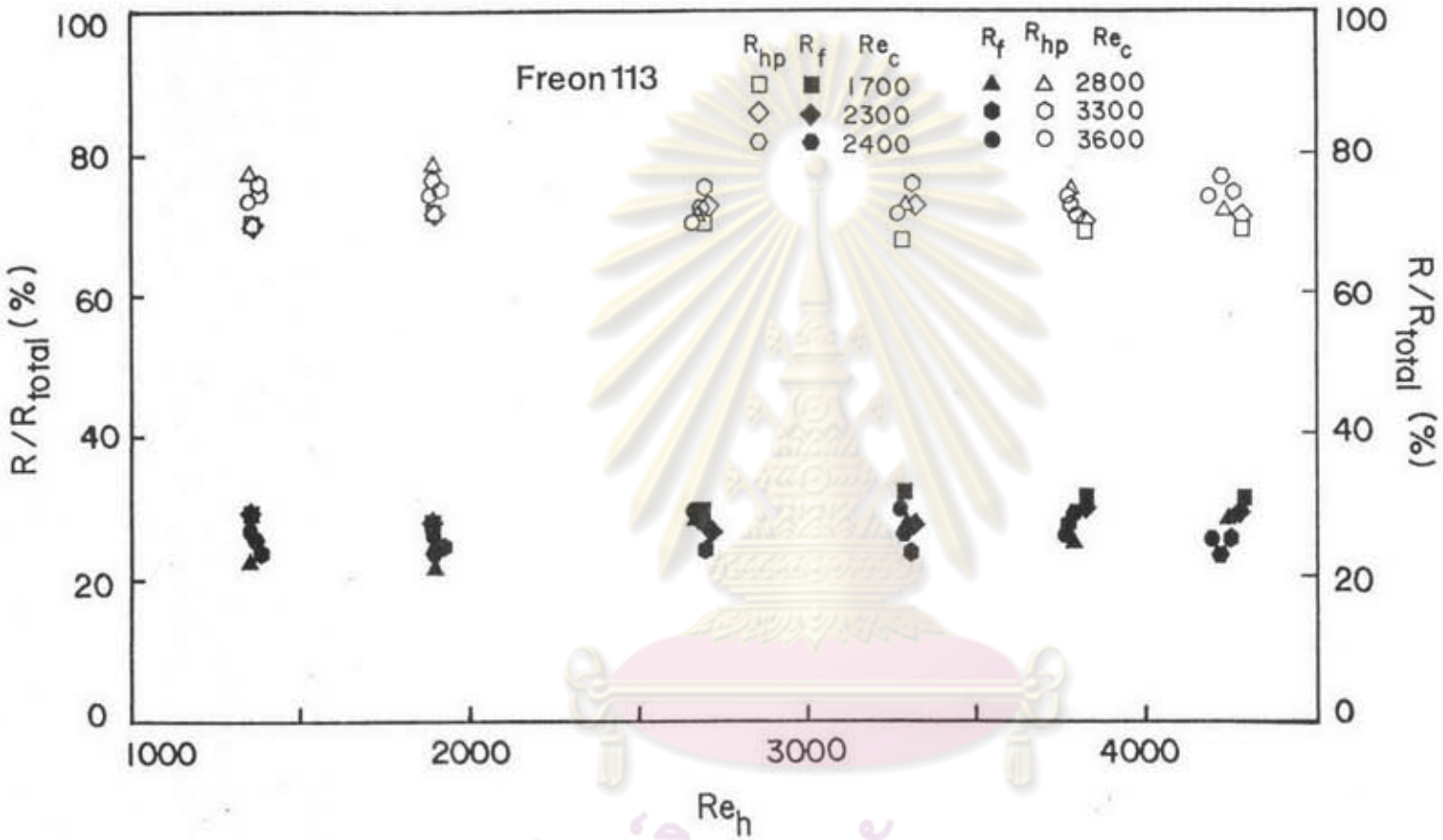

Figure 5.12 Ratio of heat pipe resistance and outside film resistance versus Reynolds number of hot water at various cold Reynolds numbers (tilt angle 50 degrees, T_h - T_c = 40-20 °C, fill ratio 30%).

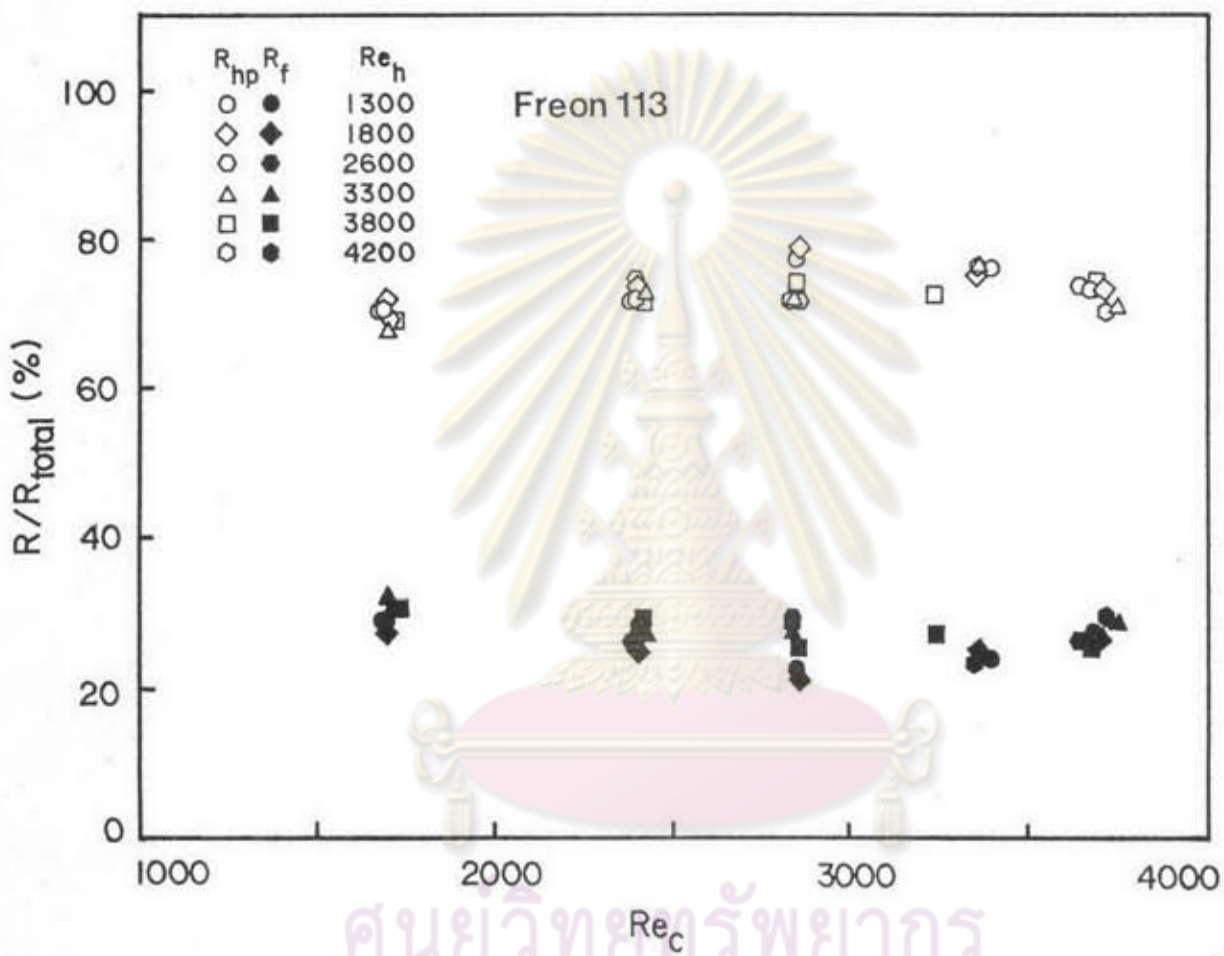

Figure 5.13 Ratio of heat pipe resistance and outside film resistance versus Reynolds number of cold water at various hot Reynolds numbers (tilt angle 50 degrees, T_h - T_c = 40-20 °C, fill ratio 30%).

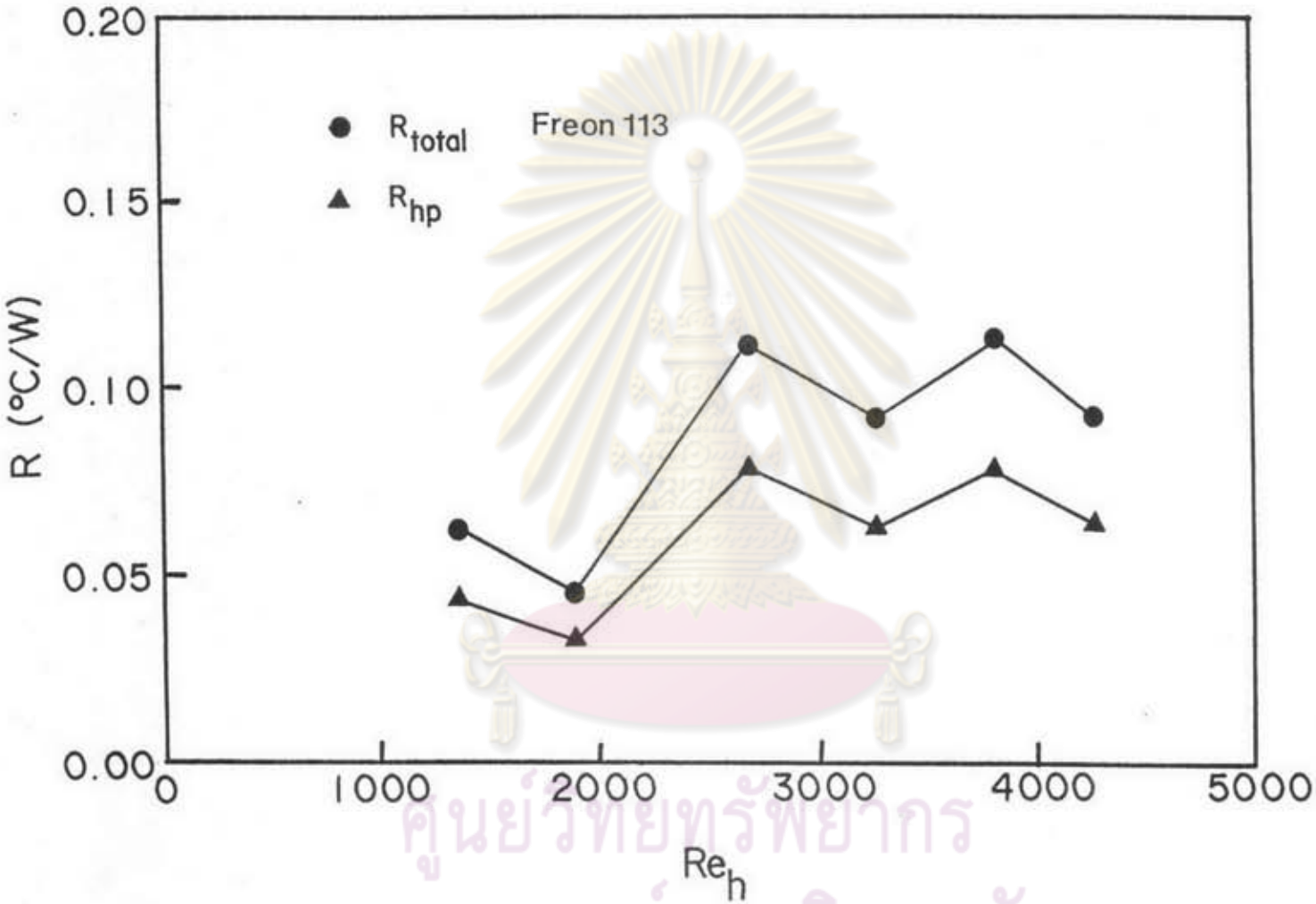

Figure 5.14 Total thermal resistance and heat pipe resistance versus Reynolds number of hot water (tilt angle 50 degrees, $T_h - T_c$ = 40-20 °C, fill ratio 30%, Re_c = 1,700).

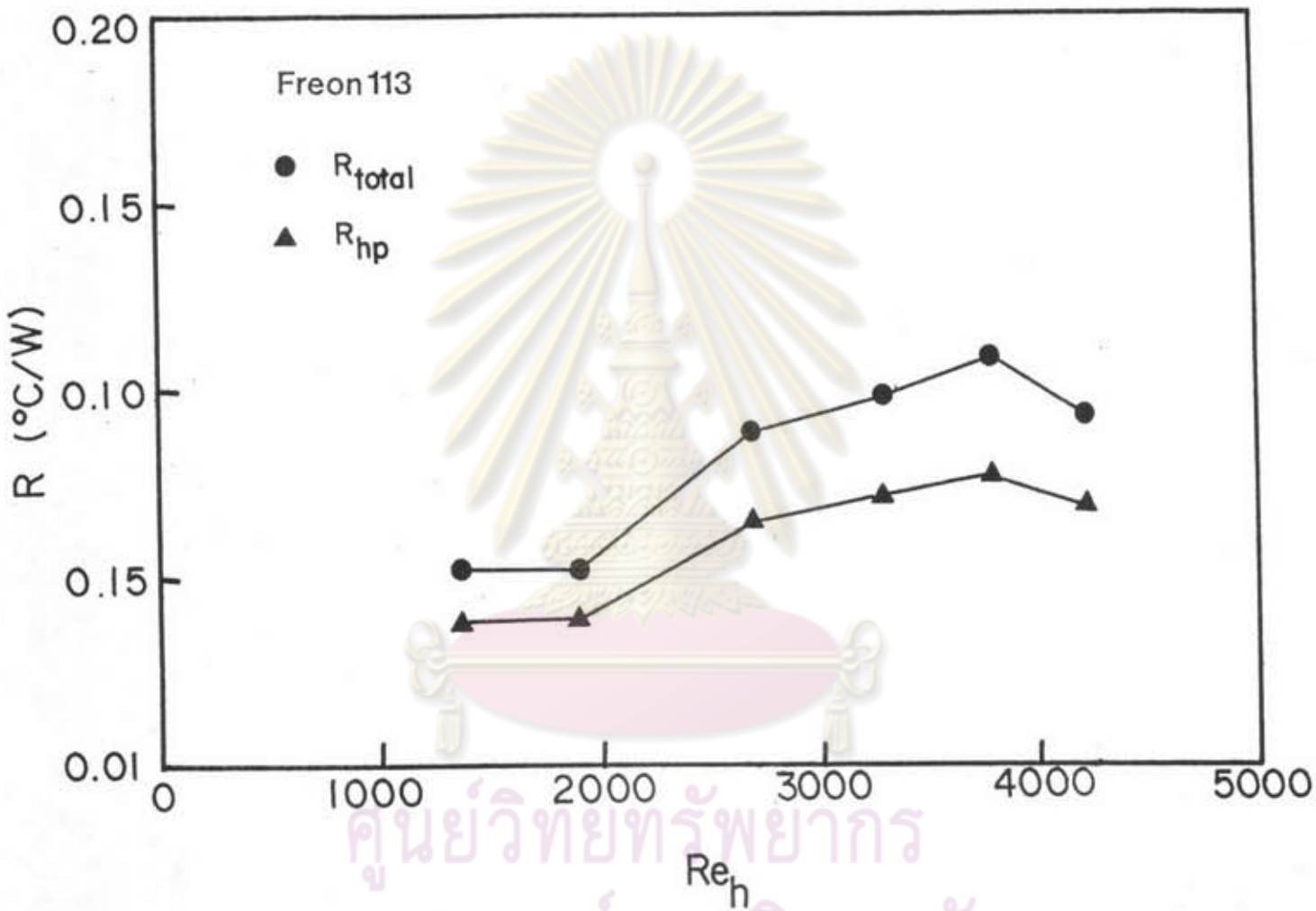

Figure 5.15 Total thermal resistance and heat pipe resistance versus Reynolds number of hot water (tilt angle 50 degrees, $T_h - T_c$ = 40-20 °C, fill ratio 30%, Re_c = 2,400).

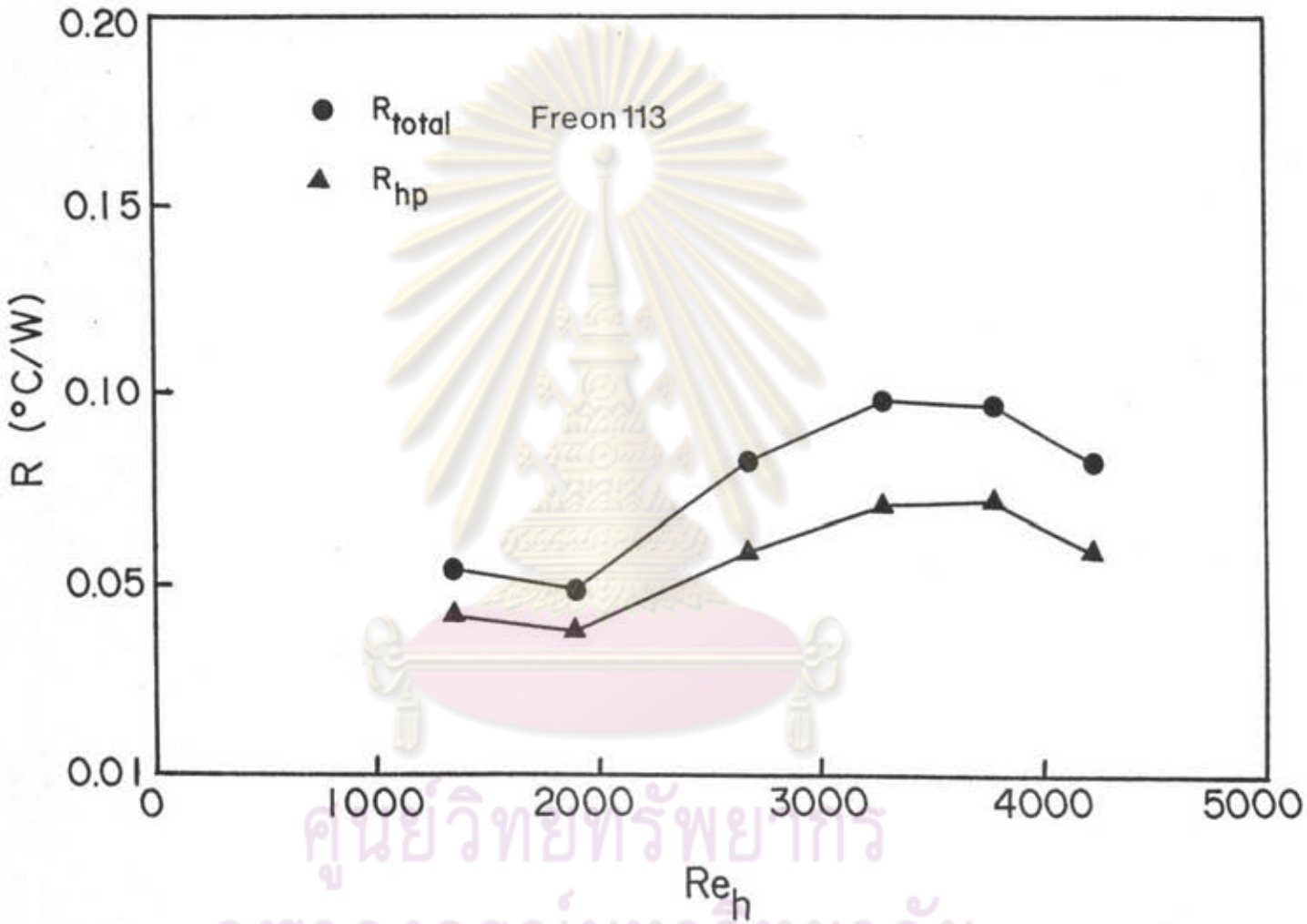

Figure 5.16 Total thermal resistance and heat pipe resistance versus Reynolds number of hot water (tilt angle 50 degrees, $T_h - T_c$ = 40-20 °C, fill ratio 30%, Re_c = 2,800).

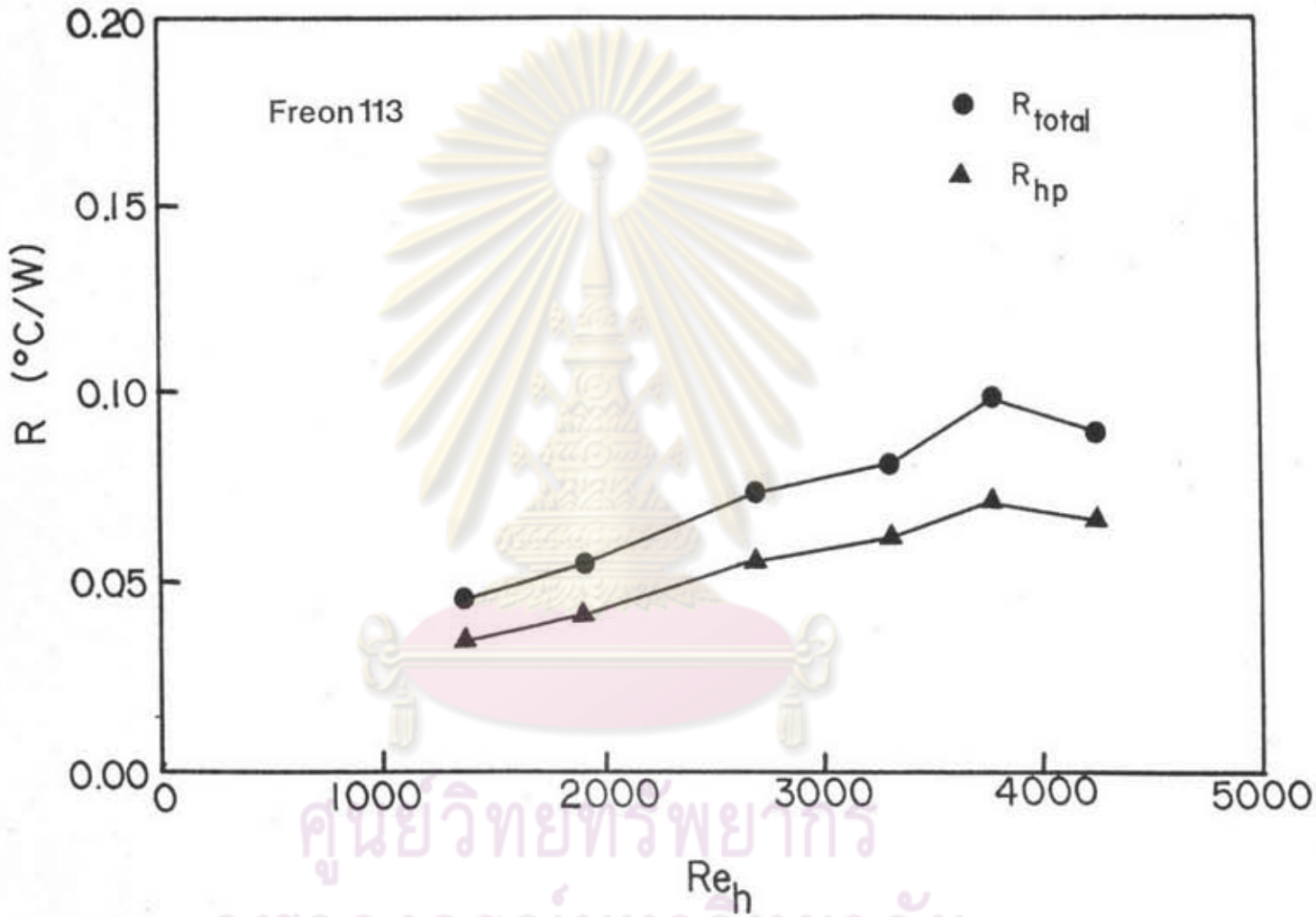

Figure 5.17 Total thermal resistance and heat pipe resistance versus Reynolds number of hot water (tilt angle 50 degrees, $T_h - T_c$ = 40-20 °C, fill ratio 30%, Re_c = 3,300).

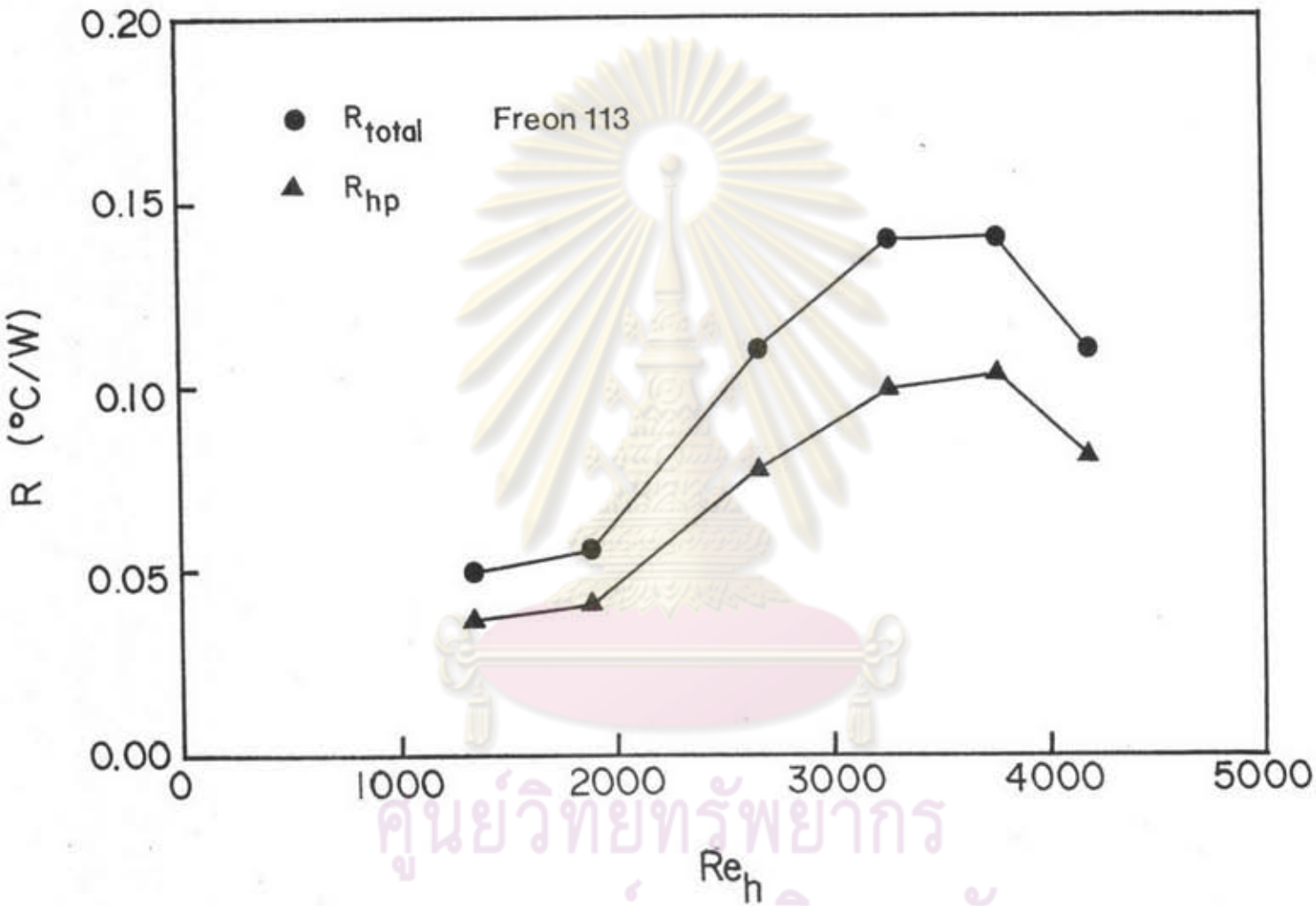

Figure 5.18 Total thermal resistance and heat pipe resistance versus Reynolds number of hot water (tilt angle 50 degrees, $T_h - T_c$ = 40-20 °C, fill ratio 30%, Re_c = 3,700).

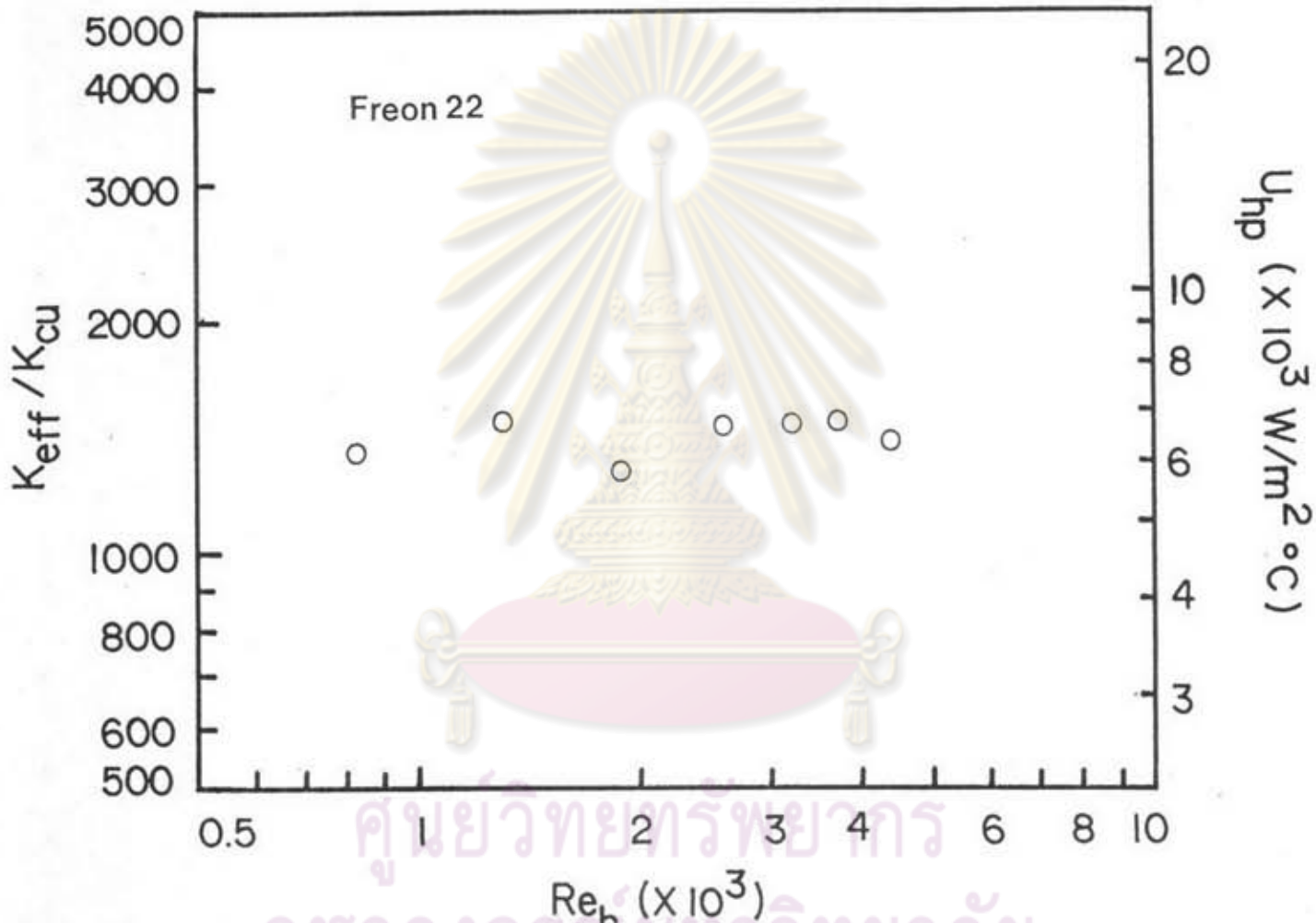

Figure 5.19 Ratio of effective thermal conductivity versus Reynolds number of hot water (tilt angle 50 degrees, $T_h - T_c$ = 40-20 °C, fill ratio 30%, Re_c = 3,600).

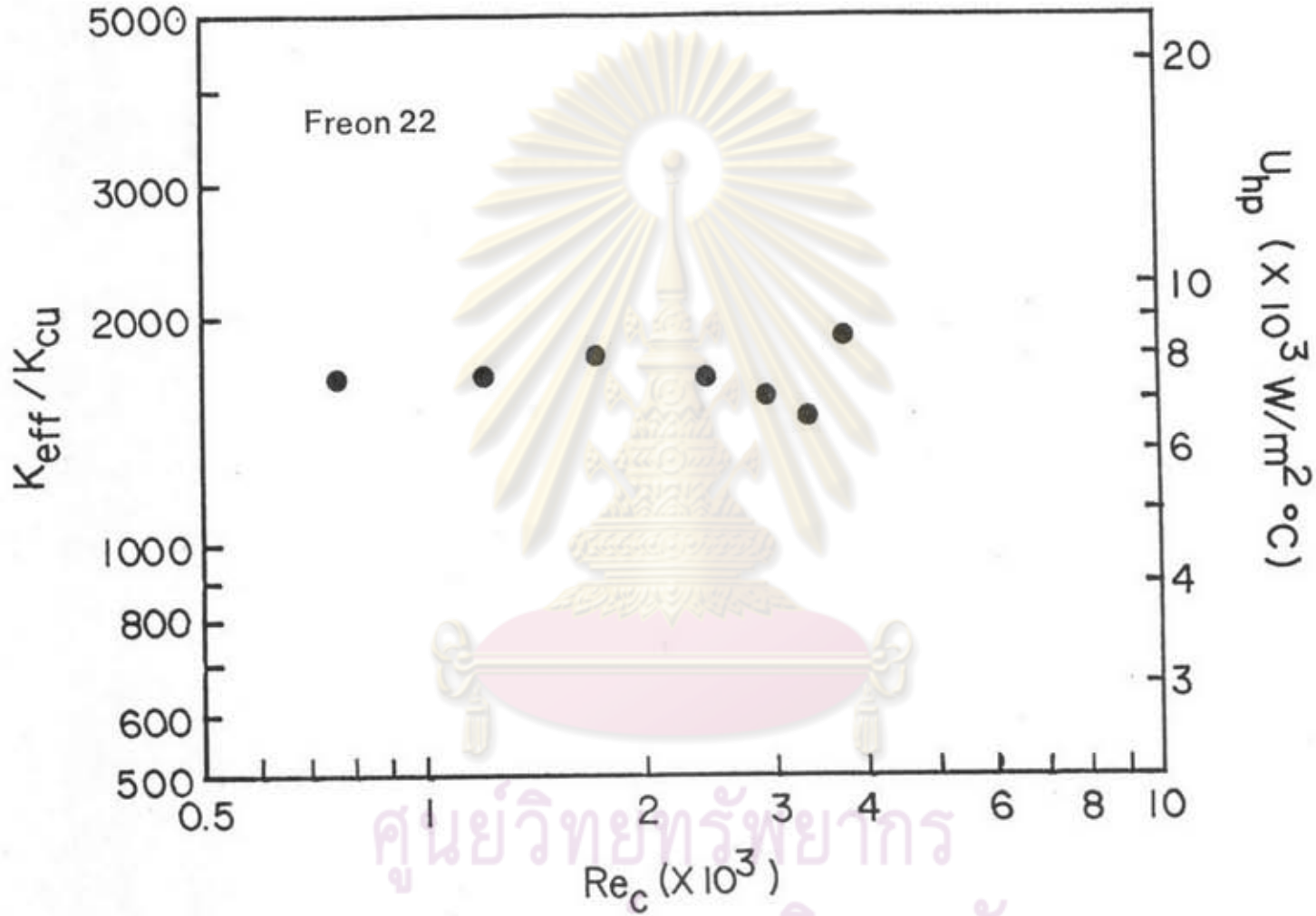

Figure 5.20 Ratio of effective thermal conductivity versus Reynolds number of cold water (tilt angle 50 degrees, $T_h - T_c$ = 40-20 °C, fill ratio 30%, Re_h = 4,200).

total and internal heat pipe resistances. We see that as the hot Reynolds number increases, the total and internal heat pipe resistances as well as the external resistances increase in such a manner that keeps the share of the outer film resistances as well as the internal resistances more or less constant.

Considering the distribution of surface temperature along the heat pipe (Figure 5.27), the temperatures within each section do not change much. Thus it may be concluded that the heat pipe is working properly. The reason that the share of the internal resistances is quite high is that the fill ratio is 30% and not an optimum. When the hot Reynolds number increases, the flow regime enters the transition region, thus adversely affecting the external resistances. This in turn causes the internal resistances to rise due to the changes in the surface temperatures.

The results for Freon-22 are similar to those of Freon-113, as can be seen in Figures 5.19-5.20.

5.5 Effect of Temperature Difference Across the Heat Pipe

Three values of the temperature difference were investigated to see their effects. For a temperature difference of 20°C, the hot water temperature is set at 40°C and the cold water temperature at 20°C; 35°C versus 25°C is used for a temperature difference of 10°C either 35 °C versus 30°C or 30°C versus 25°C is used for a temperature difference of 5°C. The results for Freon-113 are shown in Figures 5.21-5.23. Figure 5.21 shows the effect of temperature difference on the observed heat rate. Though the temperature difference of 20°C generally gives a higher heat rate than those of 10°C and 5°C, the trend is less clear when temperature differences of 5°C and 10 °C are

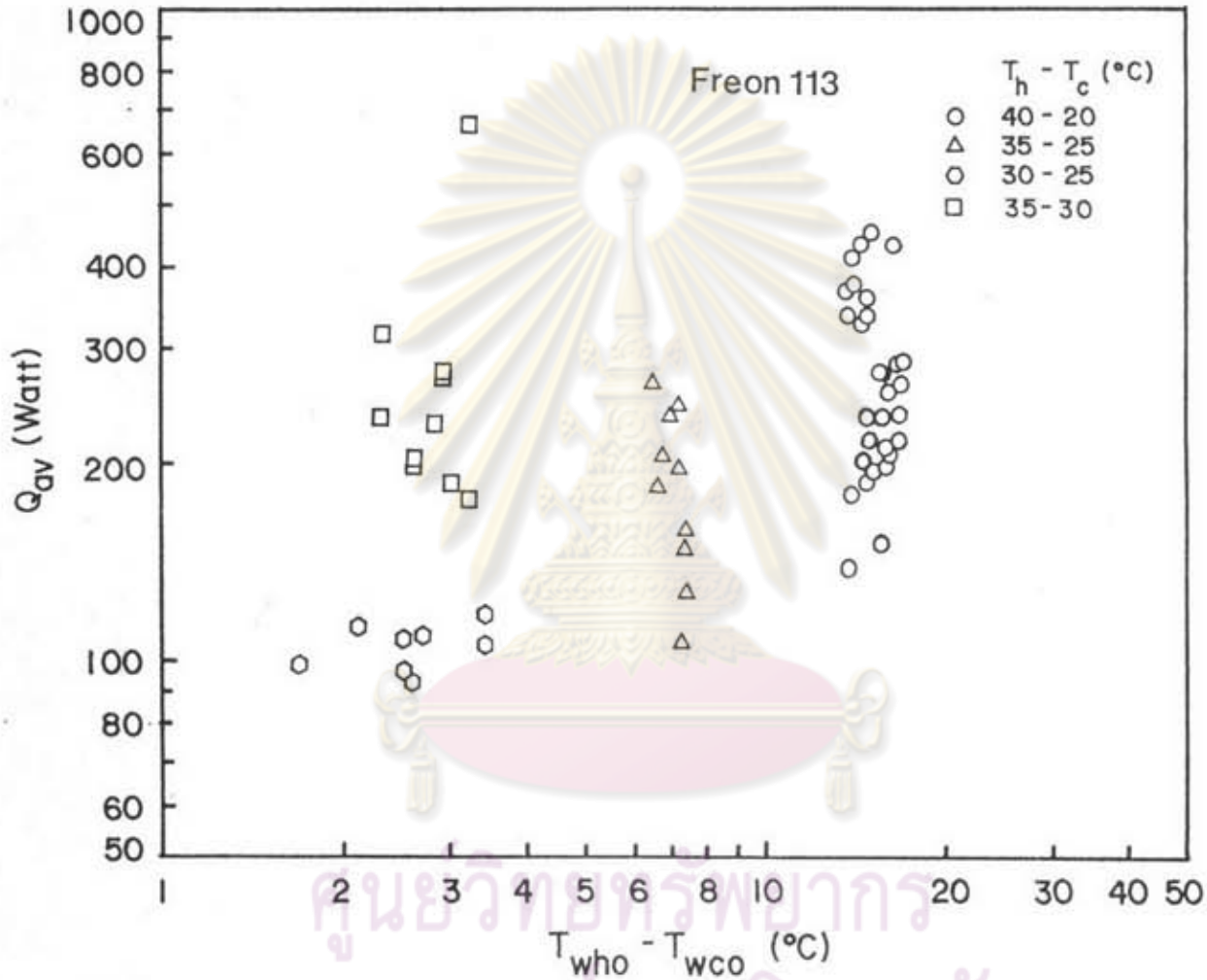

Figure 5.21 Heat transfer rate versus temperature difference between hot and cold surfaces for the case of Freon-113 (tilt angle 50 degrees, fill ratio 30%).

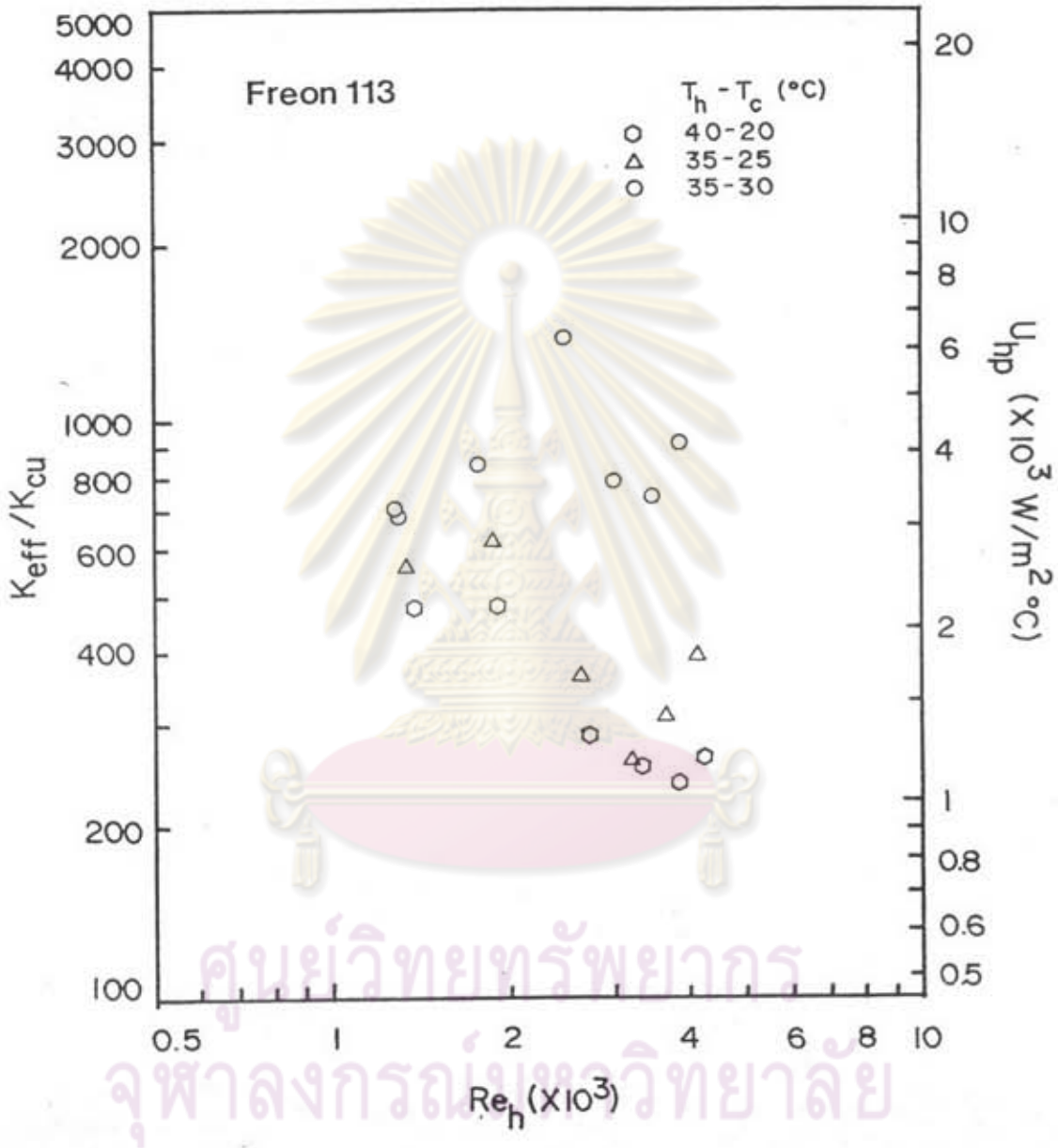

Figure 5.22 Ratio of effective thermal conductivity versus Reynolds number of hot water at varicus temperature differences between hot and cold sections (tilt angle 50 degrees, fill ratio 30%, Re_c = 2,500).

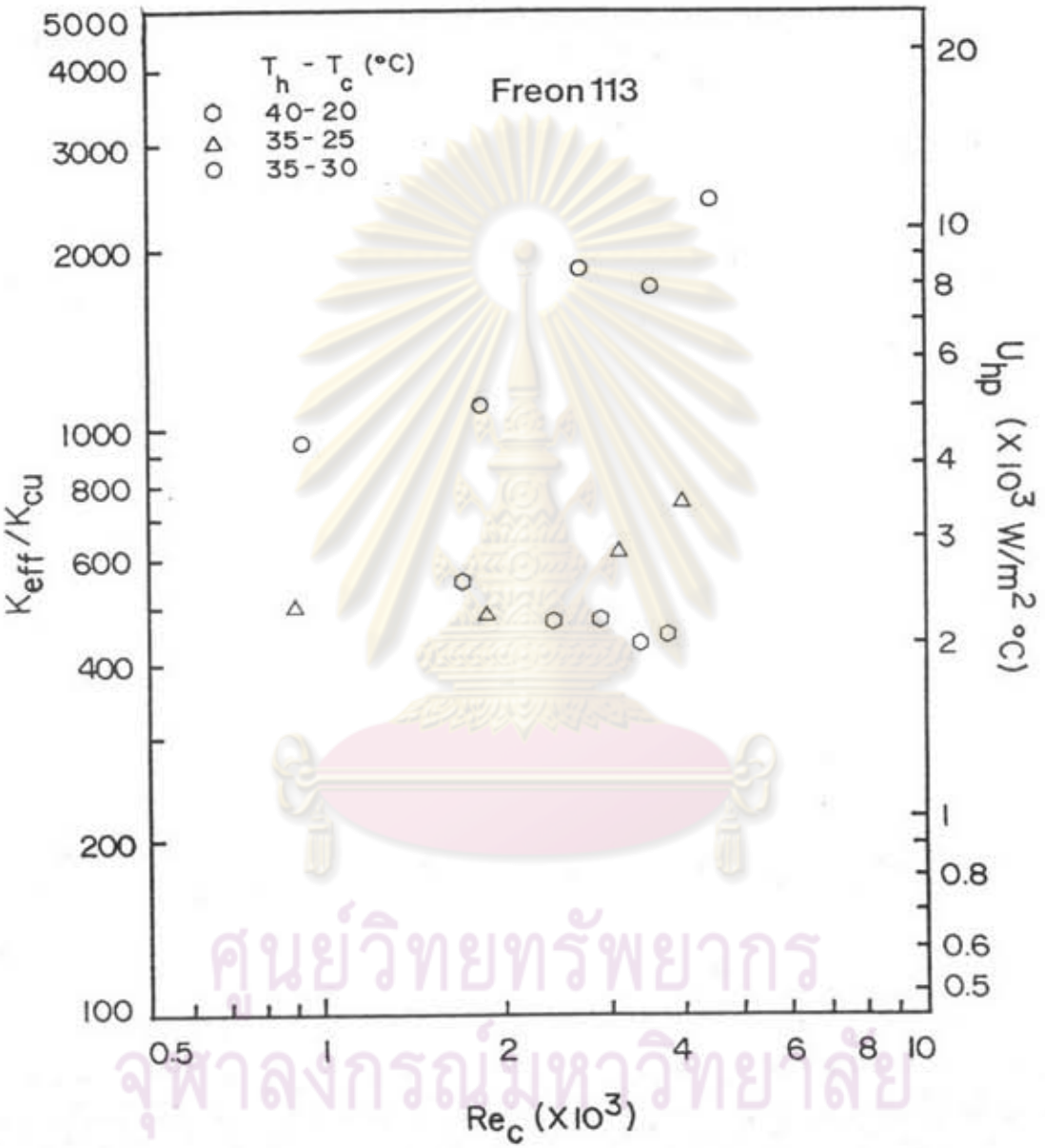

Figure 5.23 Ratio of effective thermal conductivity versus Reynolds number of cold water at various temperature differences between hot and cold sections (tilt angle 50 degrees, fill ratio 30%, Re_h = 1,900).

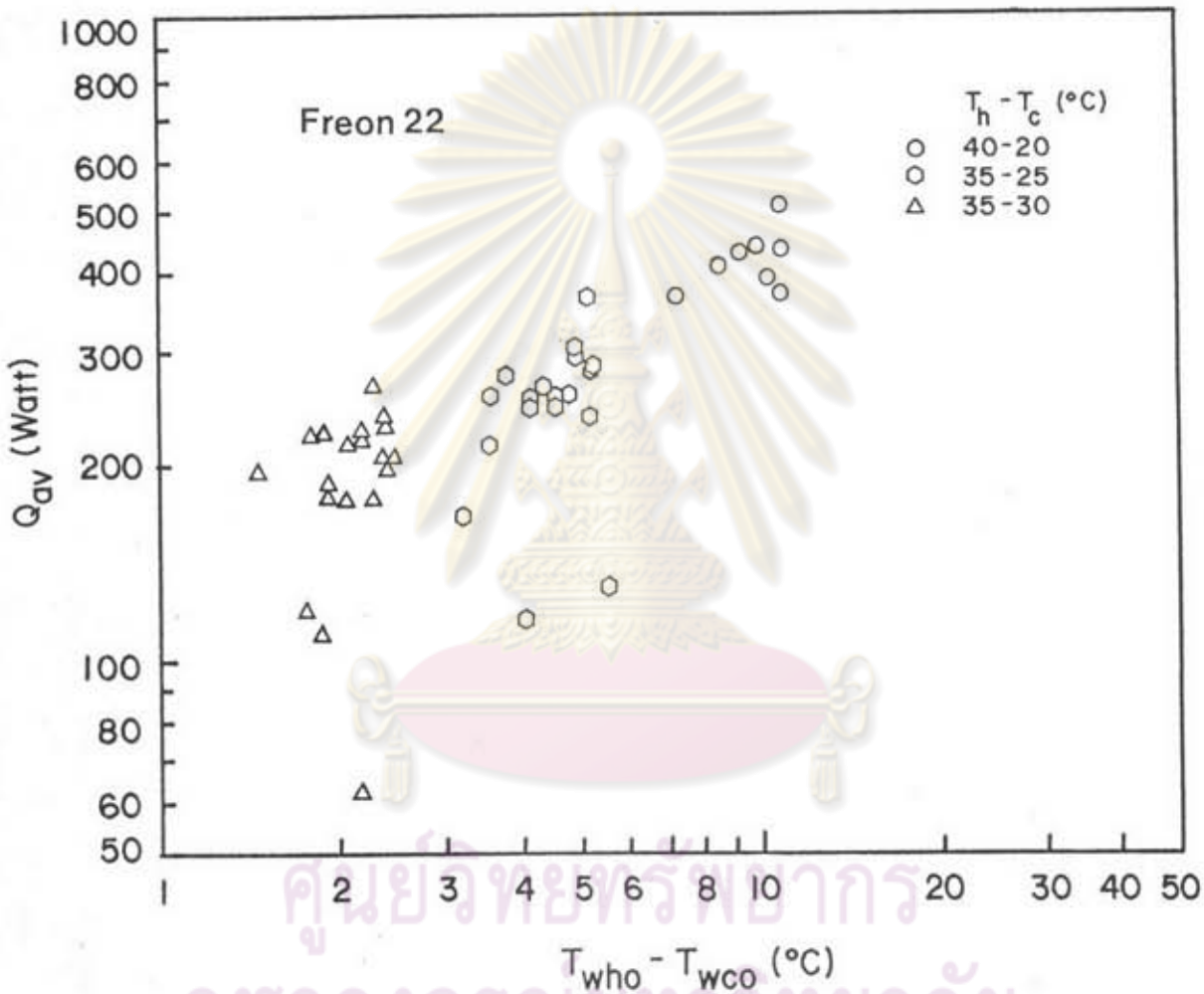

Figure 5.24 Heat transfer rate versus temperature difference between hot and cold surfaces in the case of Freon-22 (tilt angle 50 degrees, fill ratio 16.4%).

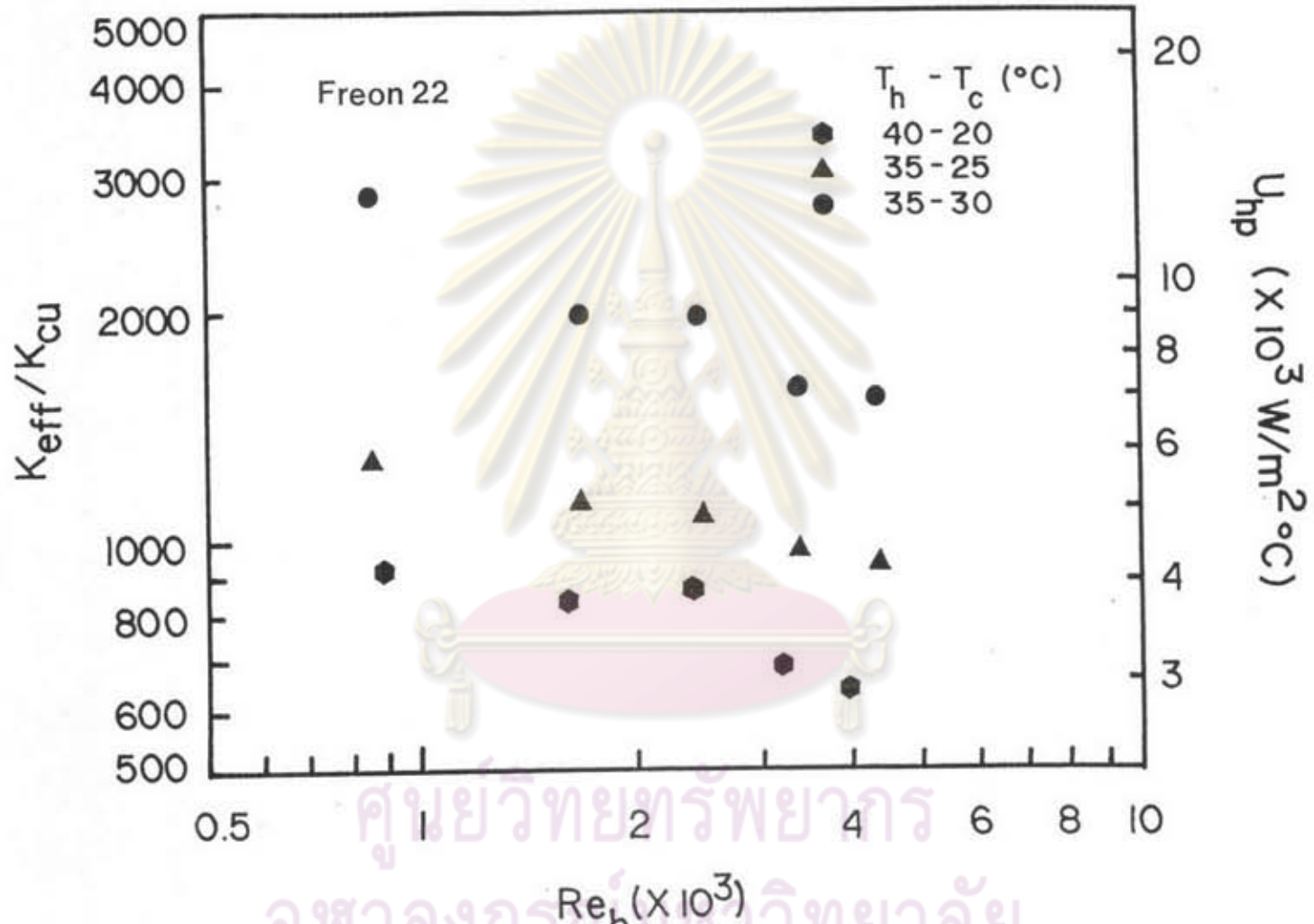

Figure 5.25 Ratio of effective thermal conductivity versus Reynolds number of hot water at various temperature differences between hot and cold sections (tilt angle 50 degrees, fill ratio 16.4%, Re_c = 3,000).

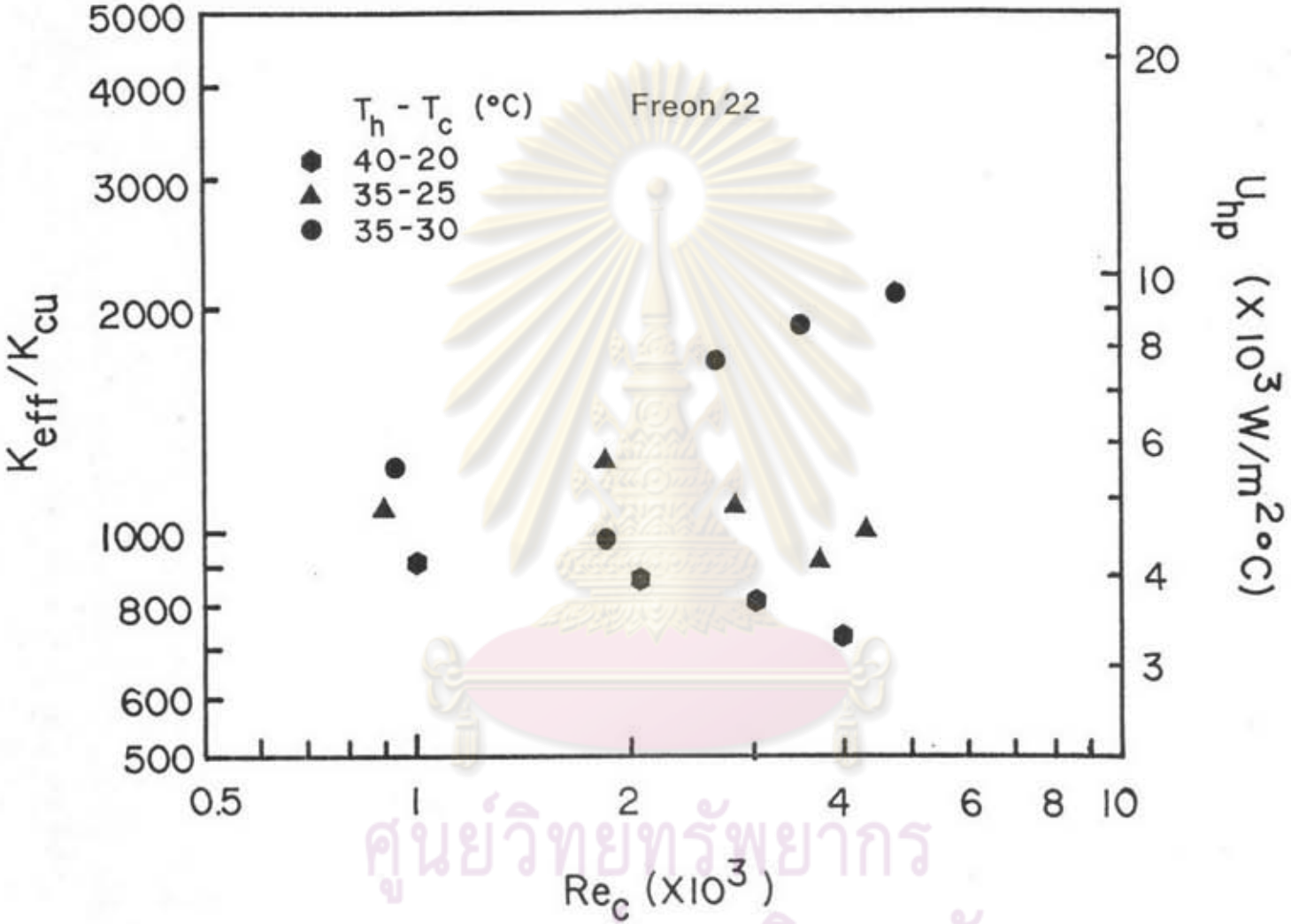

Figure 5.26 Ratio of effective thermal conductivity versus Reynolds number of cold water at various temperature differences between hot and cold sections (tilt angle 50 degrees, fill ratio 16.4%, Re_h = 1,800).

compared. In any case it is clear that the heat transfer rate does not increase linearly to the temperature driving force, but varies with ΔT^a where a is less than unity. Figures 5.22 and 5.23 clearly show that in terms of effective conductivity the temperature difference of 5 ^oC is best since $q \propto \Delta T^a$ and $a < 1$.

As shown in Figures 5.24-5.26, similar results are obtained for Freon-22.

5.6 Surface Temperature Distribution along the Heat Pipe

Surface temperature distribution along the heat pipe length is shown in Figures 5.27-5.32 for the case of Freon-113 and in Figures 5.33-5.35 for the case of Freon-22. It can be seen that the temperature distribution for different fill ratios has the same characteristics. For Freon-113 the distribution is more uniform than that of Freon-22, which is more scattered within each section.

5.7 Comparison with Published Results

Table 5.2 compares the optimum conditions obtained in the present study with those reported by other investigators.

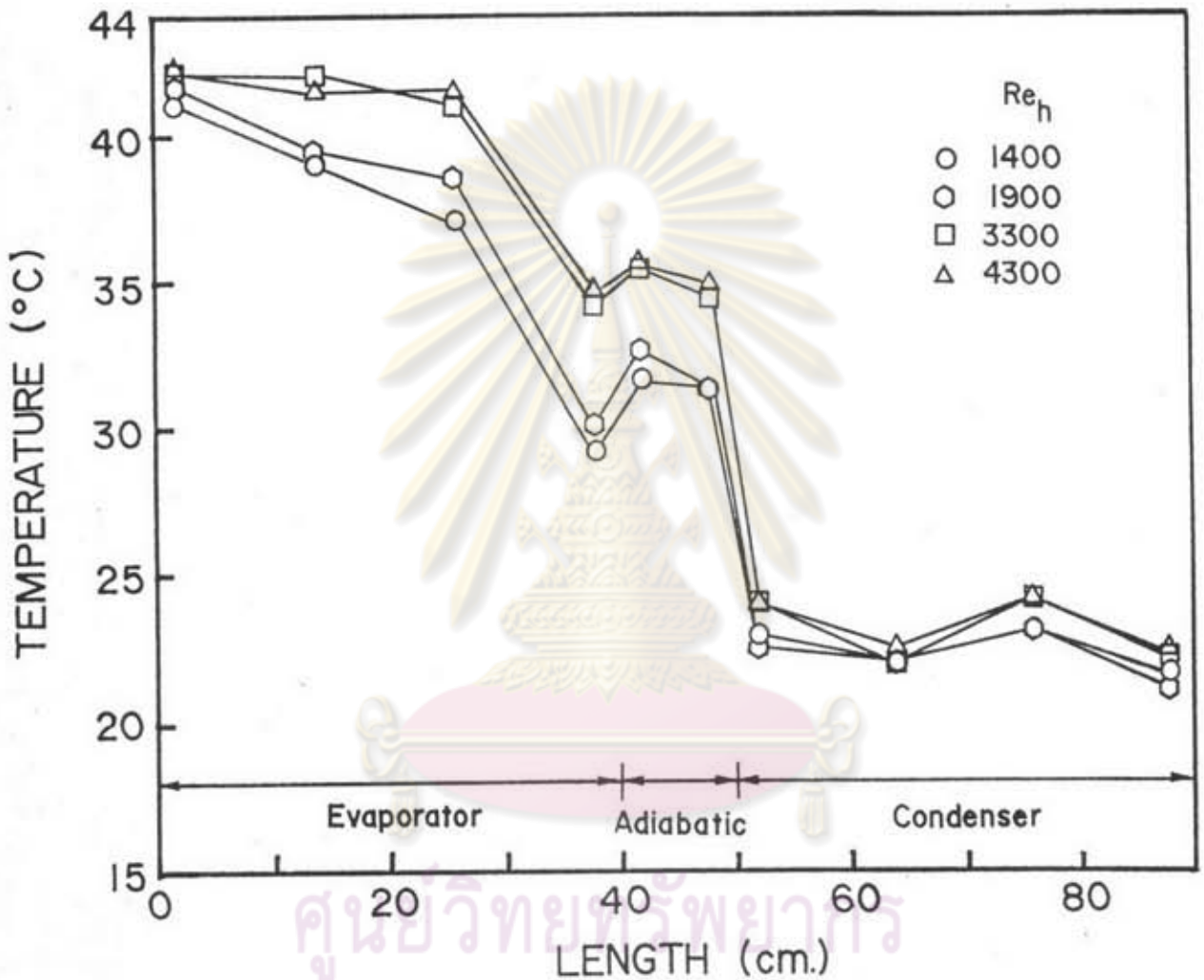

Figure 5.27 Temperature distribution along the heat pipe surface at various hot Reynolds numbers for the case of Freon-113 (Re_c = 2,400, tilt angle 50 degrees, $T_h - T_c$ = 40-20 °C, fill ratio 30%).

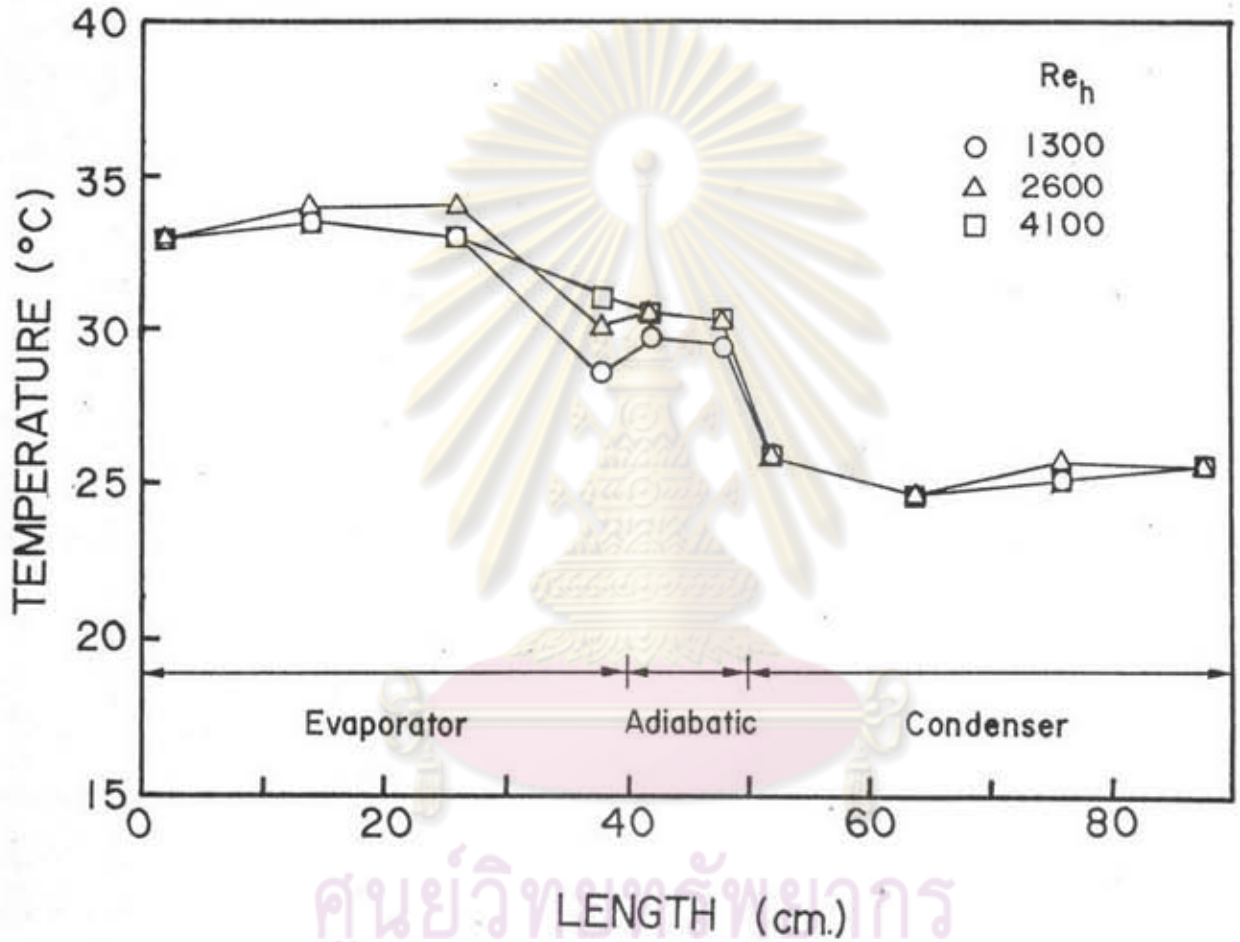

Figure 5.28 Temperature distribution along the heat pipe surface at various hot Reynolds numbers for the case of Freon-113 (Re_c = 2,500, tilt angle 50 degrees, $T_h - T_c$ = 35-25 °C, fill ratio 30%).

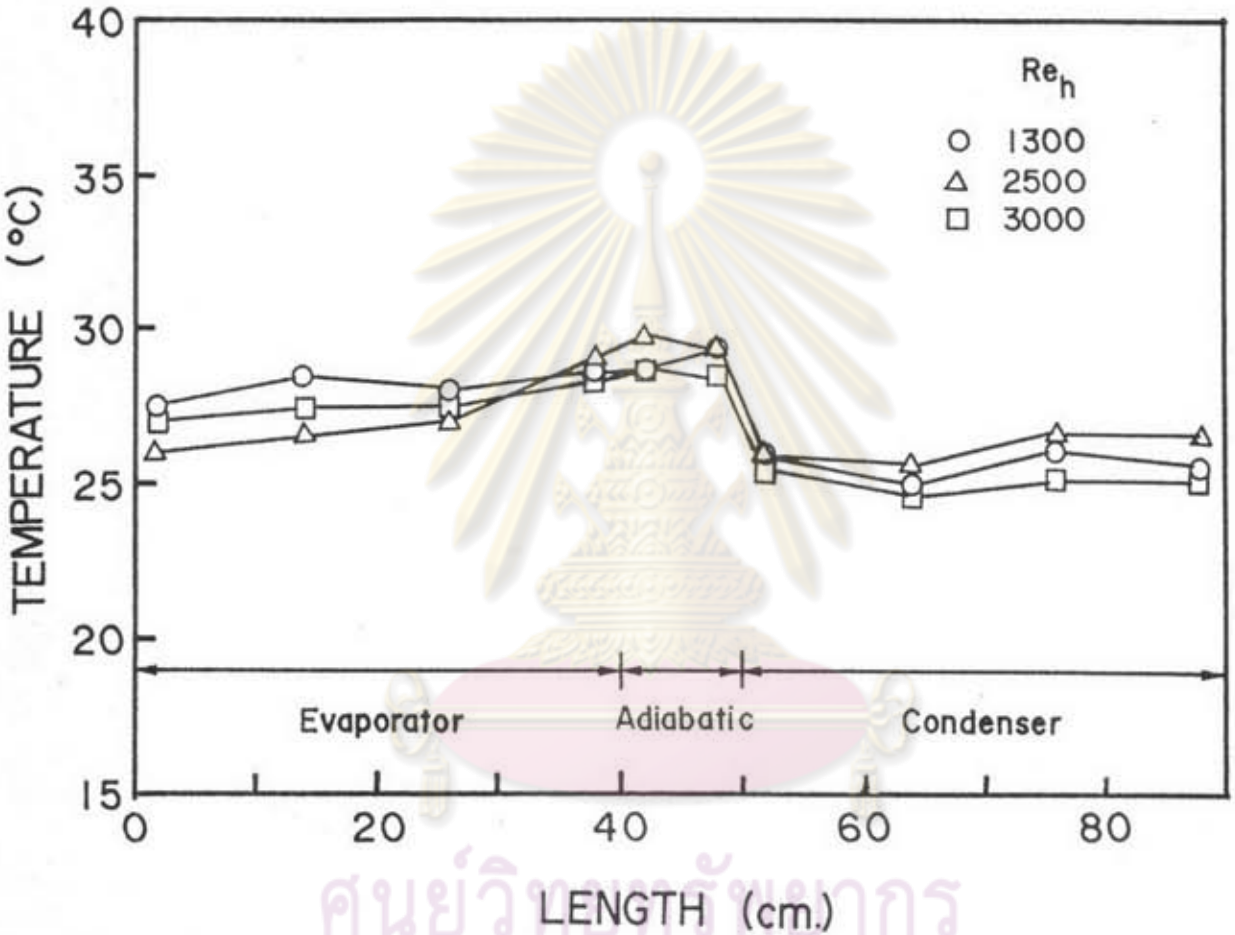

Figure 5.29 Temperature distribution along the heat pipe surface at various hot Reynolds numbers for the case of Freon-113 (Re_c = 2,500, tilt angle 50 degrees, $T_h - T_c$ = 30-25 °C, fill ratio 30%).

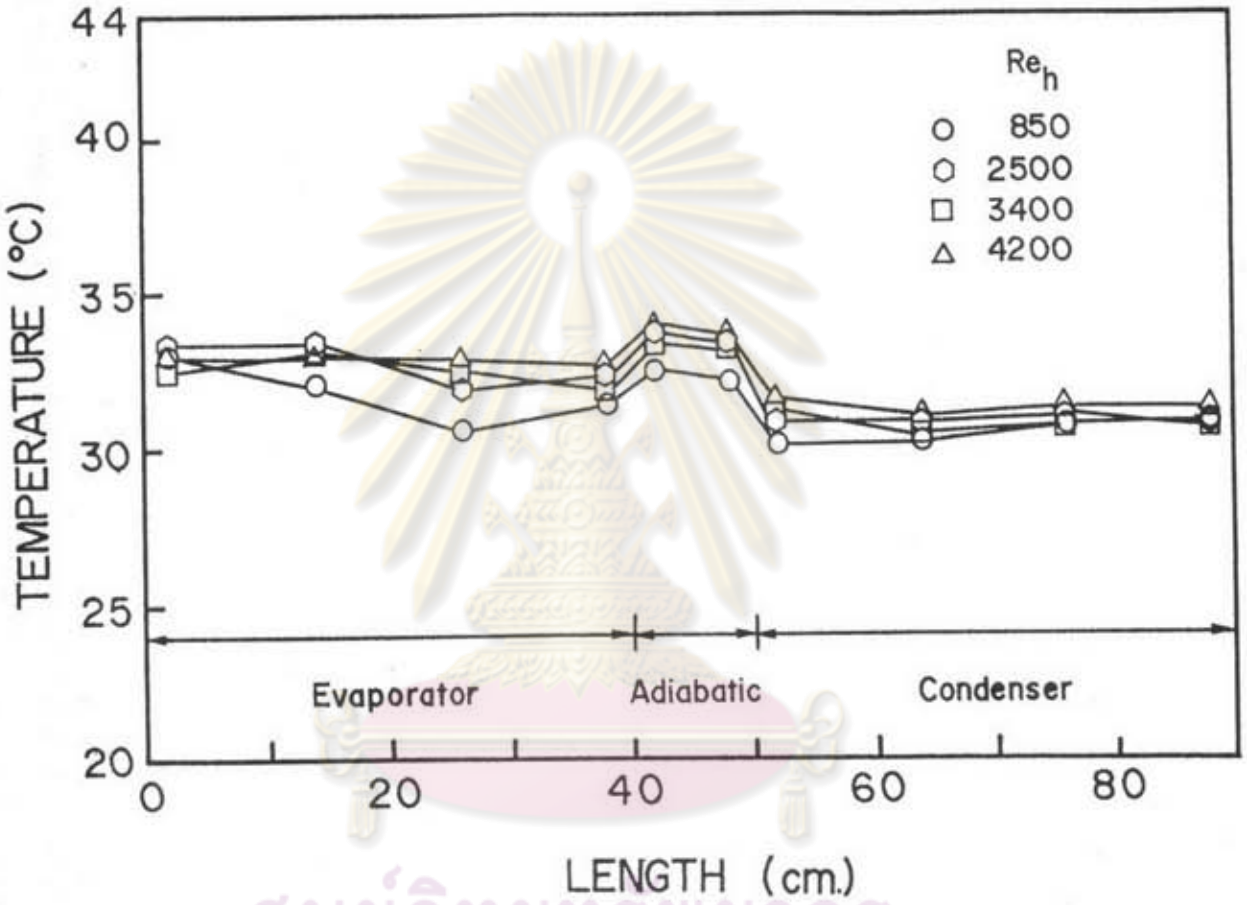

Figure 5.30 Temperature distribution along the heat pipe surface at various hot Reynolds numbers for the case of Freon-113 (Re_c = 4,400, tilt angle 50 degrees, $T_h - T_c$ = 35-30 °C, fill ratio 18.5%).

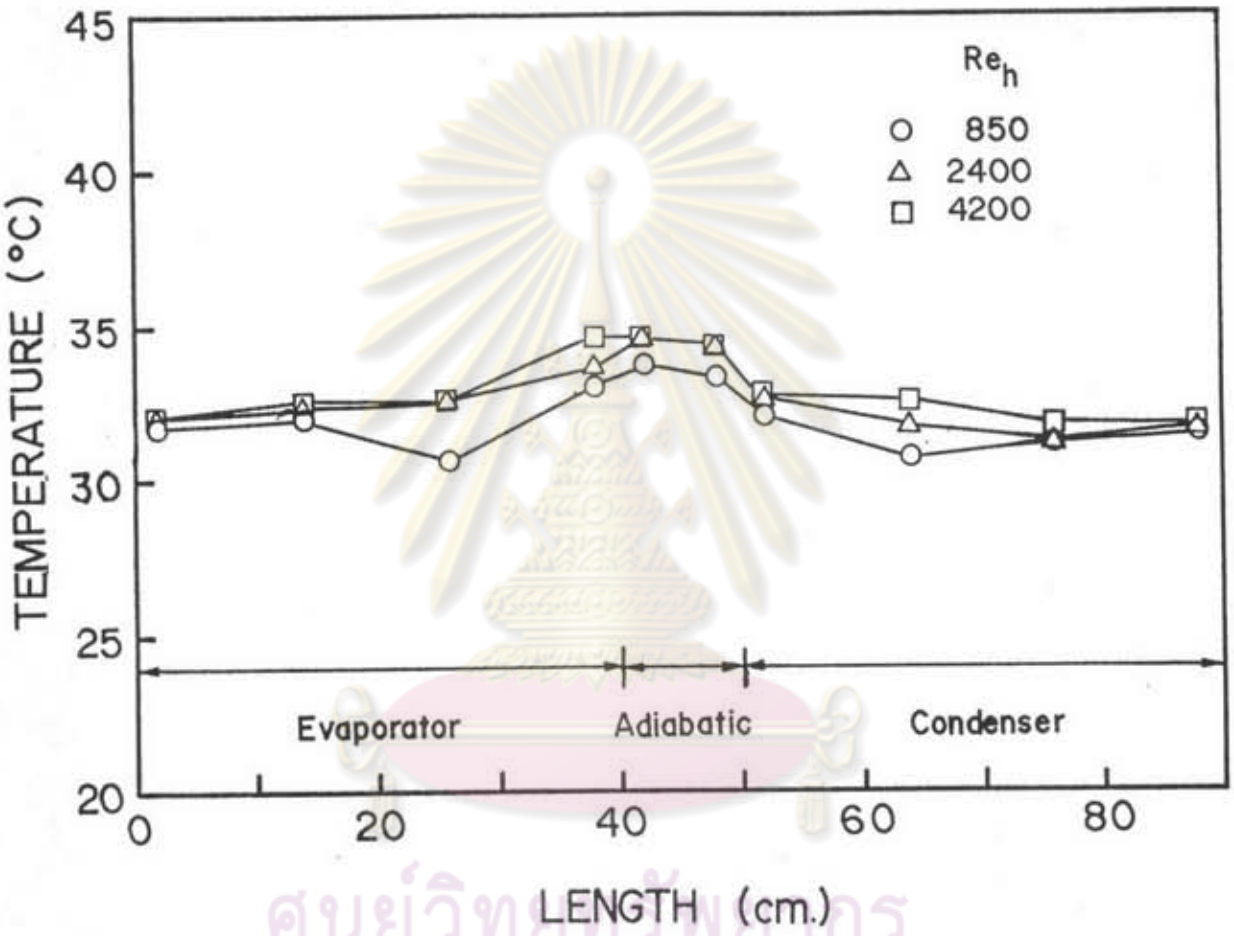

Figure 5.31 Temperature distribution along the heat pipe surface at various hot Reynolds numbers for the case of Freon-113 (Re_c = 4,400, tilt angle 50 degrees, $T_h - T_c$ = 35-30 °C, fill ratio 9.3%).

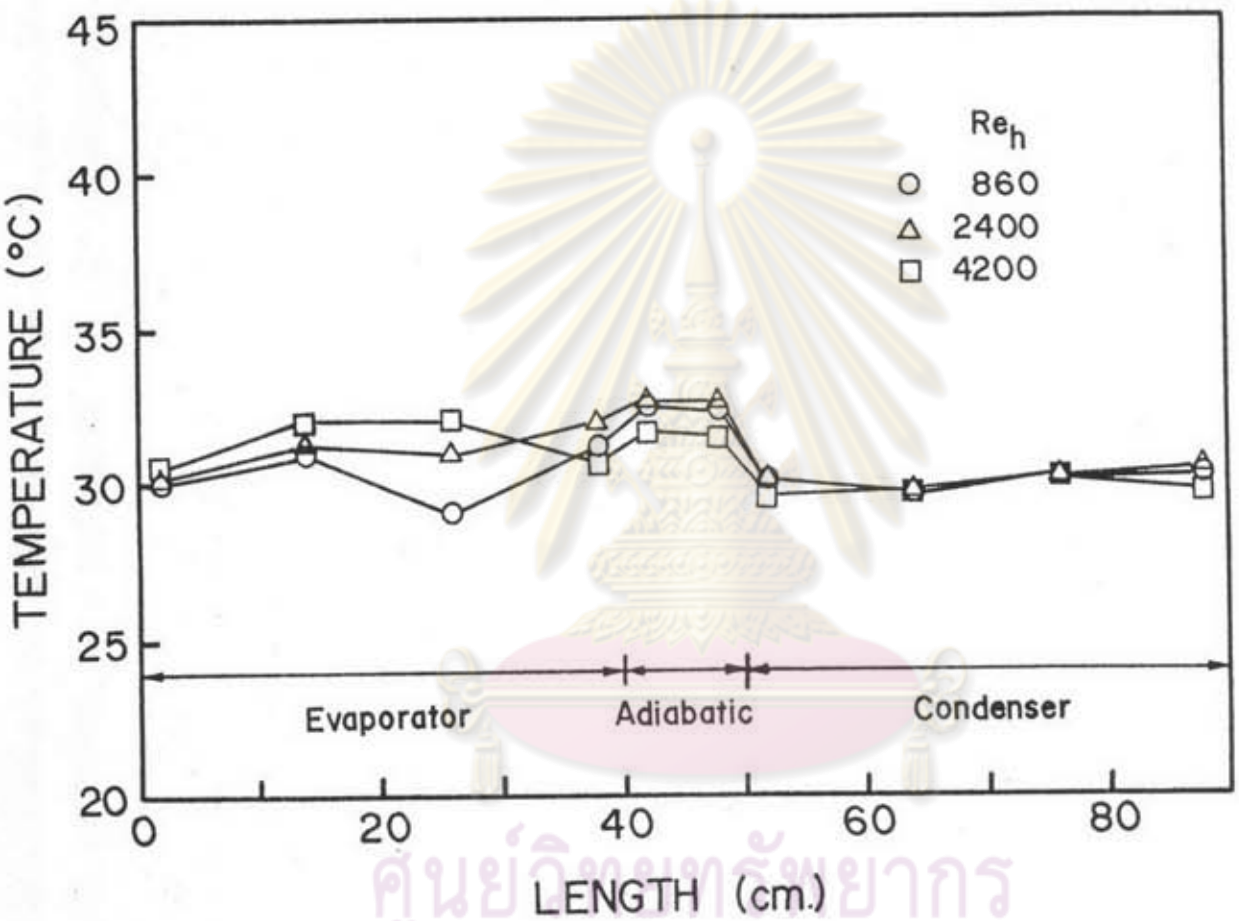

Figure 5.32 Temperature distribution along the heat pipe surface at various hot Reynolds numbers for the case of Freon-113 (Re_c = 4,400, tilt angle 50 degrees, $T_h - T_c$ = 35-30 °C, fill ratio 4.9%).

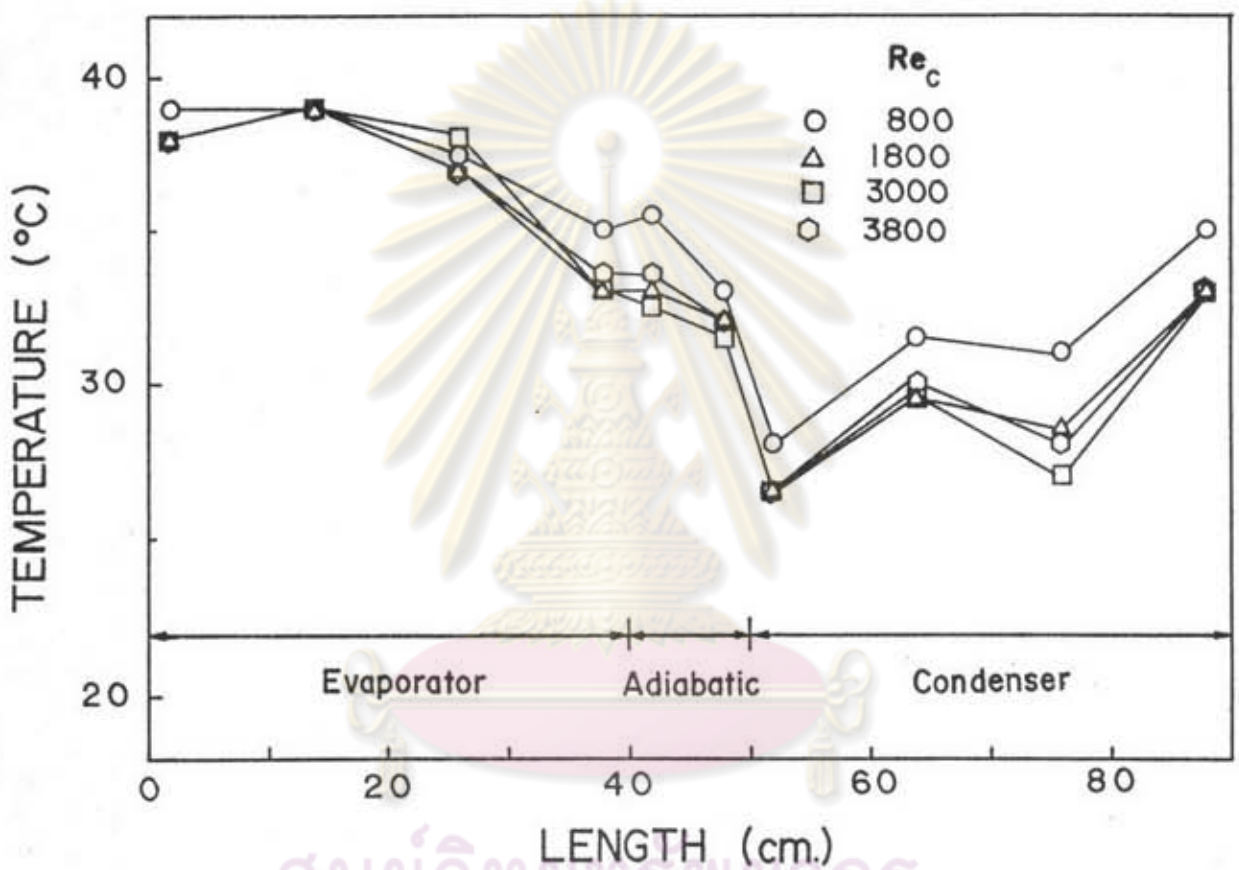

Figure 5.33 Temperature distribution along the heat pipe surface at various hot Reynolds numbers for the case of Freon-22 (Re_c = 5,300, tilt angle 50 degrees, $T_h - T_c$ = 40-20 °C, fill ratio 30%).

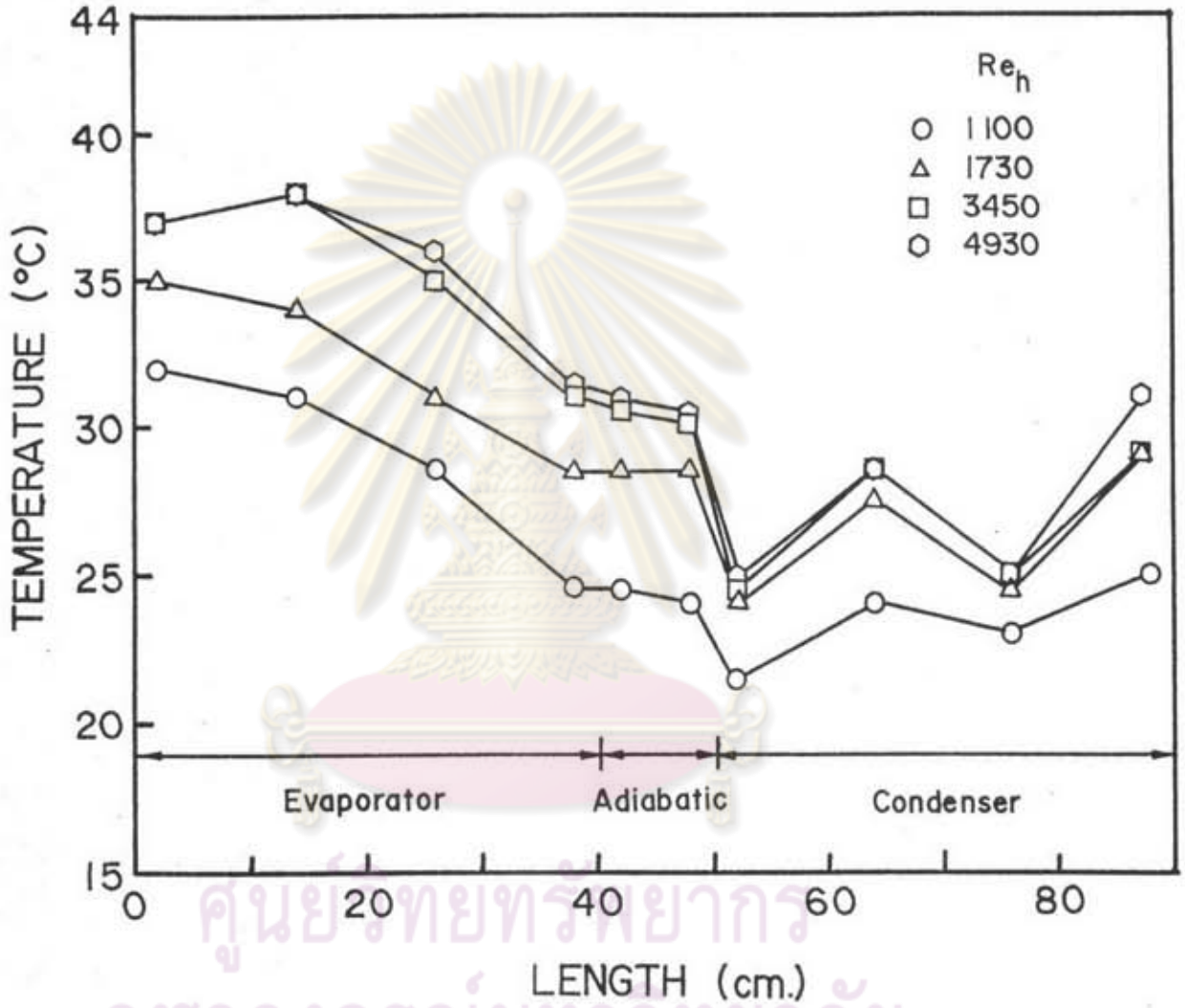

Figure 5.34 Temperature distribution along the heat pipe surface at various hot Reynolds numbers for the case of Freon-22 (Re_c = 3,400, tilt angle 50 degrees, $T_h - T_c$ = 35-25 °C, fill ratio 30%).

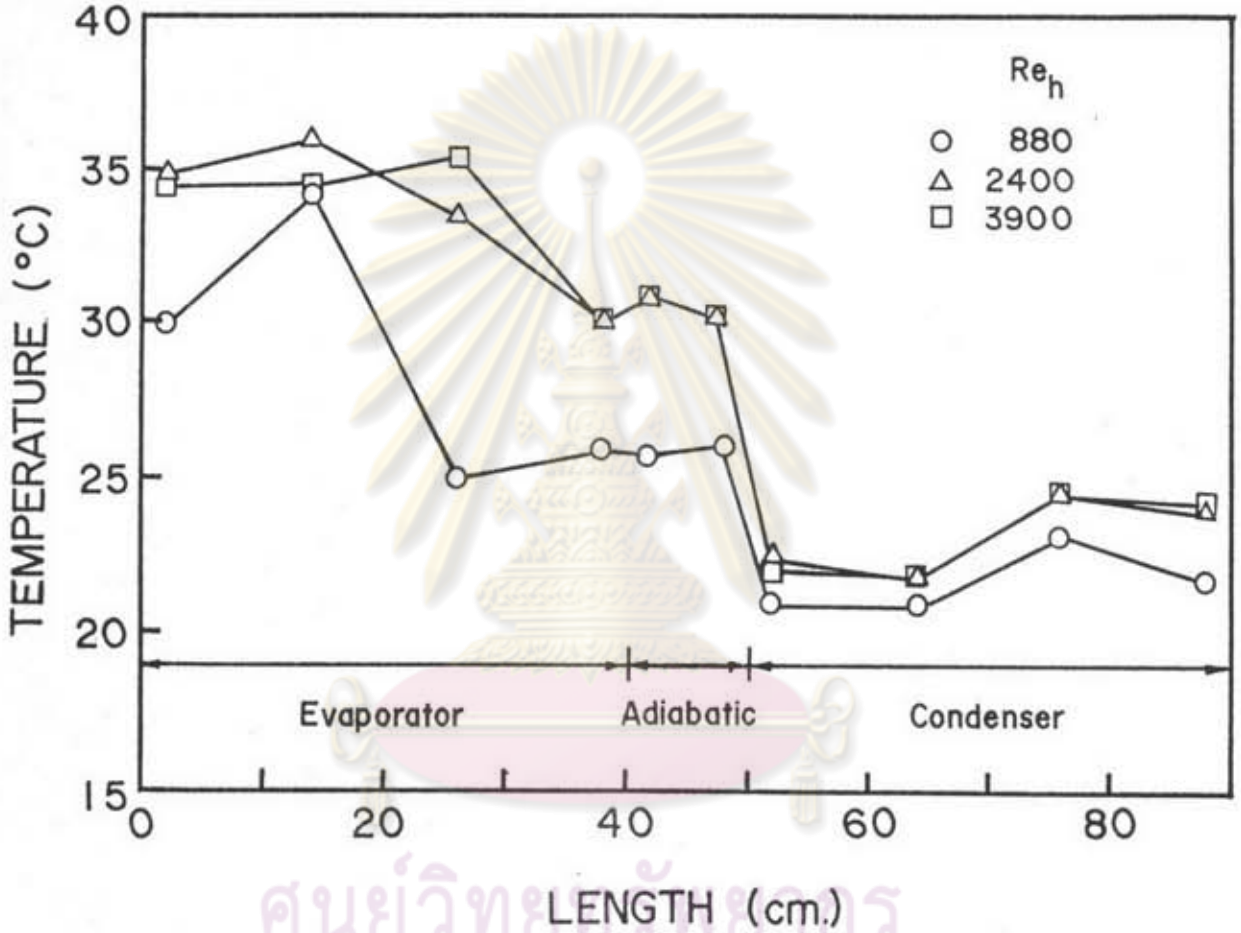

Figure 5.35 Temperature distribution along the heat pipe surface at various hot Reynolds numbers for the case of Freon-22 (Re_c = 3,000, tilt angle 50 degrees, $T_h - T_c$ = 40-20 °C, fill ratio 16.4%).

Table 5.2 Comparison of the present results with published results

Dimension	Working Fluid	Optimum Fill	Optimum Tilt
Copper tube I.D. 13 mm. Length 33 cm. Thickness 1 mm. (18)	Water	25-60% of evaporator volume	20-40 ^{o} from horizontal
Steel tube I.D. 4 cm. Length 2 m. Thickness 2 mm. (45)	Freon-115	-	40-45 ^{o} from vertical 45-50 ^{o} from horizontal
Aluminum alloy tube (axially grooved) I.D. 12 mm. Length 1 m. Thickness 4 mm. (16)	Freon-12	-	> 30 ^{o} from horizontal
Carbon steel tube I.D. 12 mm. Length 2 m. Thickness 2 mm.(20)	Methanol	3 % of total volume	40-60 ^{o} from horizontal

Table 5.2 (cont.) Comparison of the present results with published results

Dimension	Working Fluid	Optimum Fill	Optimum Tilt
Brass tube O.D. 32 mm. Length 2 m. Thickness 2 mm. (20)	Acetone	12 % of total volume	40 ° from horizontal
Stainless steel tube (axially grooved) O.D. 25.5 mm. Length 42.5 cm. (21)	Water	-	12-18 ° from horizontal
Steel pipe O.D. 3/4 " Length 21 ft. (22)	Water Freon-113 Methanol	18-22 % of total volume	-
The present study	Freon-113	9.3-18.5 % of total volume	50 ° from horizontal
	Freon-22	30 % of total volume	50 ° from horizontal

It can be seen from Table 5.2 that the optimum tilt angle obtained in the present study is 50 ^{o} from the horizontal while most of those reported by other investigators are in the range of 40-60 ^{o}, except for the stainless steel heat pipe with water as working fluid. It can be said that the optimum tilt angle in the present study agrees well with other published results.

In the case of optimum fill ratio of Freon-113, the present results also agree with those of steel pipe with water, Freon-113 and methanol as working fluid. But in the case of Freon-22, the optimum fill ratio is rather large. This indicates that the required amount of working fluid not only depends on the physical properties of working fluid but also depends on the tube geometry and the operating conditions. To design the heat pipe for using in other conditions, the optimum fill ratio should be obtained from the experiments.

5.8 Heat Transfer Correlations for the Present Single Heat Pipe

a. Inside Evaporator Section

The heat transfer mechanisms in the evaporator section are surface evaporation from a thin film and pool boiling. In the present study, the liquid fill charge ranges from moderate to large, so pool boiling should have an important role. The correlations obtained in this study are in the form of Rohsenow's pool boiling correlations as shown below:

$$\frac{C_p(T_{whi}-T_s)}{\lambda\, Pr^s} = C_{sf}\left[\frac{Q/A}{\mu\lambda}\sqrt{\frac{6g_c}{g(\rho-\rho_v)}}\right]^r \qquad (5.1)$$

Here the constant C_{sf} and exponent r have been obtained by the (logarithmic) least square method.

For Freon-113 (tilt angle 50 degrees, fill ratio 30 %) (see Figure 5.36)

$$C_{sf} = 7.021 \times 10^{-3}$$

$$r = 0.962$$

For Freon-22 (tilt angle 50 degrees, fill ratio 16.4 %) (see Figure 5.37)

$$C_{sf} = 5.654 \times 10^{-3}$$

$$r = 1.069$$

b. Inside the Condenser Section

In other studies, the Nusselt's film condensation correlations may be used to predict the heat transfer coefficient in the condenser section. In the present study, however, the inside surface of the copper tube is spirally grooved, so new correlations have to be found. Applying the least square fit method to the experimental data, the following correlations are obtained.

For Freon-113 (tilt angle 50 degrees, fill ratio 30%) (see Figure 5.38)

$$h_{ic} = 1.705 \times 10^{-6} \left[\frac{g \rho (\rho - \rho_v) \lambda k^3}{\mu (T_s - T_{wci}) L_h} \right]^{0.744}$$

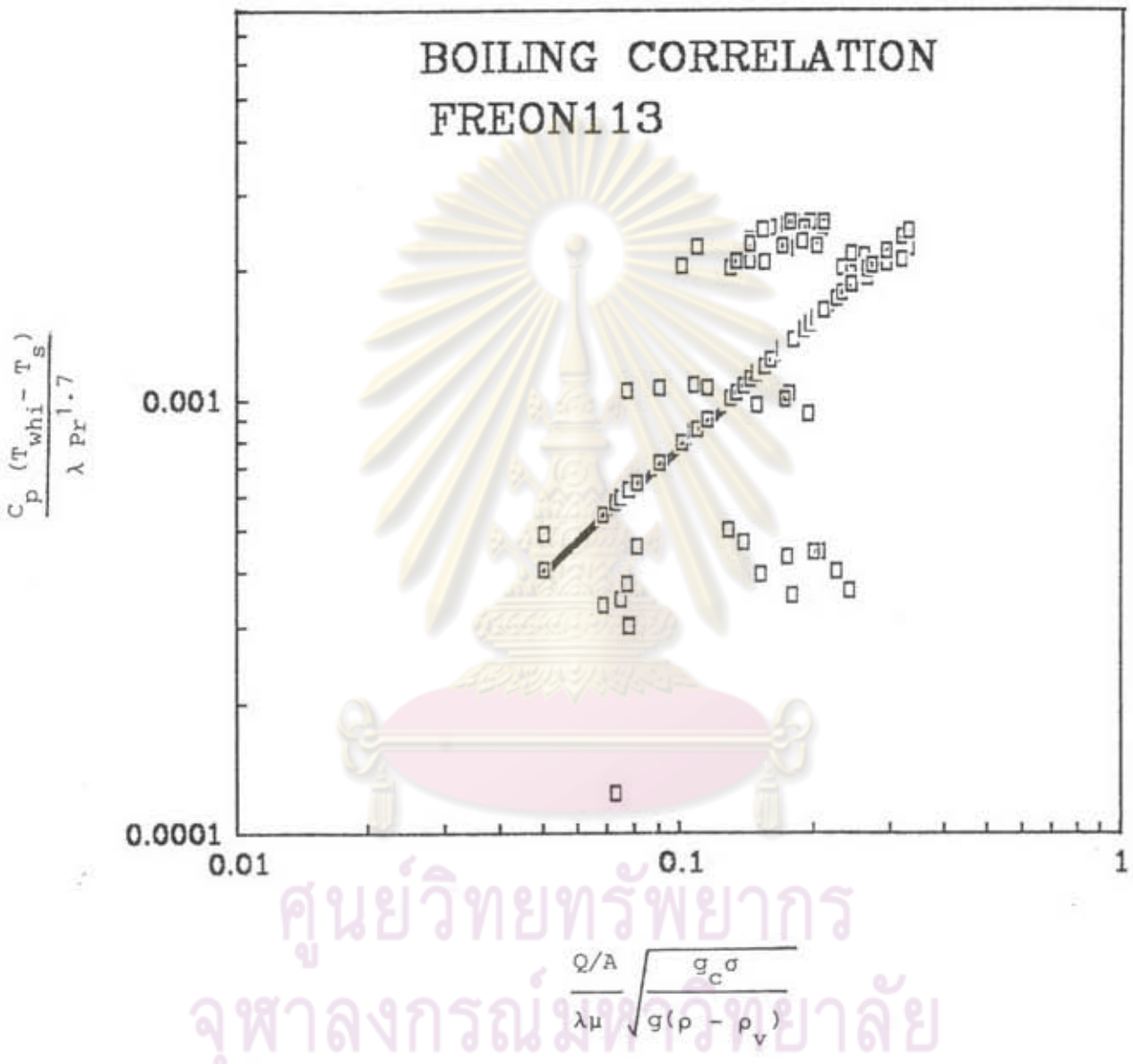

Figure 5.36 Heat transfer correlation of evaporator section for the case of Freon-113 (tilt angle = 50 degrees, fill ratio 30%).

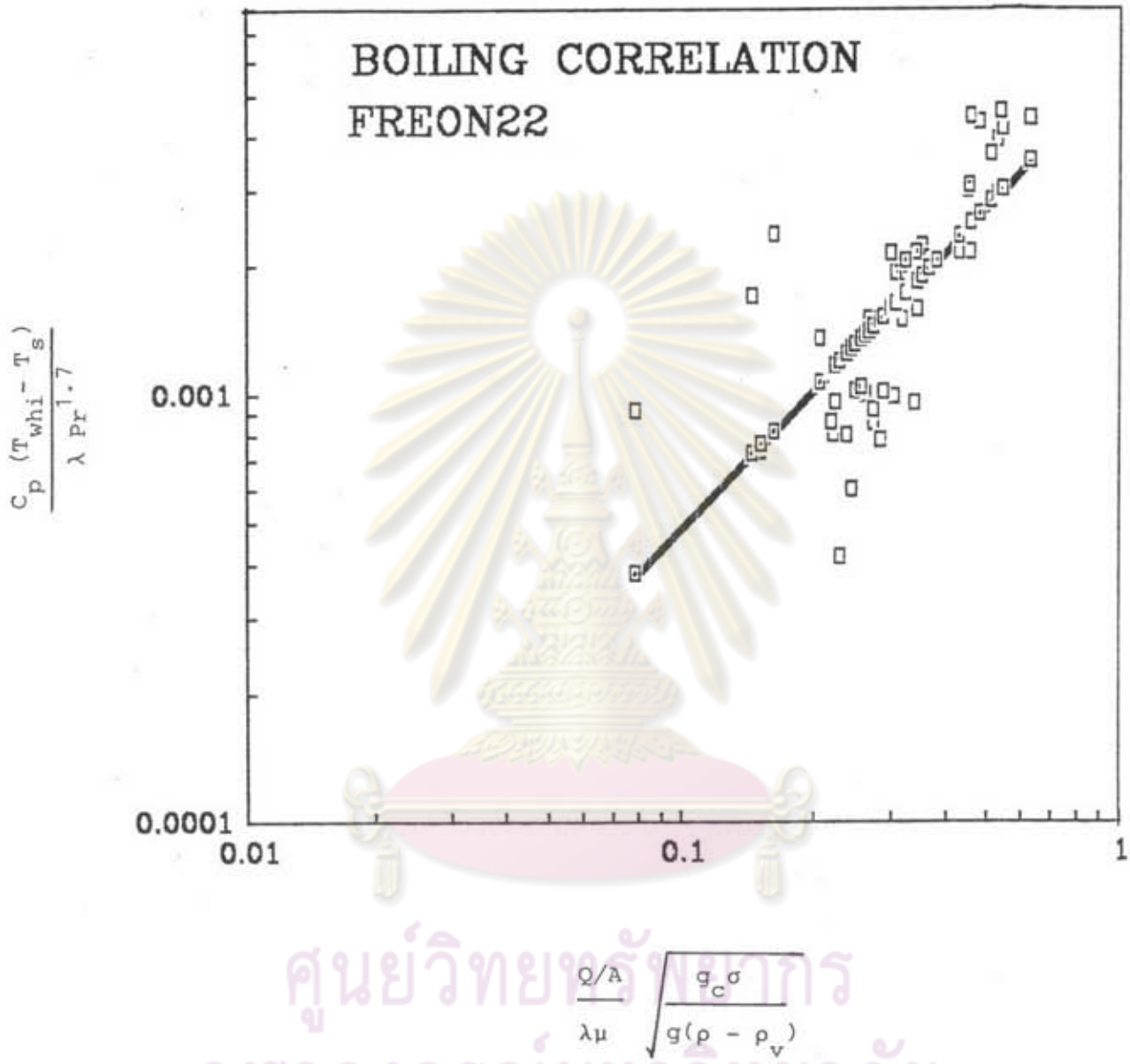

Figure 5.37 Heat transfer correlation of evaporator section for the case of Freon-22 (tilt angle = 50 degrees, fill ratio 16.4%).

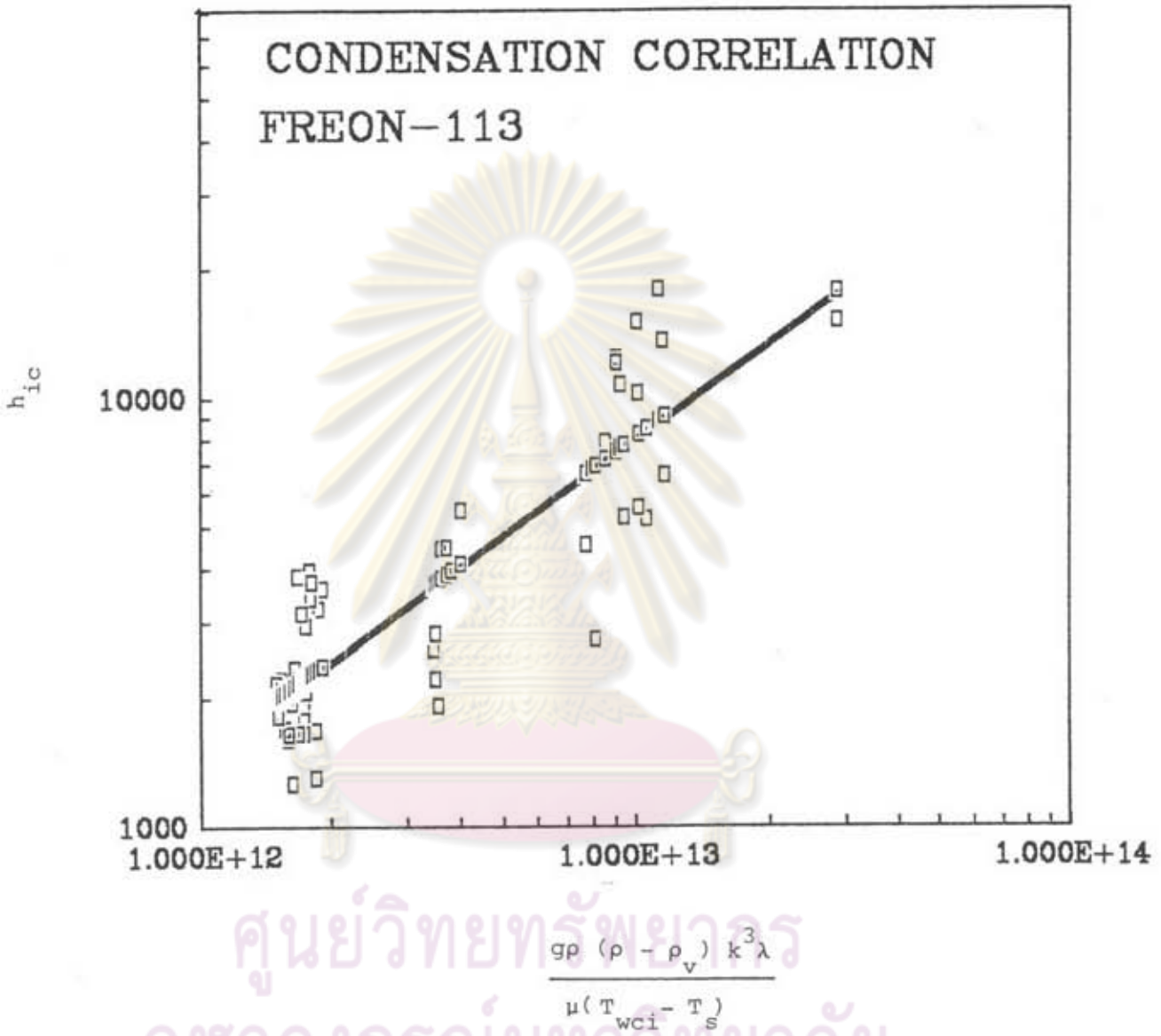

Figure 5.38 Heat transfer correlation of condenser section for the case of Freon-113 (tilt angle = 50 degrees, fill ratio 30%).

For Freon-22 (tilt angle 50 degrees, fill ratio 30%) (see Figure 5.39)

$$h_{ic} = 5.331\times10^{-4} \left[\frac{g \rho (\rho - \rho_v) \lambda k^3}{\mu (T_s - T_{wci}) L_h} \right] 0.558$$

c. Outer Film Correlations

In this study the observed values of the outer film coefficients are quite high while the flow phenomena inside the jacket is very complex. Since no suitable correlations are available, the correlations have to be obtained from the experimental results as follows.

For Evaporator Section (see Figure 5.40)

$$Nu_h = 13.228\ Re_h^{0.381} \qquad (5.4)$$

For Condenser Section (see Figure 5.41)

$$Nu_c = 0.128\ Re_c^{0.952} \qquad (5.5)$$

The above obtained correlations are graphically plotted and compared with the experimental data in the following section.

5.9 Comparison with the Experimental Results

The thermal resistance in each section of the heat pipe has been calculated using the correlations mentioned previously. The calculated results are listed in Appendix E. Comparison of the calculations with the experimental results are shown in Figures 5.42-

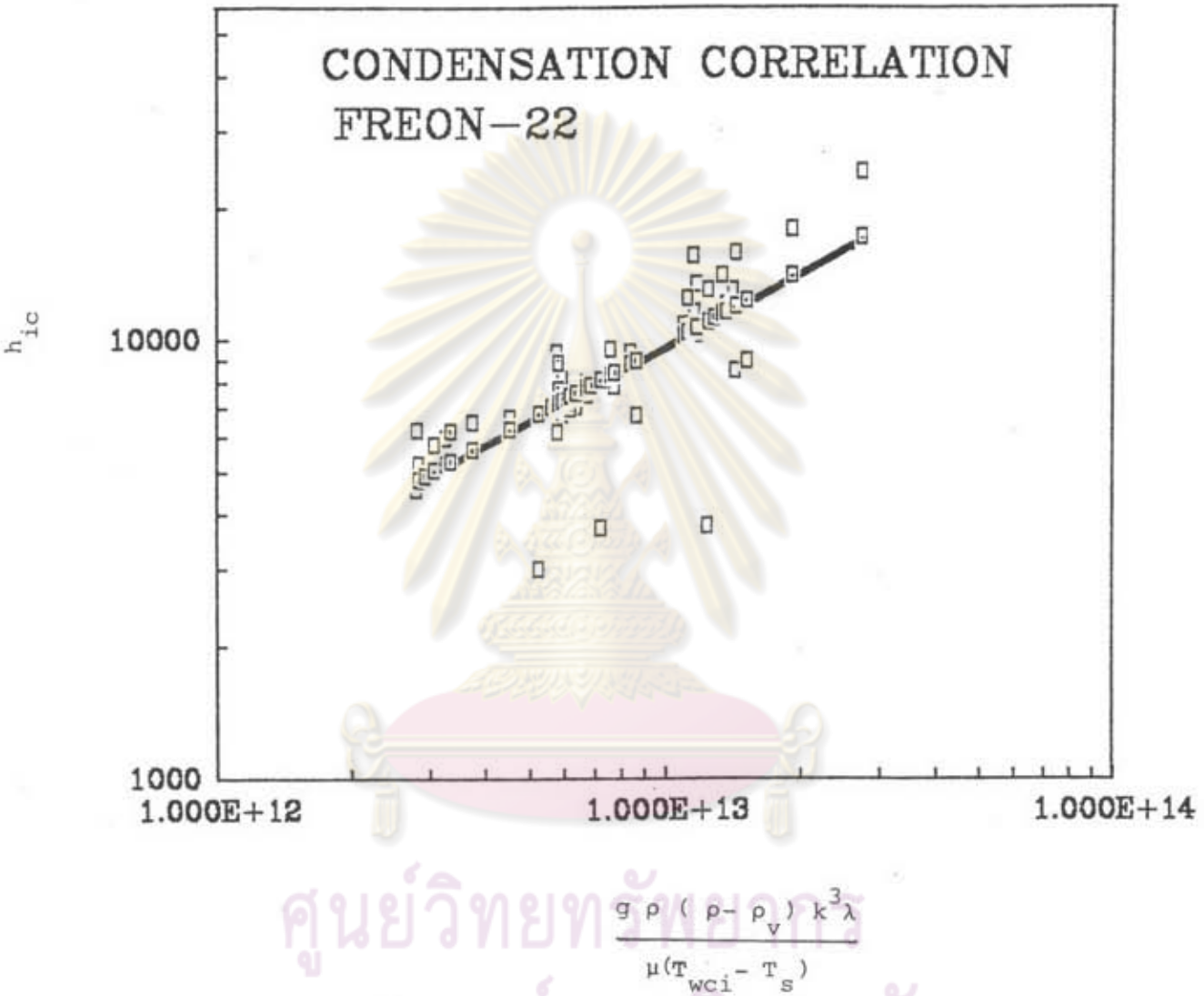

Figure 5.39 Heat transfer correlation of condenser section for the case of Freon-22 (tilt angle = 50 degrees, fill ratio of 16.4%).

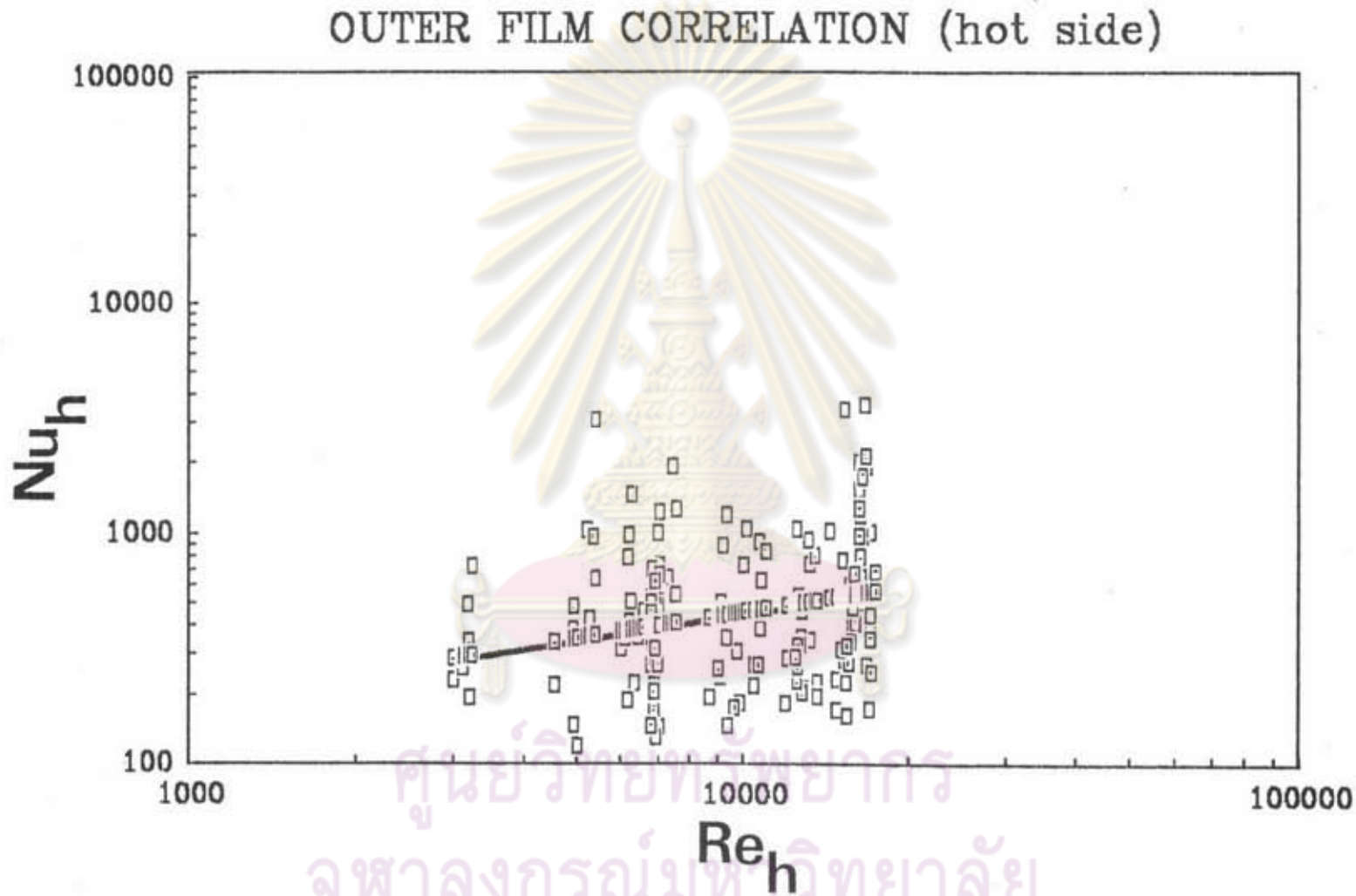

Figure 5.40 Heat transfer correlation of outside film at the evaporator section (tilt angle = 50 degrees).

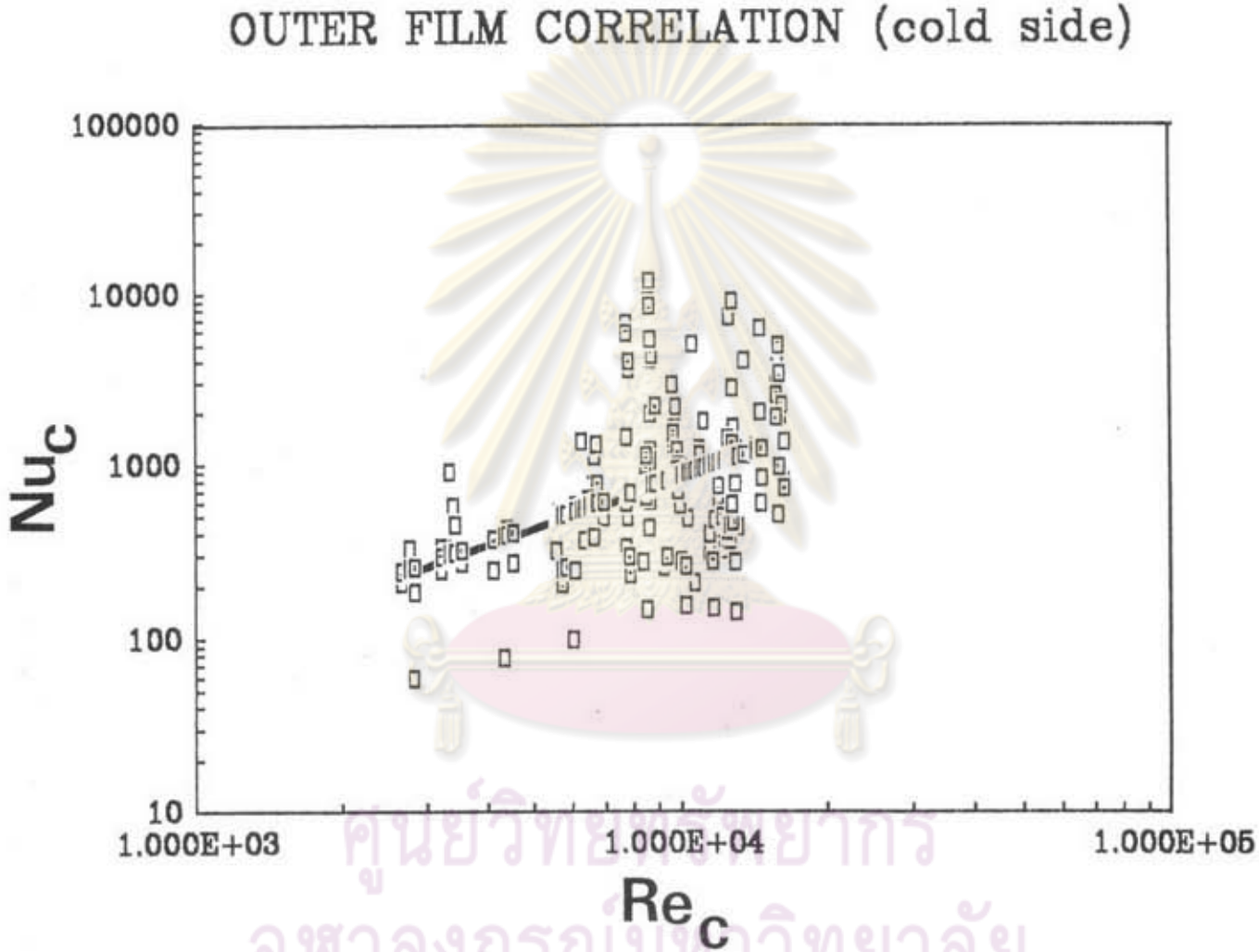

Figure 5.41 Heat transfer correlation of outside film at the condenser section (tilt angle = 50 degrees).

5.52.

It can be seen that the predicted results agree quite well with the experiments, except for the outer film resistances (R_1 and R_7) on both sides. As seen from Figures 5.43 and 5.44 the calculated values of R_1 and R_7 tend to be overestimated when the Reynolds number is small (R_1 and R_7 are small) but underestimated when the Reynolds number is large. The data from the experiments are too widely scattered to be well correlated because the Reynolds number used in the experiment falls across the laminar and transition flow regions. As is well known, the flow behavior in the transition region is highly unstable and unpredictable, and so is the accompanying heat transfer rate.

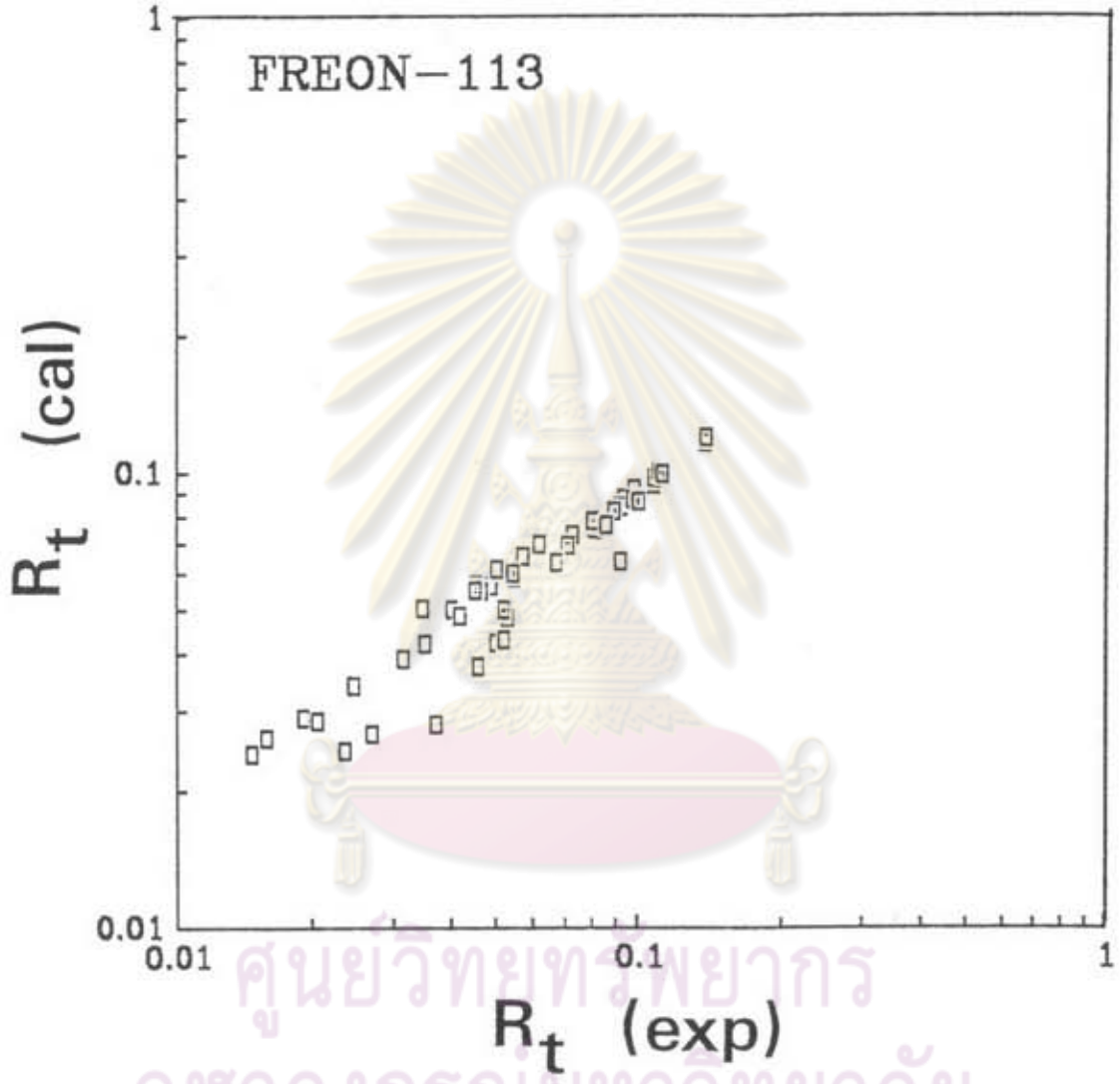

Figure 5.42 Comparison of the calculated total thermal resistance with the experimental value for the case of Freon-113 (tilt angle = 50 degrees, fill ratio 30%).

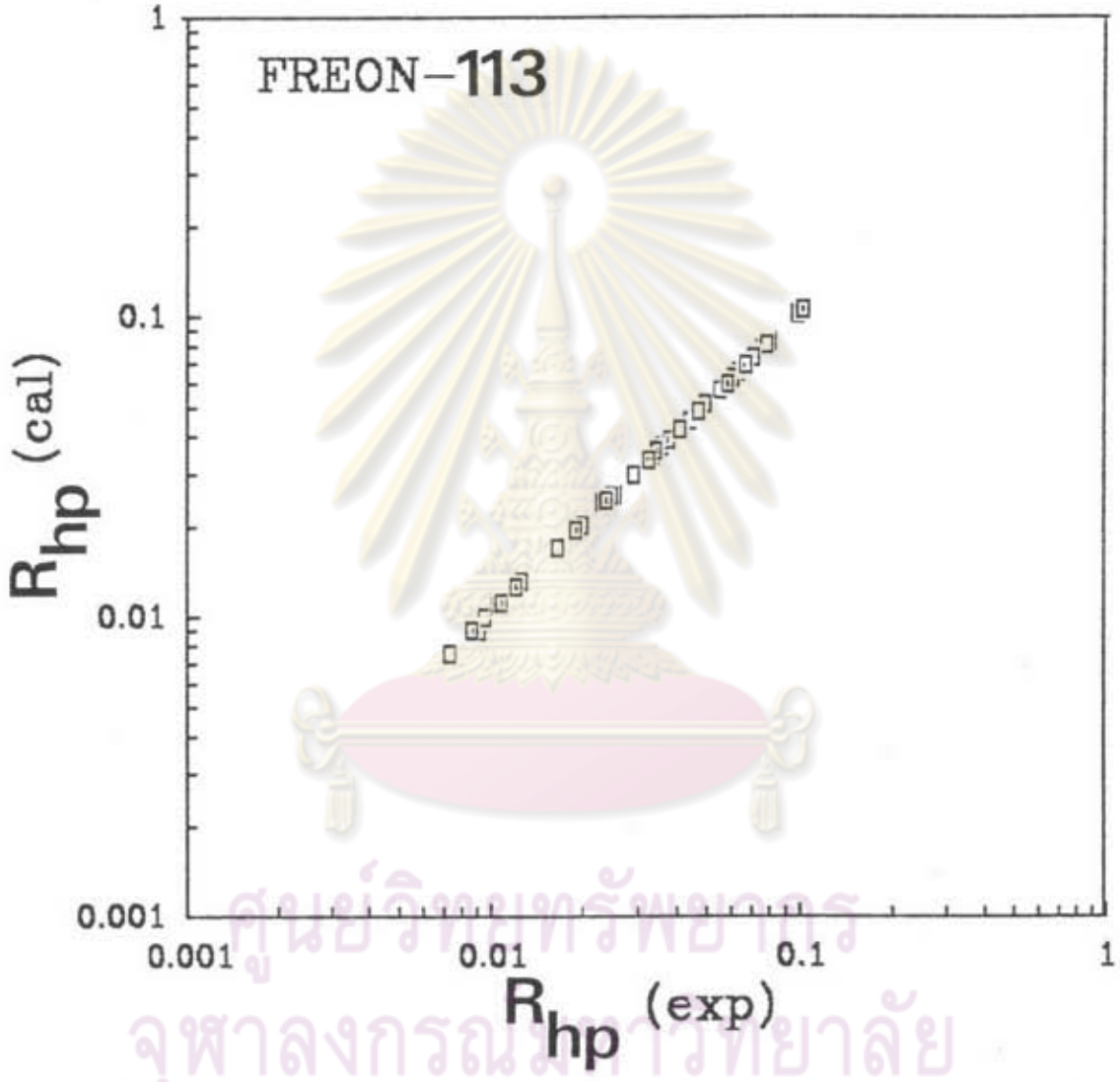

Figure 5.43 Comparison of the calculated internal thermal resistance with the experimental value for the case of Freon-113 (tilt angle = 50 degrees, fill ratio 30%).

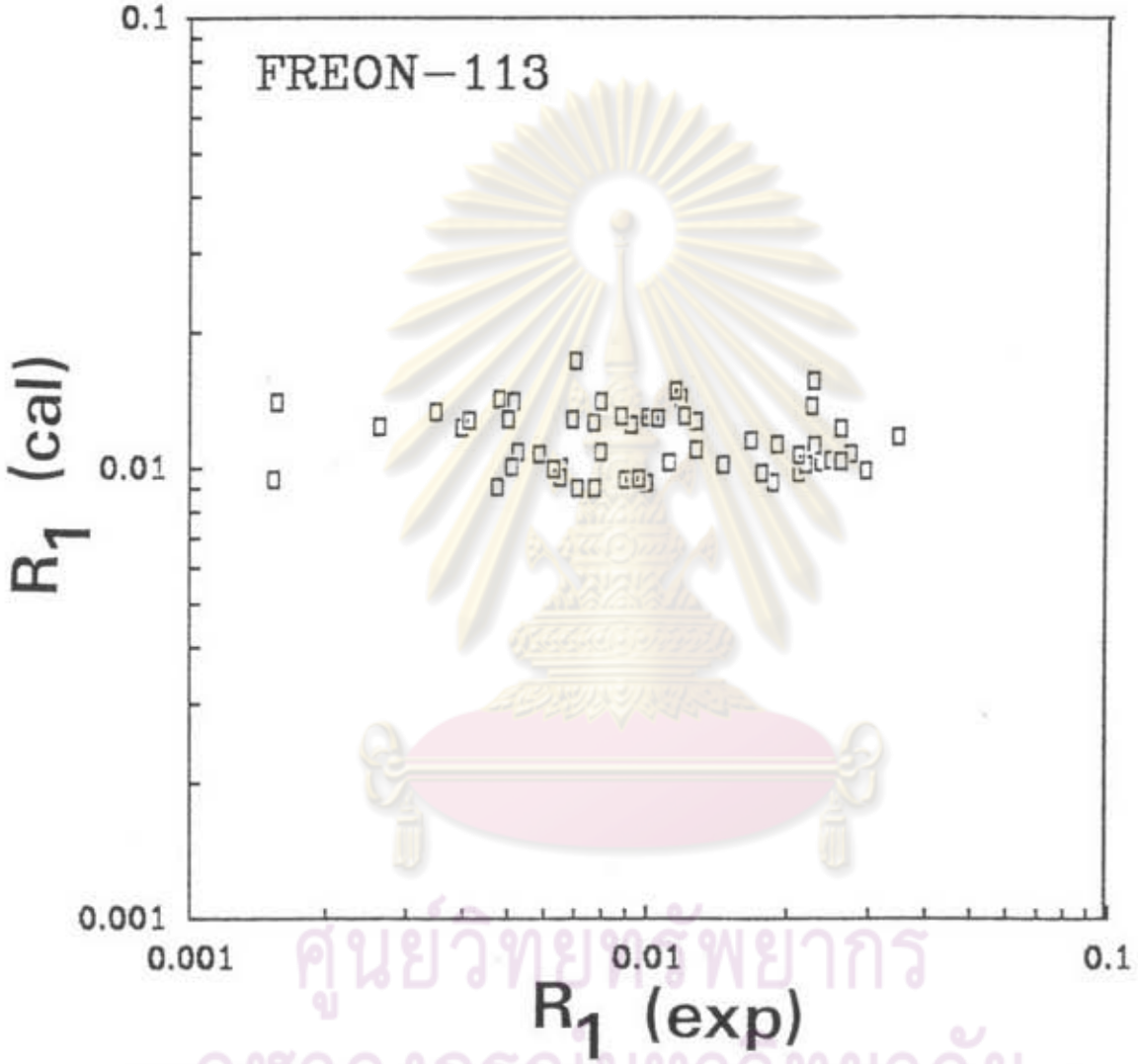

Figure 5.44 Comparison of the calculated outside film resistance at the evaporator section with the experimental value for the case of Freon-113 (tilt angle = 50 degrees, fill ratio 30%).

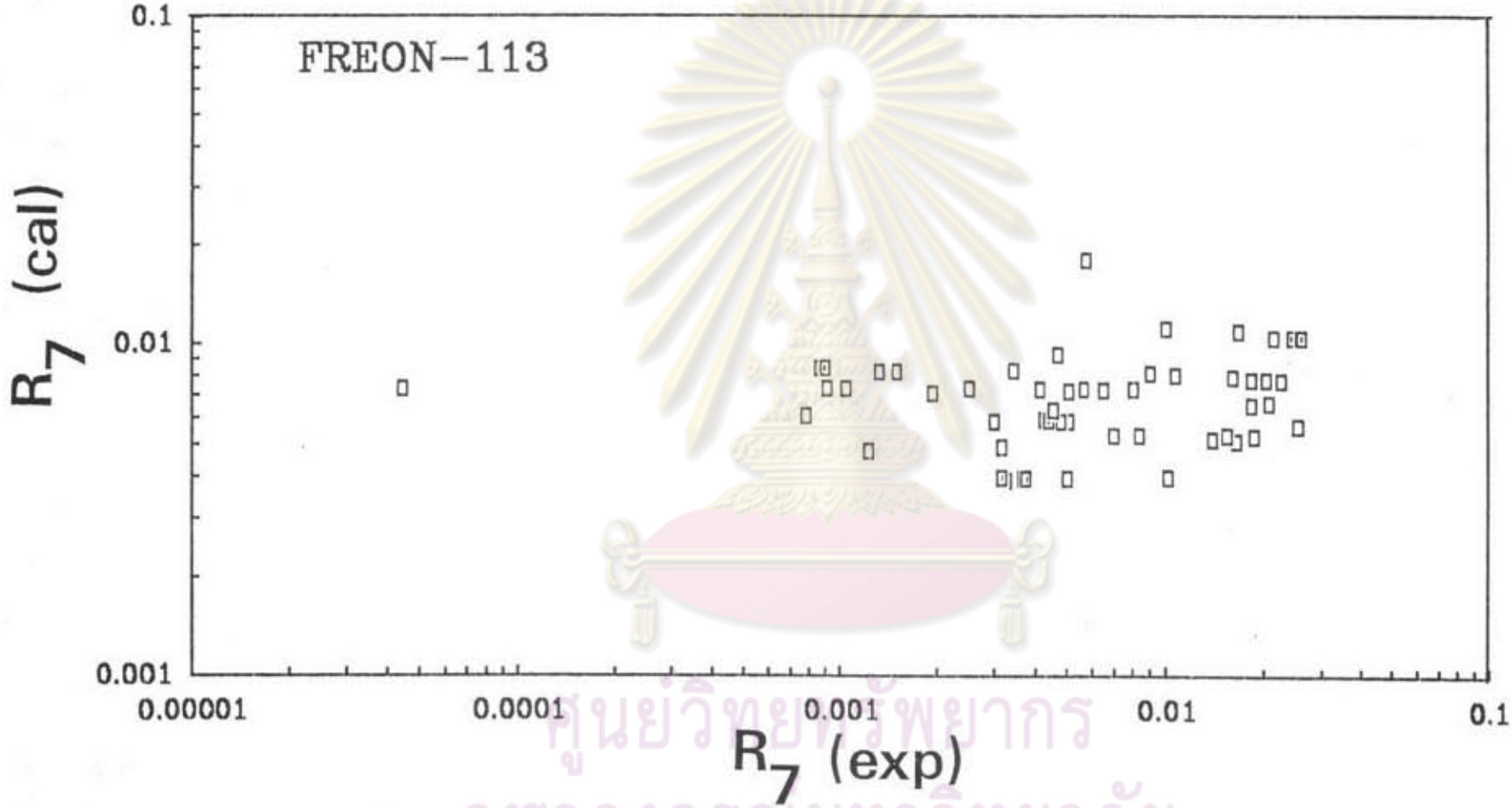

Figure 5.45 Comparison of the calculated outside film resistance at the condenser section with the experimental value for the case of Freon-113 (tilt angle = 50 degrees, fill ratio 30%).

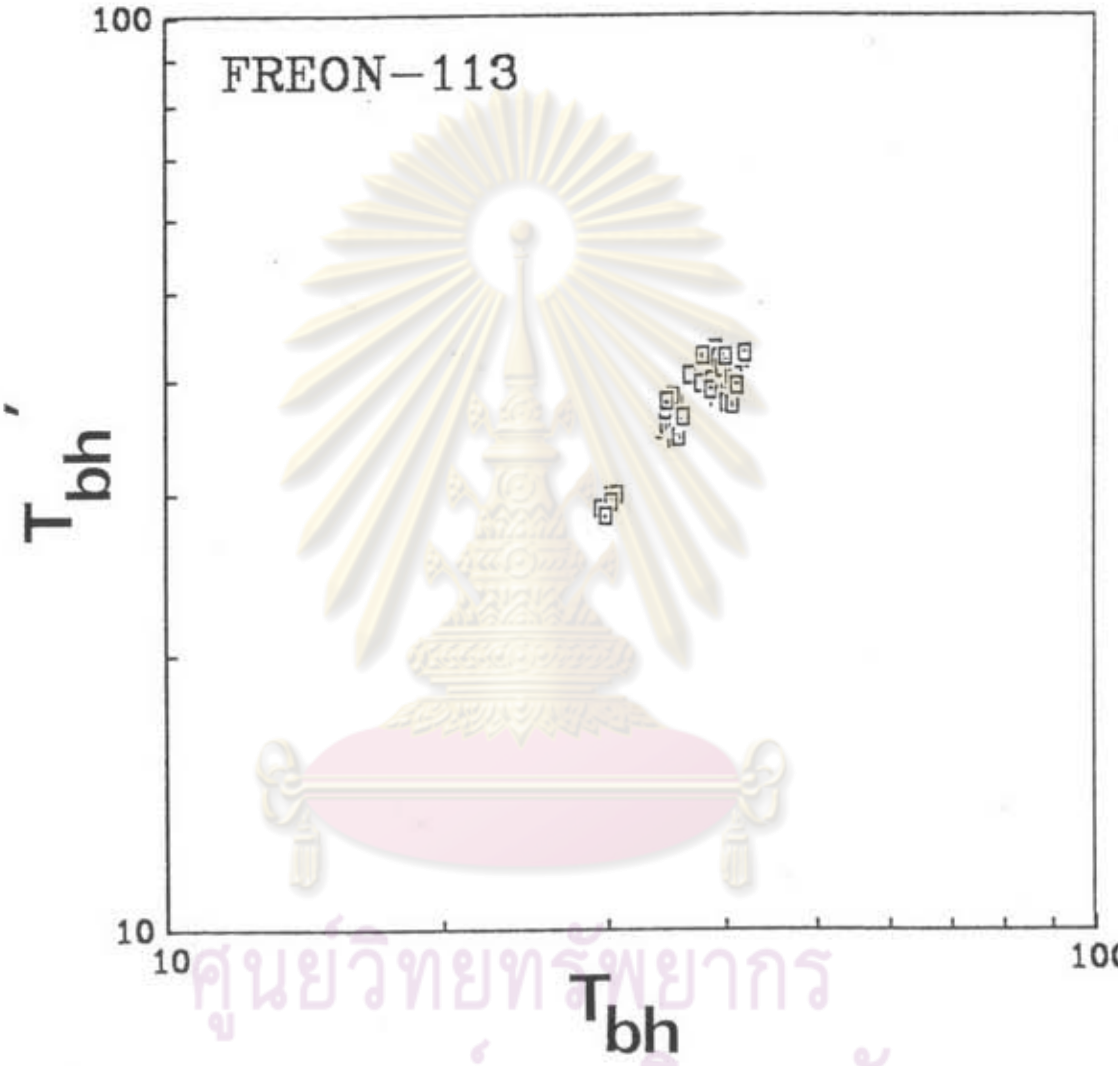

Figure 5.46 Comparison of the calculated bulk temperature of hot water with the experimental value for the case of Freon-113 (tilt angle = 50 degrees, fill ratio 30%).

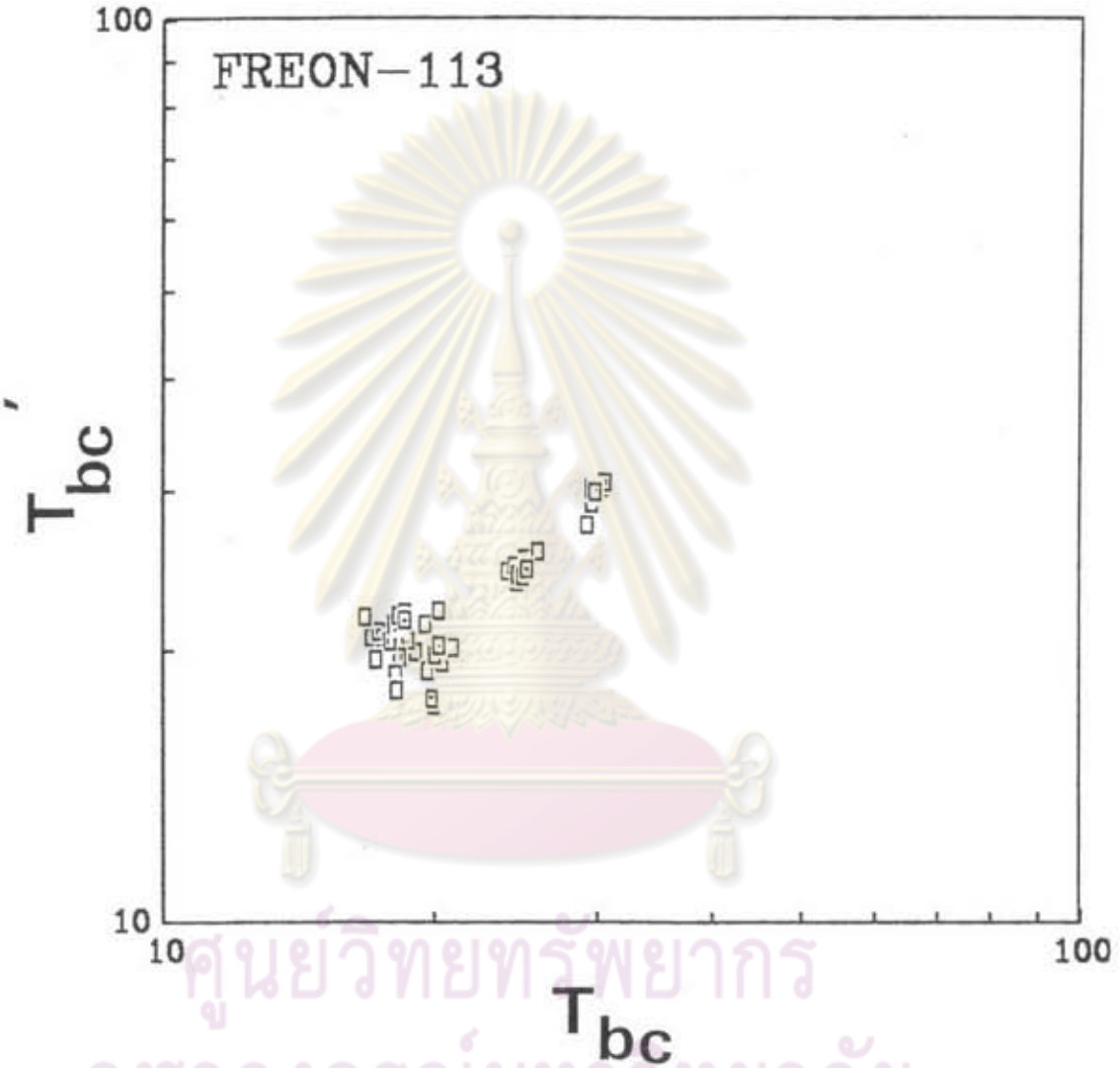

Figure 5.47 Comparison of the calculated bulk temperature of cold water with the experimental value for the case of Freon-113 (tilt angle = 50 degrees, fill ratio 30%).

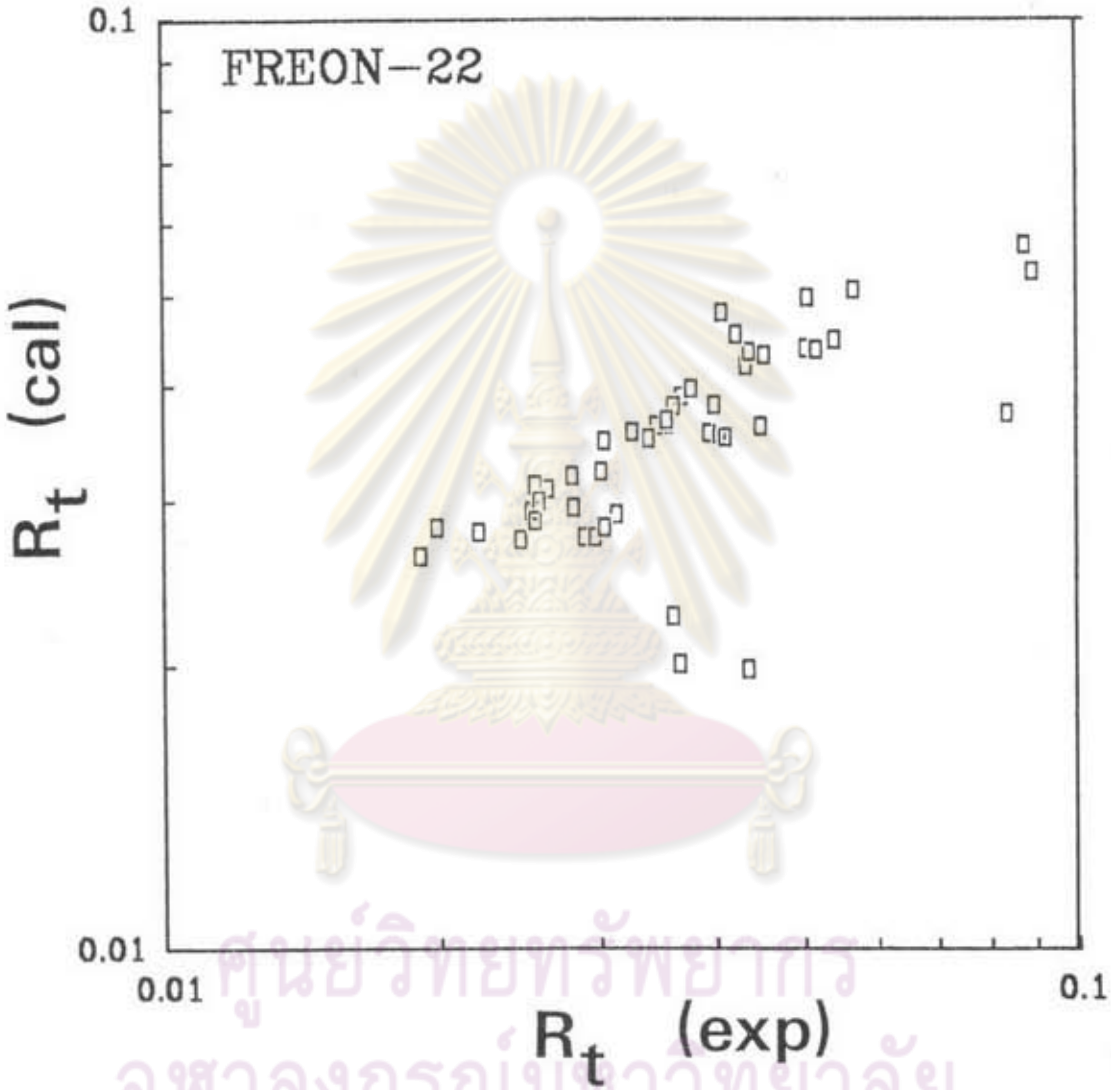

Figure 5.48 Comparison of the calculated total thermal resistance with the experimental value for the case of Freon-22 (tilt angle = 50 degrees, fill ratio 16.4%).

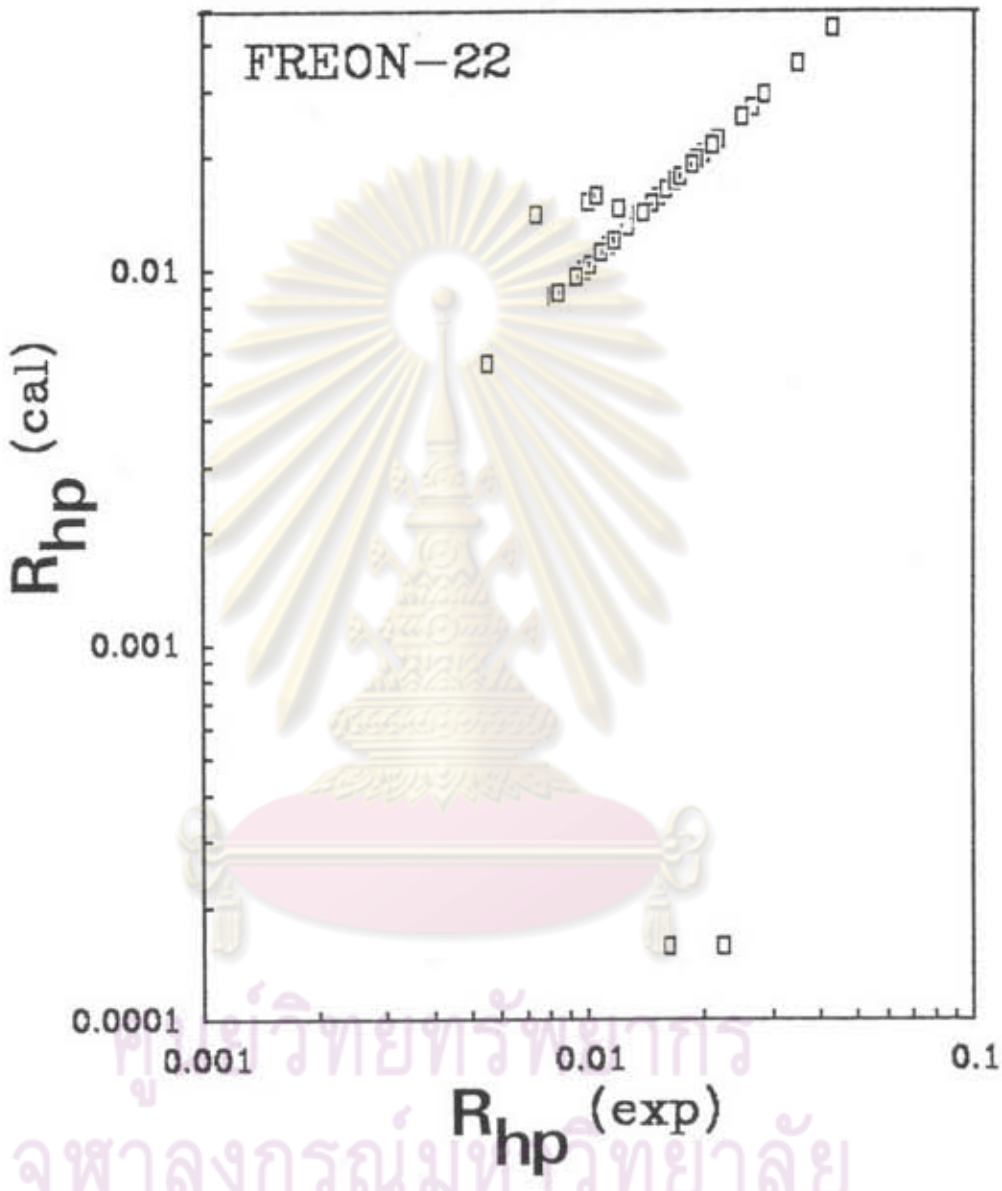

Figure 5.49 Comparison of the calculated internal thermal resistance with the experimental value for the case of Freon-22 (tilt angle = 50 degrees, fill ratio 16.4%).

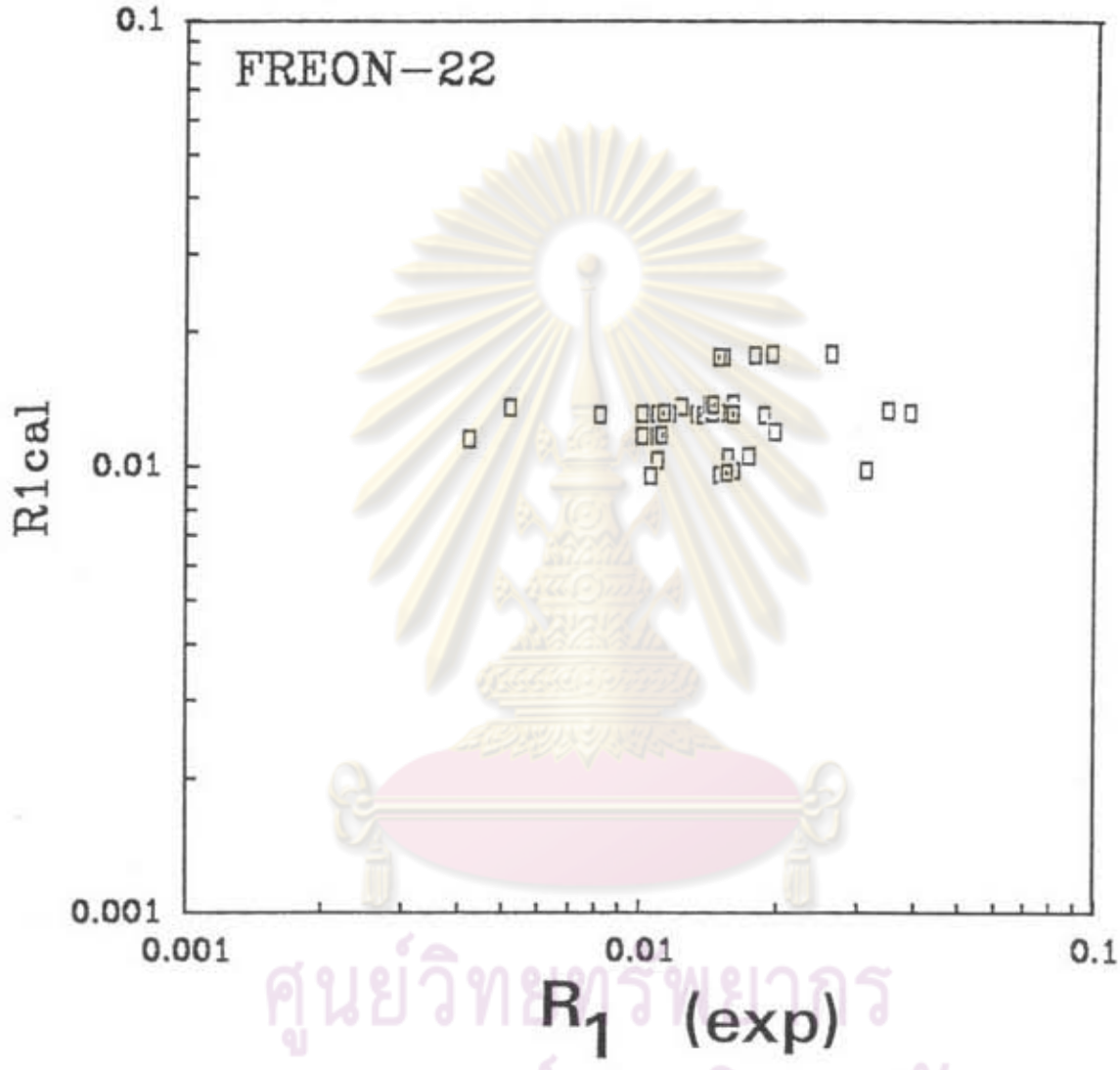

Figure 5.50 Comparison of the calculated outside film resistance at the evaporator section with the experimental value for the case of Freon-22 (tilt angle = 50 degrees, fill ratio 16.4%).

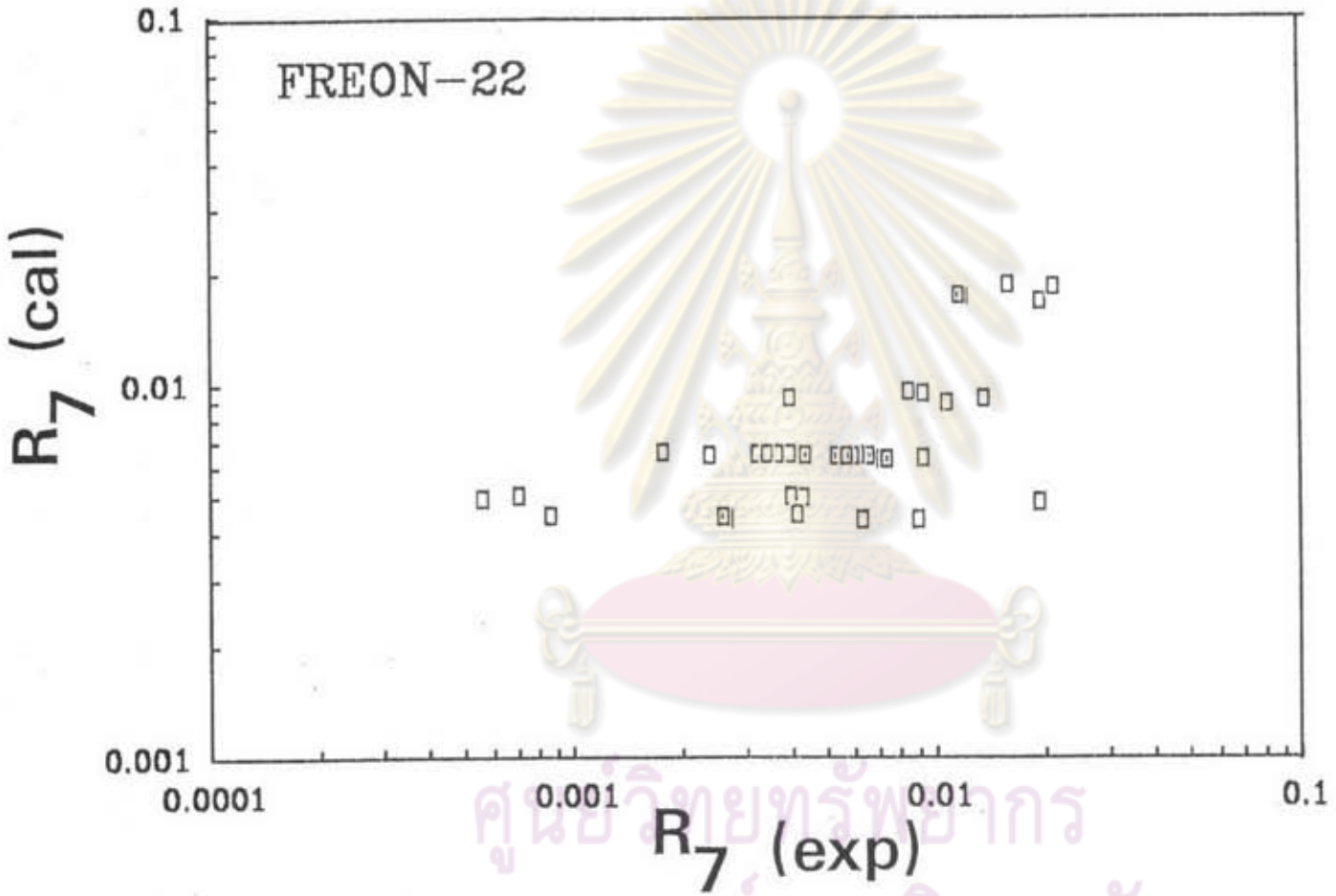

Figure 5.51 Comparison of the calculated outside film resistance at the condenser section with the experimental value for the case of Freon-22 (tilt angle = 50 degrees, fill ratio 16.4%).

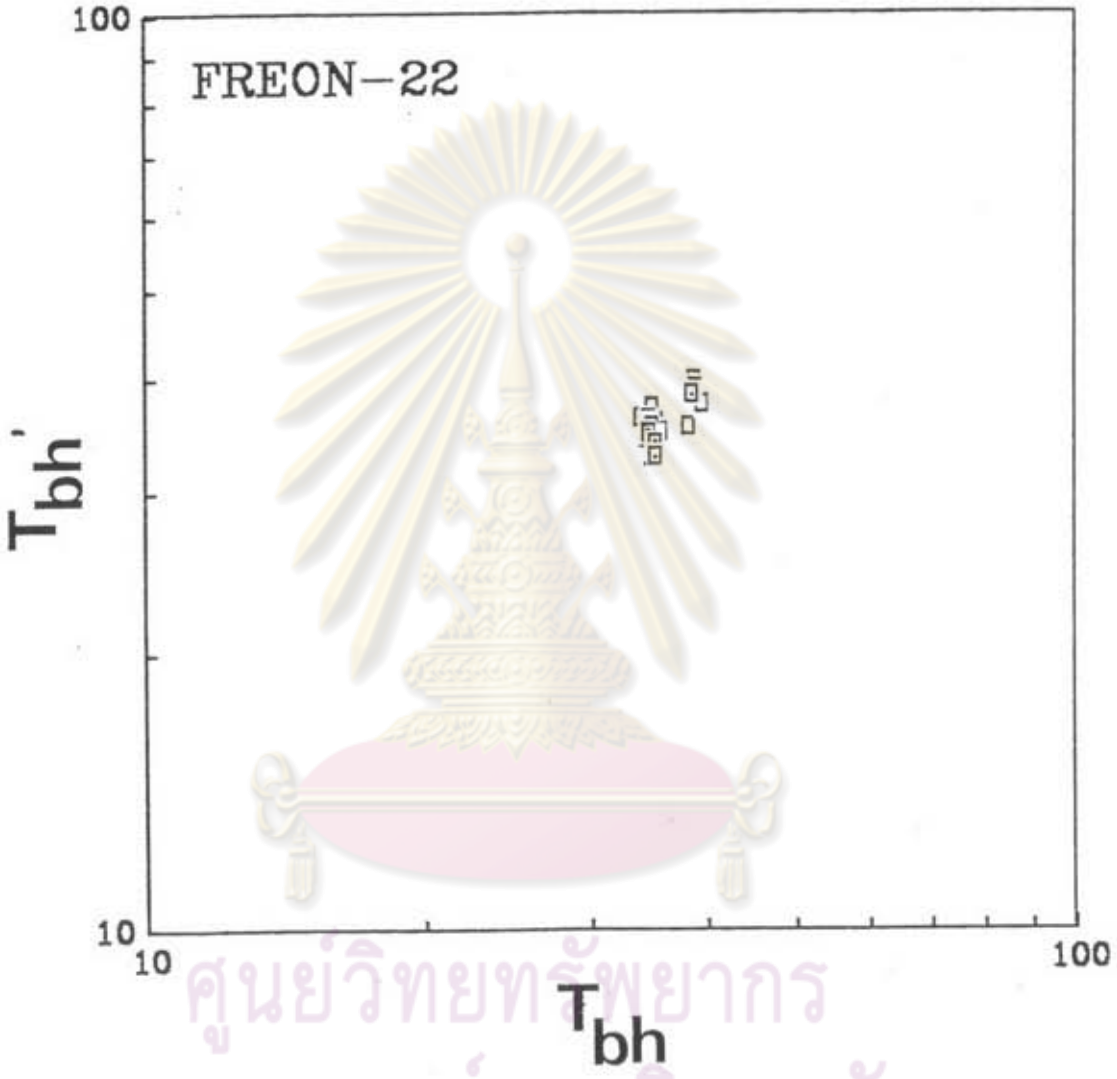

Figure 5.52 Comparison of the calculated bulk temperature of hot water with the experimental value for the case of Freon-22 (tilt angle = 50 degrees, fill ratio 16.4%).

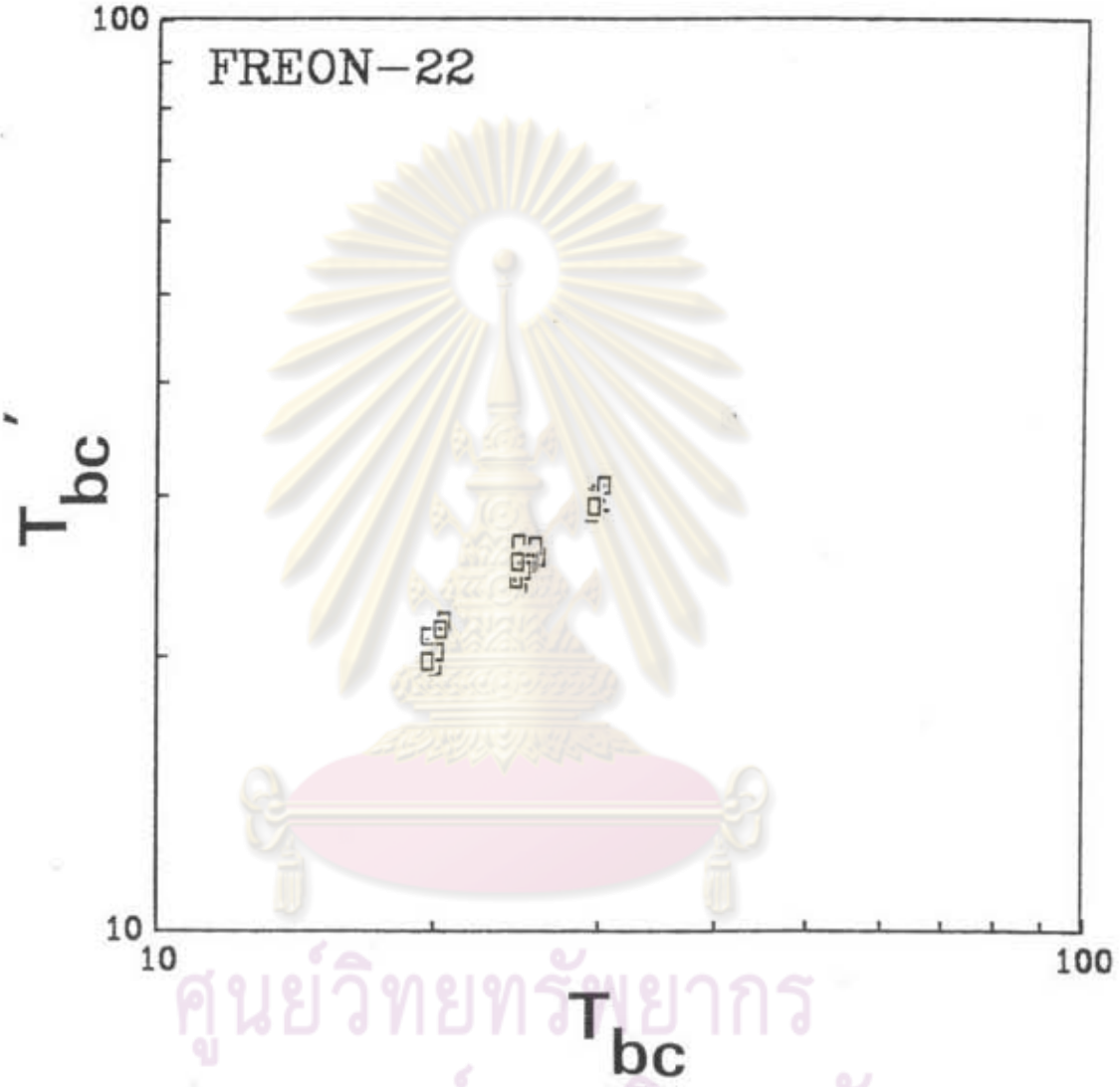

Figure 5.53 Comparison of the calculated bulk temperature of cold water with the experimental value for the case of Freon-22 (tilt angle = 50 degrees, fill ratio 16.4%).